International
Progress Report

IPR-02-42

Äspö Hard Rock Laboratory

Modelling the hydraulic regime in the fracture system at the Äspö HRL on the basis of hydrochemical measurements

Task 5. Äspö Task Force on groundwater flow and transport of solutes

L. Liedtke
N. Klennert

Federal Institute for Geosciences and
Natural Resources, Hanover, Germany

May 2001

Svensk Kärnbränslehantering AB
Swedish Nuclear Fuel
and Waste Management Co
Box 5864
SE-102 40 Stockholm Sweden
Tel +46 8 459 84 00
Fax +46 8 661 57 19

Äspö Hard Rock
Laboratory

Report no.	No.
IPR-02-42	F65K
Author	Date
Liedtke, Klennert	01-05-01
Checked by	Date
Liedtke	01-05-31
Approved	Date
Christer Svemar	02-11-19

Äspö Hard Rock Laboratory

Modelling the hydraulic regime in the fracture system at the Äspö HRL on the basis of hydrochemical measurements

Task 5. Äspö Task Force on groundwater flow and transport of solutes

L. Liedtke

N. Klennert

Federal Institute for Geosciences and
Natural Resources, Hanover, Germany

May 2001

Keywords: Groundwater flow, solute transport, coupled hydrogeochemistry, Äspö, Task 5

Summary

This study deals with the influence of the tunnel construction on the groundwater system at the Äspö site and looks at changes in the flow pattern as well as the disturbance of the chemical balance. Hydraulic and transport models were constructed to simulate the dominant hydraulic and chemical processes in the investigated area with and without the spiral tunnel.

Flow and transport calculations were carried out with a multi-fracture model including fracture zones NE-1, NE-2, NE-3, NE-4, EW-1 78°, EW-1 88°, EW-3, NNW-2, NNW-4, and NNW-7 belonging to the regional fracture system. The conditions before, during and after tunnel construction were simulated. Measured piezometric heads and the distribution of the four water types: meteoric, Baltic Sea, glacial, and brine at different control points were compared to simulated values. Model parameters were varied corresponding to the deviations to achieve a better match between the measured and simulated values.

The flow modelling confirmed the observed drawdown beneath the island of Äspö and the resulting change in the flow pattern and flow velocities. In contrast to initial conditions, the model indicates downward groundwater flow above the tunnel and upward flow in the fractures beneath the tunnel. Conservative transport calculations demonstrate the changing mixing ratio of groundwaters of different origin at the site (meteoric, Baltic sea, glacial, brine water). This effect can be compared to observed chemical compositions at specific control points. The change of the flow directions owing to the drawdown results in dilution of dissolved substances by meteoric water flowing into the aquifer. The upward groundwater flow of brine increases the salinity in the deeper part of the investigated area.

Chemical analyses of non-conservative elements in the water samples show a clear deviation compared to simulated concentrations from the mixing model. For this reason, different approaches were pursued to identify chemical processes and to increase the understanding of the groundwater changes associated with tunnel excavation. A general conceptual model of the essential hydrochemical conditions at the site during the tunnel excavation was composed. Chlorine, Bromine and also Sodium behave conservatively and can largely be reproduced by a pure mixing approach. In general, the groundwater components SO_4^{2-}, HCO_3^-, K^+, Ca^{2+}, and Mg^{2+} are affected by chemical processes. Cations are for the most part controlled by exchange processes. Sulphate, hydrogen carbonate, and calcium are influenced by dissolution and precipitation of calcite and gypsum. Additionally, organic redox reactions and organic decomposition may account for the observed carbonate and sulphate chemistry. Nevertheless, it can be assumed that a few chemical reactions, that influence the groundwater composition, cannot be identified because of different processes that lead to opposite effects concerning loss or gain of elements.

Sammanfattning

Denna studie handlar om tunneldrivningens påverkan på grundvattensystemet på Äspö, och undersöker förändringar i flödesmönstret liksom störningar i kemibalansen. Hydrauliska modeller och modeller för transport utvecklades för att simulera de dominerande hydrauliska och kemiska processerna i det undersökta området med och utan en spiraltunnel.

Flödes-och transportberäkningar genomfördes med en flerspricksmodell som inkluderade sprickzonerna NE-1, NE-2, NE-4, EW-1 78^{o}, EW-1 88^{o}, EW-3, NNW-2, NNW-4 och NNW-7, vilka hör till det regionala spricksystemet. Förhållandena före, under och efter tunneldrivningen simulerades. Uppmätta piezometriska tryck och distributionen av de fyra vattentyperna: meteoriskt, Östersjöiskt, glacialt och saltrikt vid vissa kontrollpunkter jämfördes för att simulera värden. Modellparametrar varierades i förhållande till avvikelser för att få en bättre överensstämmelse mellan uppmätta och simulerade värden.

Flödesmodelleringen bekräftade de observerade avsänkningarna under Äspö ö och härav ändrade flödesmönster och flödeshastigheter. I kontrast till de ursprungliga förhållandena indikerade modellen ett nedåtgående flöde ovanför tunneln och uppåtriktat flöde i sprickor under tunneln. Konservativa transportberäkningar demonstrerade den förändrade blandningskvoten i grundvatten av olika ursprung på platsen (meteoriskt, Östersjöiskt, glacialt och saltrikt vatten). Denna effekt kan jämföras med observerade kemiska sammansättningar i specifika kontrollpunkter. Förändringen i flödesriktningar till följd av avsänkningen resulterar i utspädning av upplösta ämnen i meteoritiskt vatten, som rinner in i akvifären. Det uppåtriktade flödet av saltrikt vatten ökar salthalten i de djupare delarna i det undersökta området.

Kemiska analyser av sorberande ämnen i vattenproven visar en klar avvikelse jämfört med simulerade koncentrationer från blandningsmodellen. Av detta skäl användes olika tillvägagångssätt för att identifiera kemiska processer och för att öka förståelsen om grundvattenförändringar till följd av tunneldrivning. En generell konceptuell modell upprättades för de viktiga hydrokemiska förhållandena på platsen under tunneldrivningen. Klor, brom och även natrium sorberar ej och kan i stort representeras av en ren blandningsmodell. I allmänhet påverkas grundvattenkomponenterna SO_4^{2-}, HCO_3^-, K^+, Ca_2^+ och Mg_2^+ av kemiska processer. Katjoner kontrolleras för det mesta av utbytesprocesser. Sulfat, vätekarbonat och kalcium påverkas av upplösning och utfällning av kalcit och gips. Därtill kan organiska redoxreaktioner och organisk ämnens separation förklara den observerade kalcium-och sulfatkemin. Oberoende av detta kan antas att det inte går att identifiera endast några få kemiska reaktioner, som påverkar grundvattnets sammansättning. Olika processer förekommer, som leder till motstridiga resultat beträffande förlust eller vinst av olika ämnen.

Contents

List of Figures

List of Tables

Appendices

1 Introduction

1.1 Background

The pre-investigations for the Äspö Hard Rock Laboratory (HRL) started in 1986 and a large number of investigation boreholes have since been drilled on Äspö and in adjacent areas. The borehole lengths vary from 22 m to 1700 m. They are usually equipped with borehole packers to divide the borehole into different hydraulic units.

The Äspö Hard Rock Laboratory was constructed from October 1990 to October 1994. The maximum depth of the laboratory is 450 m and the tunnel has a total length of 3.6 km. Tunnel excavation affected the groundwater flow and the chemical composition of the groundwater in the fractures. This can be observed by monitoring the pressure heads and the chemical composition in the borehole sections.

At the Äspö Hard Rock Laboratory, the groundwater flow, chemical composition, and piezometric levels in the borehole sections have been monitored at undisturbed sites and then at successive intervals as the tunnel approaches the HRL target area under Äspö island. The change in the chemical composition indicates groundwater flow and solute transport.

Different types of groundwater with different origins were identified on the basis of the consistency and composition of element concentrations using the M3 – Multivariate Mixing and Mass Balance Calculations approach (LAAKSOHARJU & WALLIN 1997).

Potential chemical reactions can be considered to explain the difference between the present water composition and a conservative transport model. An important task is to assess the extent of reactions taking place as water-rock interactions or between different types of groundwater. Another significant aspect is the influence of the boundary conditions on the mixing processes depending on changes in the flow pattern.

Hydraulic processes as well as transport phenomena in specific conductor domains were simulated in the study presented in this report. Borehole sections associated with specific major fracture zones were studied and changes in chemical composition were compared with simulations. In this way, the models were calibrated using the information derived from the response.

1.2 Objectives

The aim of Task 5 is to compare and ultimately integrate hydrochemistry and hydrogeology. The general method is to compare the outcome of the hydrochemical models with the groundwater flow models. The Task 5 modelling will also be useful for a future assessment of the stability of the hydrodynamic and hydrochemical conditions at Äspö. This modelling approach could, if successful, then be used for any future repository site investigation and evaluation, especially in a crystalline bedrock environment. The objectives of this study derive from the general objectives stated for Task 5 (WIKBERG 1998).

The specific objectives are:

- to assess the consistency of groundwater flow models and hydrochemical mixing-reaction models through integration and comparison of the hydraulic and chemical data obtained before, during and after tunnel construction

- to develop a procedure for integrating hydrological and hydrochemical information which could be used to assess potential disposal sites.

1.3 Performance

The following procedure was used during the performance of this working draft:

1. evaluating groundwater flow and chemical composition in specific fracture zones in the Äspö HRL target area

   - during undisturbed (natural) conditions before October 1990;
   - during and after the construction of the tunnel;

2. compare and interpret the undisturbed and influenced conditions with the prediction, and assess the influence of chemical reactions on the varying groundwater composition.

2 Site Description

The Äspö Hard Rock Laboratory is located about 2 km north of the Oskarshamn Nuclear Power Station on the island of Äspö. The access tunnel extends from Simpevarp island, runs under the sea floor and reaches the spiral part of the HRL beneath the island. The total length of the tunnel is 3600 metres and reaches a maximum depth of 450 metres below ground level, (Figure 2-1).

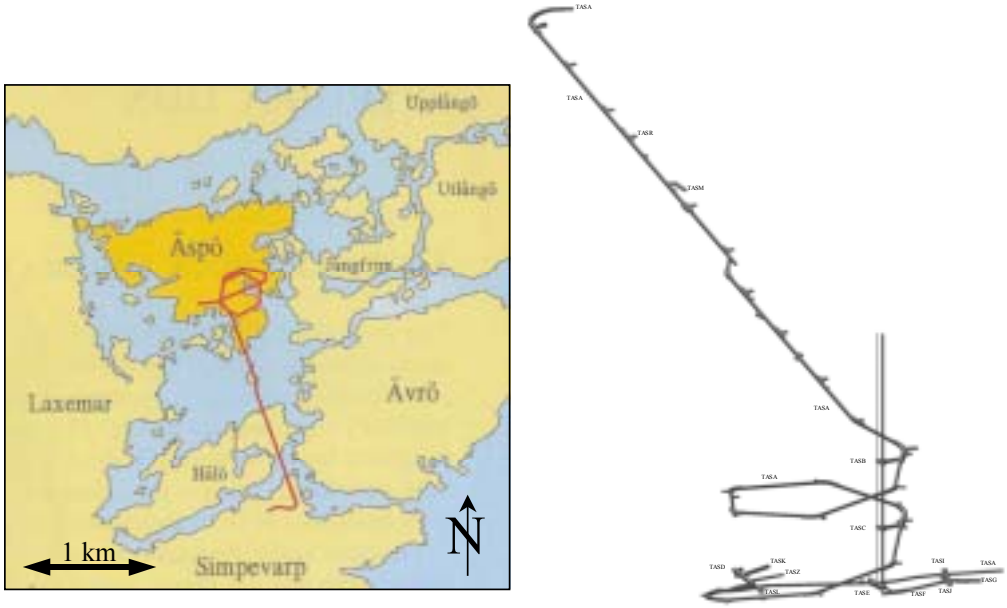

Figure 2-1 *Location of the Äspö HRL and tunnel geometry (from RHÉN et al. 1997).*

The geology of the Äspö site is characterised by a Småland type medium-grained porphyritic granite to quartz monzodiorite and in the south of the island by the red granite Ävrö variety. Furthermore, some intersections with fine-grained alkali granite, altered greenstone and dacitic metavolcanics occur as lenses and dikes. During tunnel investigations the existence end extensions of fractures, fracture filling minerals, the tunnel geology as well as geohydrology and groundwater chemistry data were mapped (MARKSTRÖM & ERLSTRÖM 1996).

The annual mean precipitation in the investigated area is about 675 mm. The groundwater recharge (precipitation minus evaporation) is assumed to be 150 - 200 mm/a (RHÉN et al. 1997). Groundwater flow or discharge and recharge mainly take place along major tectonic fractures and discontinuities. Figure 2-2 shows the major fracture zones in the investigated area in relation to the HRL tunnel. The structures modelled in this study using a part of the collected data set are pointed out.

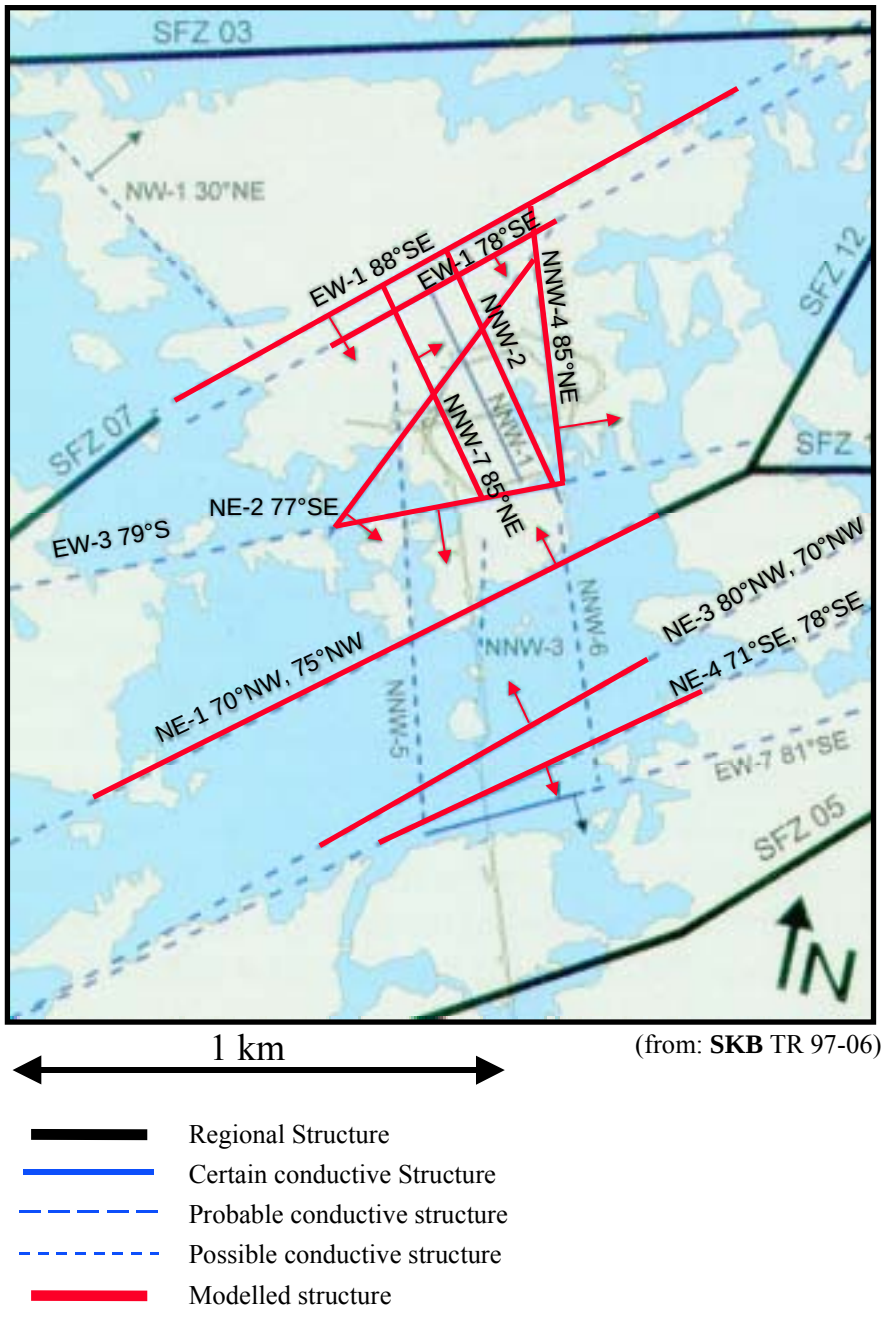

(from: **SKB** TR 97-06)

Figure 2-2 *Hydraulic conductors at the Äspö site.*

3 Basic Conceptual Assumptions

3.1 Aim of the Modelling

The aim of the modelling is to understand the hydraulic conditions at the Äspö site and the effects of tunnel excavation on the groundwater dynamics. The corresponding change in the chemical composition of the groundwater, associated with a different distribution of the water types, helps to develop a conceptual model for the site characteristics. For this reason, site scale flow and conservative transport models were constructed.

Apart from the additional chemical modelling approach some general aspects are discussed that look at the chemical environment at the site, e.g. the salinity distribution. Ultimately, the modelling concepts and results have to be related to measurements. The scope of the groundwater model comprises natural flow and flow to the HRL tunnel, transport phenomena, and chemical characteristics.

The modelling helps to understand the interrelationships between the hydrological and hydrochemical processes and to identify possible chemical reactions affecting the groundwater composition. Therefore, the information on different water compositions at the selected control points can be used for the modelling with the chemical data applied as tracer information.

3.2 Processes

The construction of the tunnel has an influence on the groundwater flow and the distribution of the main groundwater types: meteoric, Baltic sea, glacial, and brine. This effect can be observed by considering the major fracture zones. A disturbance of the flow pattern can be continuously observed. The lowering of the water table beneath the island of Äspö is a distinct sign of the influence of leakage into the tunnel.

Furthermore, the change in salinity caused by the mixing of different water types causes a change in the distribution of element concentrations and also in the density balance. Chemical reactions may occur which did not take place during the initial, undisturbed conditions.

3.3 Basic Conceptual Model

The numerical site model in this study consists of several discrete hydraulic conductor domains. They occur as major discontinuities in the surrounding rock mass volume and are realised in the model as two-dimensional planar zones.

As recharge and discharge at the Äspö site is controlled mainly by these major discontinuities, it is assumed that groundwater flow can be simulated by considering the processes taking place in the fractures. The influence of the hydraulic rock mass domain is ignored in this study.

Under initial conditions, the groundwater table at the Äspö site has a level up to +4 m above sea level (masl) due to a slightly undulating surface not exceeding +14 masl (RHÉN et al. 1997). For modelling purposes, the fracture zones are considered to be initially completely filled with groundwater.

Chemical reactions can be disregarded if the assumption of groundwater mixing leading to the present groundwater composition is confirmed. However, a combined model for transport and chemical reactions is necessary if chemical processes influence the groundwater composition to the extent that the sampled water analyses cannot be reproduced with a mixing approach, e.g. with a conservative transport model.

4 Model Concepts and Formulation

The DURST/Rockflow software used to simulate flow (SM2 - flow model) and solute transport (TM2 - transport model) in the modelling of Task #5 are based on the assumption of a double porosity continuum for the fractured rock. This software was developed jointly by BGR and the University of Hanover (LIEDTKE et al. 1994; LEGE 1996; KOLDITZ 1997; KOLDITZ et al. 1998).

4.1 Basic Assumptions

In particular, the finite element method is used for the numerical simulation of flow and transport in subsurface systems. Time derivatives were evaluated by using different schemes with various order of accuracy. The stability of numerical solutions will depend on the reference point in time of difference formula. In general, a distinction is made between explicit and implicit schemes. A number of approximate schemes with respect to stability and consistency are examined. The stability criterion from Neumann states that the intrinsic values of the amplification matrix of the discretized equation must be lower or equal to unity. Important stability criteria are stated in terms of the Courant number Cr,

$$Cr = \left| \frac{v \cdot \Delta t}{\Delta l} \right| \leq 1$$

the grid Peclet number Pg,

$$Pg = \left| \frac{v \cdot \Delta l}{D} \right|$$

and the Neumann number Fo.

$$Fo = \frac{D}{\Delta l^2} \Delta t \leq \frac{1}{2}$$

For the non-linear problems, where no exact discretization criteria exist, the consideration of physical conservativity and the grid convergence test may be appropriate proofs of solution stability. Spatial and temporal discretizations can introduce spurious dispersion effects where the amount of the (physical) hydrodynamic dispersion is enlarged by a numerical one. Truncation errors must be determined to estimate the actually resulting dispersion effective in the numerical approach.

4.2 Governing Equations

The transient saturated groundwater flow is described by

$$S_0 \frac{\partial h}{\partial t} + \nabla v = q\,, \qquad (4\text{-}1)$$

where h is the piezometric head,

t the time,

S_0 the specific storativity,

v the average fluid velocity vector, and

q the fluid sink/source.

The velocity is given by the three-dimensional, linear Darcy law:

$$v = -K \cdot \nabla h\,, \qquad (4\text{-}2.a)$$

where K is the hydraulic conductivity tensor, or by the general form of various non-linear laws for fracture or tube flow:

$$v = -K^* \cdot (\nabla h)^{\alpha}\,, \qquad (4\text{-}2.b)$$

where K^* is the hydraulic conductivity as a function of the piezometric head or its gradient and

α a coefficient for different non-linear flow laws.

If v is substituted into the mass balance equation (3-1), the equation may be rewritten as

$$S_0 \frac{\partial h}{\partial t} + \nabla(K \cdot \nabla h) = q\,, \qquad (4\text{-}3)$$

which is the governing equation for the flow model.

The differential equation for solute transport is [SM 2 , Version 1.04, 1992]

$$\begin{aligned} &(n\rho_G + (1-n)\,\rho_G \rho_F\, K_d)\,\frac{\partial c}{\partial t} \\ &+ \rho_G v \cdot (grad\ c) \\ &- div\ (D_G\ (grad\ (n\rho_G c)) \\ &+ (n\lambda\rho_G + (1-n)\lambda\rho_F \rho_G K_d)c \\ &+ q\,(c - c^*) = 0 \end{aligned} \qquad (4\text{-}4)$$

where c is the mass fraction of solute per fluid mass,

n the volumetric porosity,

t time

D_F	the diffusion/dispersion tensor,
F	fluid
v	velocity of fluid flow
q	source / drain term
$\lambda = \ln 2 / t_{1/2}$	the radioactive decay constant of the injected radioelement,
$t_{1/2}$	half – life time
K_d	distribution coefficient
ρ_F ; ρ_G	density rock ; density fluid and
c*	the concentration of solute in the source fluid.

This formulation includes dispersion effects according to Fick's first law. The three-dimensional diffusion/dispersion tensor in a ξ, η, ζ-co-ordinate system oriented according to the flow path is written as

$$Ds = \begin{bmatrix} \alpha_L |v| + d_0 & 0 & 0 \\ 0 & \alpha_T |v| + d_0 & 0 \\ 0 & 0 & \alpha_T |v| + d_0 \end{bmatrix}, \qquad (4\text{-}5)$$

where α_L, α_T are the longitudinal and transverse coefficients of mechanical dispersion and

d_0 is the moleculary diffusion coefficient.

This is identical to the Scheidegger approach after transformation of D_s into a global x-, y-, z-co-ordinate system.

The term $n\lambda c$ describes the non-conservative behaviour of the solute and can be interpreted as a decay term for radioactive solutes, with λ for the decay constant in the decay law.

The last term of equation (4-4) is the source term for fluid sources within the modelled domain.

4.3 Numerical Realization

Equations (4-3) and (4-4) are both solved numerically using a finite-element method. An implicit Crank-Nicolson finite difference scheme is employed to approximate the time-dependent terms, while in space, a Bubnow-Gelerkin technique is used. In this case, the test and shape functions are the same.

The modelling system consists of one-, two- and three-dimensional isoparametric elements with linear shape functions. The position of nodes and elements in the domain to be modelled can be arbitrary, with the restriction that each quadrangular element must be in a plane (Figure 4-1).

Time-dependent piezometric heads at the boundaries and time-dependent fluxes at arbitrary nodes act as the boundary conditions of the flow model. The velocities are used as input data for the transport model. Time-dependent concentrations at the inflow boundary are to be given, as well as the initial concentration distribution.

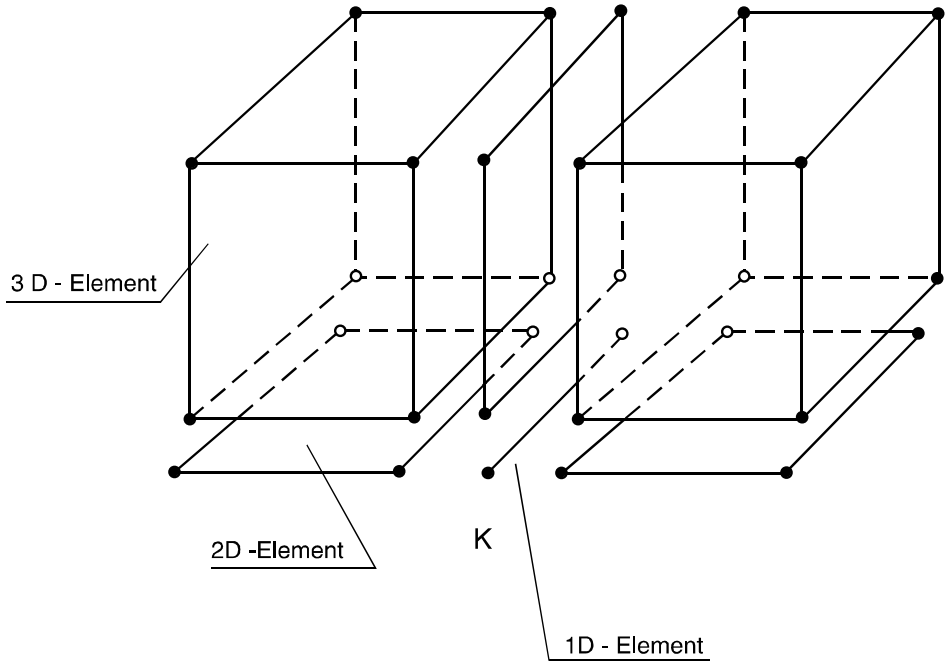

Figure 4-1 *Arbitrary combination of elements of different dimensions.*

The time step increments for transport simulations can be controlled in different ways. They can be taken directly from the flow model or described independently. In the latter case, the velocities are linearly interpolated if the time steps for the transport model are different from the flow field calculation.

Solute transport in the fracture is advection-dominated. A Taylor series expansion describing artificial diffusion was used to modify the numerical formulation in order to reduce the instability of the modelling.

5 Model applications

5.1 Introduction

A multi-fracture model is used to simulate flow and transport including the fracture zones NE-1, NE-2, NE-3, NE-4, NNW-2, NNW-4, NNW-7, EW-1 78°, EW-1 88°, and EW-3. The study comprises a time period for the calculation of about 3700 days (1990-10-01 to 2001-12-31). It includes a prediction of conditions during and after the excavation of the tunnel. The positions of the working face of the tunnel at different stages were included in the model in order to simulate the development of the groundwater system during excavation.

The different approaches that concern the chemical evolution of the groundwater mainly refer to specific time series or water samples from selected measurement points. Equilibrium calculations were carried out for the whole fracture network to characterise the varying chemical conditions at the site.

5.2 Basic Approach and Data

The final multi-fracture model includes 10 discrete fracture zones that are mostly in hydraulic contact and demonstrate the complex connections between the major hydraulic discontinuities, see Figure 5-1. The fracture zones reveal a distinctive groundwater system that is characterised by a large influence of fracture NE-1 (ITTNER & GUSTAFSSON 1995). Some conductors that were intersected by the tunnel several times show a more significant change in the dynamic conditions than others (RHÉN & STANFORS 1993). Non-steady-state flow was calculated and a detailed pressure model for the following transport calculations was constructed.

The fractures are influenced by the island of Äspö and the Baltic Sea and partly by Hålö Island (fracture NE-4). Therefore, different boundary conditions influencing the dynamic system are considered, e.g. the recharge rate on Äspö island and constant pressure heads at the Baltic sea. The modelled fractures are intersected by a number of boreholes in which pressure and chemical data are measured (RHÉN & STANFORS 1995). These data were used for a comparison with the simulated data. Hydraulic head measurements from several surface drilled boreholes (KAS) were also considered. The groundwater composition was compared with measured water samples taken from exploration holes in the tunnel. In this way, 6 control points were chosen to compare the simulated pressure heads, and 18 control points were used to compare the mixing fractions and the chemical composition.

5.3 Geometric Framework

The final model includes the location and orientation of the hydraulic fracture zones NE-1, NE-2, NE-3, NE-4, NNW-2, NNW-4, NNW-7, EW-1 78°, EW-1 88°, and EW-3. They are assumed to be two-dimensional, planar fracture zones, see Figure 5-1.

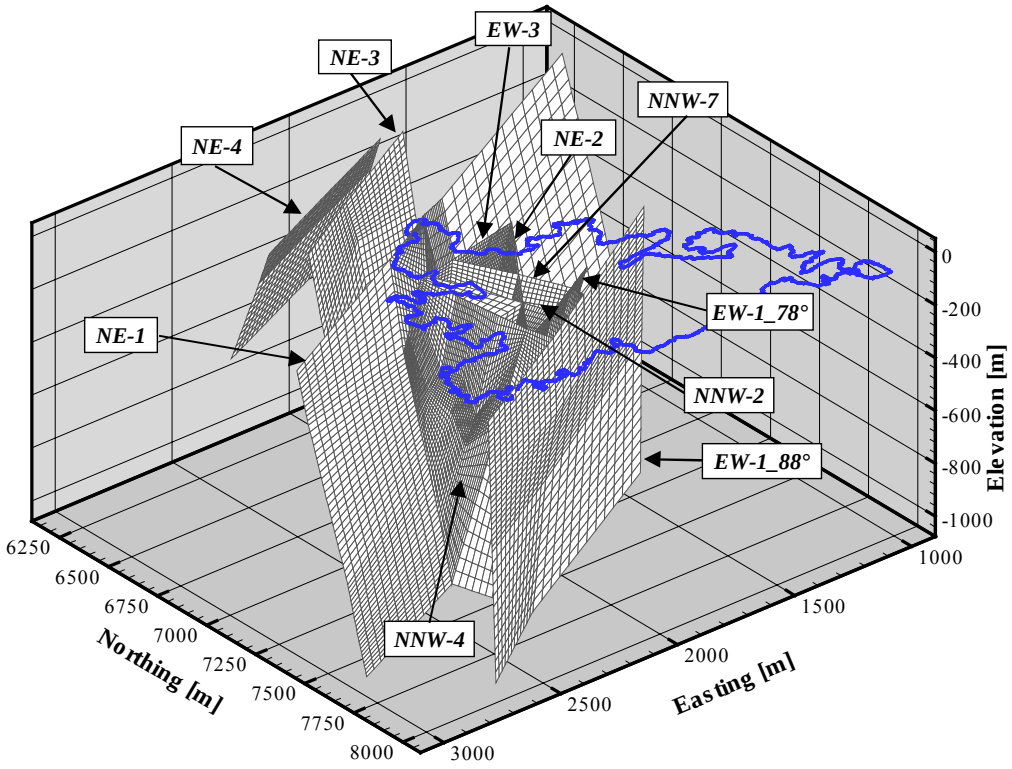

Figure 5-1 *Survey of the modelled structures.*

Co-ordinates or dip and azimuth of the fractures as well as fracture intersections were included in the model as described below and proposed in RHÉN et al. (1997). The extension of the fracture zones in the z-direction were made according to the consideration of the proposed fracture intersections and the position of the tunnel penetration points. The planar quadrangular areas of the fracture zones were extended downwards from the surface with respect to assumed hydraulic connections. The orientations of the fractures and co-ordinates of the corner points are given in Tables 5-1 and 5-2.

The geometry of zone NE-1 was approximated using the average values of x, y and z for NE-1 with a dip of 70°NW and with a dip of 75°NW, as proposed in RHÉN et al. (1997). NE-1 is presented with extensions down to a depth of -1024 masl and a length of 2000 m. In situ, NE-1 is assumed to be approximately 60 m wide and to consist of three branches. In the model a width of 35 m is assumed.

Table 5-1 Orientation of the fracture planes.

	NE-1	NE-2	NE-3	NE-4	EW-3
Dip [°]	72.5	77	74.3	74.7	79
Azimuth [°]	332.7	126	330	153.7	168.3

	EW-1 78°	EW-1 88°	NNW-2	NNW-4	NNW-7
Dip [°]	78.5	88.1	90	85	85
Azimuth [°]	150.7	150.7	66.3	82.8	65.2

The fractures NE-4 and NE-3 were approximated using an average value of the two defined planes NE-4, 71° SE and NE-4, 78° SE and NE-3, 80° NW and NE-3, 70° NW respectively. As mentioned above, the fracture geometries of NE-4 and NE-3 were extended to a depth of about –450 masl according to the position of the tunnel penetration points and the fact, that there are no intersections with other fracture tones.

Fracture zone EW-3 intersects the tunnel with a width of about 13 m. It consists of a 2–3 m wide crushed section in the centre resulting from contact between fine-grained granite and Äspö diorite. The intersections of EW-3 with NE-2 and NNW-4 form the boundaries of the planes, see Figure 5-1. At the base, EW-3 stops at fracture NE-1.

The fracture EW-1 can be divided into two main parallel hydraulic structures (EW-1, 78° and EW-1, 88°), that represent the northern boundary of the modelling area.

Although fracture NNW-4 belongs to a swarm of minor fractures forming a NNW system, this discrete fracture is characterised by a clear indication in the tunnel and a significant water inflow that justifies closer consideration (ITTNER & GUSTAFSSON 1995). All NNW trending structures intersect the fractures NE-2 and EW-1 78° and stop at their vertical boundaries at EW-3 to the south and at EW-1 88° to the north. In contrast to the proposal in RHÉN et al. 1997, NNW-2 and NNW-4 terminate at EW-3, and at the basal boundaries at NE-1.

The fracture zones NNW-2, NNW-4, NNW-7, EW-3 and NE-2 are essentially influenced by NE-1. They represent the central zone of the investigated area and are penetrated by the tunnel several times.

Quadrilateral, two-dimensional finite elements are used to construct the mesh of the fracture zones. After a refining process of 144 macro-elements, the modelled domain of the multi-fracture model includes 13761 nodes and 13536 two-dimensional elements. Every macro-element consists of 144 finite elements. Refinement was carried out in areas of interest e.g. where the tunnel penetrates the fracture zones. The edge lengths of the cells are between 8 and 86 metres. With respect to the corner points of the computational domain, the modelled fractures can be placed in a cube of 2000 x 1800 x 1000 m^3.

Table 5-2 Fracture co-ordinates used in the multi-fracture modelling study (in Äspö co-ordinate system).

Fracture Zone	Northing [m]	Easting [m]	Elevation [masl]
NE-1	6307	1000	0
	7340	3000	0
	6662	1000	-1000
	7695	3000	-1000
NE-2	7050	1838	0
	7614	2248	0
	6965	1921	-510
	7383	2368	-1024
NE-3	6365	1728	0
	6782	2481	0
	6457	1702	-545
	6891	2451	-545
NE-4	1816	6354	0
	2575	6695	0
	1847	6200	-457
	2606	6537	-457
NNW-2	7640	2090	0
	7140	2274	0
	7667	2142	-500
	7171	2272	-299
NNW-4	7147	2307	0
	7718	2220	0
	7097	2339	-288
	7720	2310	-1000
NNW-7	7562	1960	0
	7113	2143	0
	7597	1982	-250
	7097	2339	-288
EW-1 78°	7434	1840	0
	7649	2239	0
	7270	1840	-700
	7495	2240	-700
EW-1 88°	7250	1440	0
	8000	2735	0
	7250	1455	-1000
	8000	2702	-1000
EW-3	7050	1838	0
	7147	2307	0
	6965	1923	-511
	7097	2339	-288

During the construction of the FE-mesh, the calculated corner points, points of intersection with the tunnel, and mutual intersections were taken into consideration. The co-ordinates where the tunnel penetrates the fractures are presented in Table 5-3. All penetration points are included even if they were not clearly found in situ. Fracture zones EW-1 78° and EW-1 88° show no tunnel intersections but are intersected by the NNW trending structures. The tunnel with its shafts as well as the coast of Äspö are represented by one-dimensional elements.

Table 5-3 Co-ordinates of the tunnel intersecting fracture zones (in Äspö co-ordinate system).

Fracture Zone	Northing [m]	Easting [m]	Elevation [masl]	Tunnel Face Position [m]
NE-1	6944.6	2109.2	-179.2	1296.9
NE-2	7233.3	2034.7	-221.6	1599.6
	7413.7	2174.5	-252.3	1860.1
	7204.4	2045.6	-333.5	2491.6
	7452.8	2240.0	-382.1	2875.3
	7284.6	2134.2	-439.6	3329.1
NE-3	6637.5	2149.8	-135.8	986.9
NE-4	6476.3	2145.0	-112.7	821.8
NNW-2	7411.4	2166.4	-251.1	1851.6
	7171.3	2271.8	-298.8	2231.1
	7435.4	2159.5	-370.4	2791.7
	7297.9	2208.5	-428.6	3253.6
NNW-4	7350.7	2304.6	-273.1	2021.4
	7261.9	2317.0	-285.3	2121.6
	7423.6	2305.9	-392.2	2947.4
	7318.1	2321.5	-417.7	3138.3
NNW-7	7338.8	2061.0	-233.2	1711.9
	7139.4	2161.0	-315.0	2346.3
	7280.0	2108.4	-443.4	3355.3
EW-3	7063.5	2093.2	-196.0	1416.8

5.4 Material Properties

The material properties and transport parameters assigned to the fracture zones are presented in Table 5-4 a and 5-4 b. Transport calculations are based on a hydraulic model calculated for non-steady-state conditions with a specific storage coefficient of 0.0001 [1/m] and a varying permeability. The fracture width varies within a range of 0.1 - 35 m, the permeability lies between 8e-07 to 1e-07 m/s for the different macro-elements of the FE-mesh.

Table 5-4 Material properties for the hydraulic conductor domains in the multi-fracture model.

Fracture	Macroelements (me)	Permeability K [m/s]	Fracture width b [m]
NE-1	**me 1 - 20**	8E-7	35
NE-2	**me 1 - 4**	5E-7	10.0
NE-2	**me 5 - 7**	5E-7	0.1
NE-2	**me 8 - 9**	5E-7	1.0
NE-2	**me 10 - 11**	5E-7	10.0
NE-2	**me 12**	5E-7	30.0
NE-3	**me 1 - 4**	1E-7	35.0
NE-4	**me 1 - 4**	5E-7	35.0
NNW-2	**me 1 - 7**	5E-7	10.0
NNW-4	**me 1 - 4**	5E-7	20.0
NNW-4	**me 5 - 7**	5E-7	0.1
NNW-4	**me 8 - 9**	5E-7	1.0
NNW-4	**me 10 - 11**	5E-7	10.0
NNW-4	**me 12**	5E-7	30.0
NNW-7	**me 1 - 8**	5E-7	10.0
EW-1 78°	**me 1 - 9**	5E-7	10.0
EW-1 88°	**me 1 - 9**	5E-7	10.0
EW-3	**me 1 - 3**	5E-7	5.0
EW-3	**me 4**	5E-7	10.0
EW-3	**me 5 - 7**	5E-7	0.1
EW-3	**me 8 - 9**	5E-7	1.0

Table 5-4 (continued) Material properties for the hydraulic conductor domains in the multi-fracture model.

Spec. Storage Coefficient [1/m]	Effective Porosity [%]	Longitudinal Dispersion [m]	Transversal Dispersion [m]	Diffusion [m^2/s]	Tortuosity [-]
0.0001	25.0	25.0	2.5	1e-09	1

5.5 Time Discretization and Spatial Assignment Method

The modelling period for the flow and transport calculations starts with the beginning of tunnel construction, representing natural initial conditions. The starting date is 1st October 1990 (0 days). After more than 310 days, the tunnel crosses the first fracture zone in the model (NE-4), the last fracture is intersected after 1369 days. The modelling period ends after 3765 days. A time discretization of one day was chosen for the transport model resulting in a total of 3765 time steps. For the hydraulic model several flow fields were calculated representing the modelling period between the penetrations of the fractures by the tunnel. This approach depends on the position of the tunnel face during the excavation progress (see Figure 5-2).

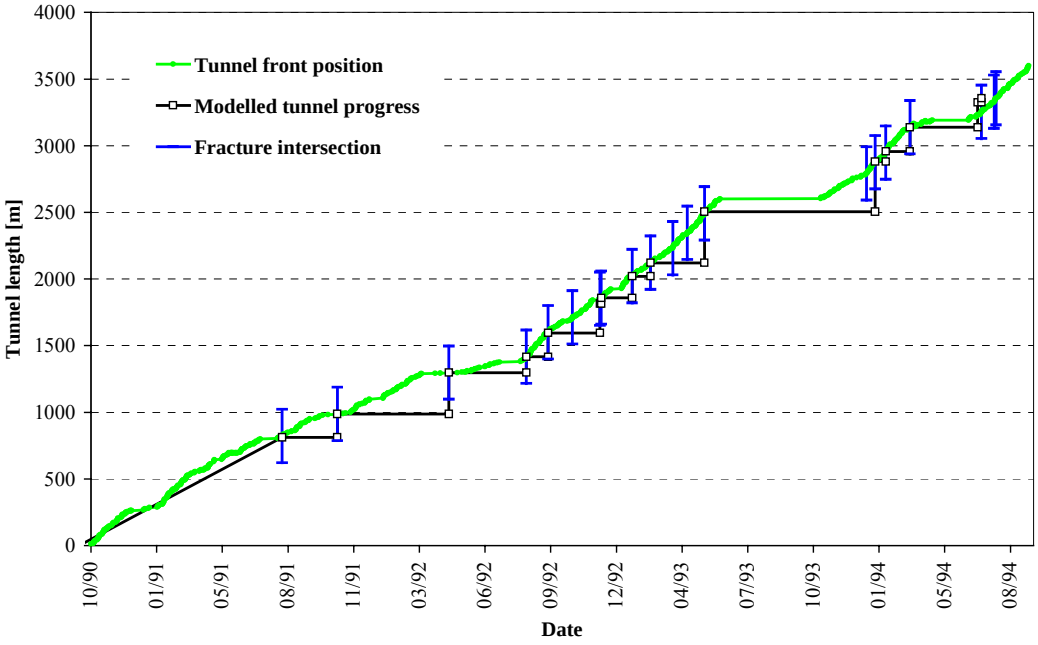

Figure 5-2 *Advance of the tunnel front during the excavation process.*

All hydraulic structures used in this study represent discrete fracture zones whose existence has been reasonable confirmed. They were indicated topographically and/or found in the tunnel and are partly proved by refraction seismic or magnetic data. They were approximated as planes according to the co-ordinates given in RHÉN et al. 1997 and are assumed to crop out at the surface.

The properties of the hydraulic conductors in the multi-fracture model as well as transport and hydraulic parameters are mostly constant values for every fracture as presented in Table 5-4. Apart from this, the fracture width and permeability vary within a fracture where penetrated by the tunnel. The elements around this area are defined with a smaller fracture width or permeability, respectively, to control the inflow to the tunnel.

5.6 Boundary and Initial Conditions

The following description of assigning the boundary and initial conditions to the multi-fracture model refers to all stages of the model development, i.e. the final 10-fracture-model as well as the preceding model containing less fracture zones. This refers to the boundary and initial conditions for flow and and transport calculations, especially the interpolation method for the initial distribution of the four water types used for transport calculations.

Initially, the fractures are assumed to be completely water-filled. The boundary conditions for the vertical, bottom and the upper boundary (Baltic sea) of the flow model are constant pressure heads of zero (Dirichlet conditions) except for the intersection lines of some of the fracture zones. No boundary conditions were assigned to their vertical intersections and basal boundaries with the aim of taking into consideration the mutual hydraulic connections.

Concerning the recharge on Äspö island (upper boundary) the asumption is made that the natural throughflow of meteoric water is relatively small before the tunnel excavation compared to the induced gradients after the beginning of the construction. For this reason the recharge is defined to be negligible for the periods before the tunnel excavation and the beginning of the drawdown and no significant dilution with meteoric water takes place under natural, undisturbed conditions. The recharge rate is assigned to each node of the upper boundary belonging to Äspö island. It is assumed that the amount of fresh water infiltrating the deeper areas grows with the expansion of the drawdown funnel. The initial rate is $7 \cdot 10^{-7}$ m^3/s; after the beginning of the drawdown it increases following a defined time function and reaches a value of $2.4 \cdot 10^{-5}$ m^3/s after tunnel construction.

At the internal boundaries where the tunnel intersects the fractures, an assumed head of zero is temporarily assigned until the tunnel reaches the fracture. After the penetration date, a piezometric head corresponding to the geodetic height is assigned to every penetration point in the fracture and a value for the inflow to the tunnel is calculated (Dirichlet conditions). The three penetration points in fracture NNW-7 are defined with Neumann conditions.

Initial and boundary mixing ratios of the four water types for transport calculations were interpolated according to the grid information available from GURBAN et al. (1998). The grid data from the data delivery for the inital distribution are arranged as ten planar zones. Each of them consists of ten nodes in x-direction with a distance of about 417 m and ten nodes in y-direction with a distance of about 280 m covering an area of about 116760 m^2 with the island of Äspö in the centre. The distance of the planes in z-direction is 168.9 m starting with the first plane at +20 masl and ending with the last plane at –1500 masl. These planar zones show the mixing fractions as they were interpolated with the M3 computer program.

The grid data were transferred to the multi-fracture model by placing the fracture model in the pile of the interpolated data planes and determining the grid nodes of the data set that were nearest to the modelling domain of the fracture grid. The mixing fractions of the selected nodes were extracted from the data set and a depth depending distribution of the four water types was derived as presented in Appendix 1. In this way, the spatial dependency of the ground water distribution was taken into account concerning the horizontal variation (separation of the regions belonging to Äspö island or the Baltic sea, respectively) as well as the vertical variation.

Some of the selected nodes of the given data set showed a deviation of more than 5% (sum of the four proportions = 100%) and thus were not used for fitting the initial conditions (open circles in Appendix 1). Different distributions were assigned to the area below Äspö island and the Baltic Sea. Initial conditions for the transport calculations were assigned to each node in the FE grid.

The chemical concentrations of the model boundaries depend on the initial proportions of the different water types. The upper boundary in the area of the Baltic Sea shows a concentration of 100 % Baltic Sea water, the island of Äspö 100 % meteoric water. The lower and side boundaries represent constant concentrations according to the initial conditions.

6 Chemical modelling

6.1 Introduction

The investigations in the present study concerning the geochemical and hydrochemical characteristics at the site are connected with the excavation of the underground facility. Different approaches were pursued to acquire knowledge about the chemical situation. The approaches are based on the available data sets distributed within the scope of the Task 5 project. The data include measurements of physical parameters, e.g. pH, temperature, electrical conductivity, as well as chemical analyses of water samples including the main species sodium Na^+, potassium K^+, calcium Ca^{2+}, magnesium Mg^{2+}, hydrogen carbonate HCO_3^-, chlorine Cl^-, and sulphate SO_4^{2-}. Isotopic data for ^{18}O, deuterium and partly for tritium are available. Additionally, some measurements of alkali and alkaline-earth elements, silica, bromine, and iron also exist.

The different chemical approaches imply different aspects for studying the chemical conditions, partly using the PHREEQC computer program. These procedures arose from a point of issue that was raised at the beginning of the study. It concerned the basic data necessary for further investigations and raised the question of whether to use the element concentrations derived from the conservative mixing model (based on the M3 data) or to use the originally analysed data from specific boreholes. After a general evaluation of both data sets, clear discrepancies are revealed that lead to variably differing results with respect to the quantitative chemical calculations.

The advantage of using the conservative mixing model (four water types) is an evenly distributed grid of information matching the fracture geometry of the FE model. On the other hand, the analysed data set seemed more trustworthy considering the quantitative element concentration, although it was irregularly distributed in time and space. So as not to ignore potentially important data, and to incorporate both aspects, the compromise was to use the grid data for a more general approach and for implicit conclusions on potential interactions. The original water analyses were used for more precise investigations at a smaller scale, e.g. equilibrium calculations for time series of water samples at boreholes.

6.2 Reaction Modelling Plan

The groundwater composition at the Äspö site is a result of mixing and reaction processes. It is assumed that almost stagnant conditions prevailed prior to the tunnel construction such that groundwater was for the most part in equilibrium with the host rock and over a long time water-rock-interactions influenced the water composition. Since the beginning of tunnel excavation, the increased hydraulic gradients almost certainly have enhanced the influence of the mixing processes.

The DURST/Rockflow software is used to simulate flow (SM2 – flow model) and solute transport (TM2 – transport model) in the modelling of Task 5. The PHREEQC

computer program was applied for the chemical part of the Task 5 exercise. This program includes speciation, batch-reaction, one-dimensional transport, and inverse geochemical calculations (PARKHURST & APPELO 1999). In this way, hydrological and hydrochemical modelling are carried out in two different steps which have to be combined in succession (see Figure 6-1).

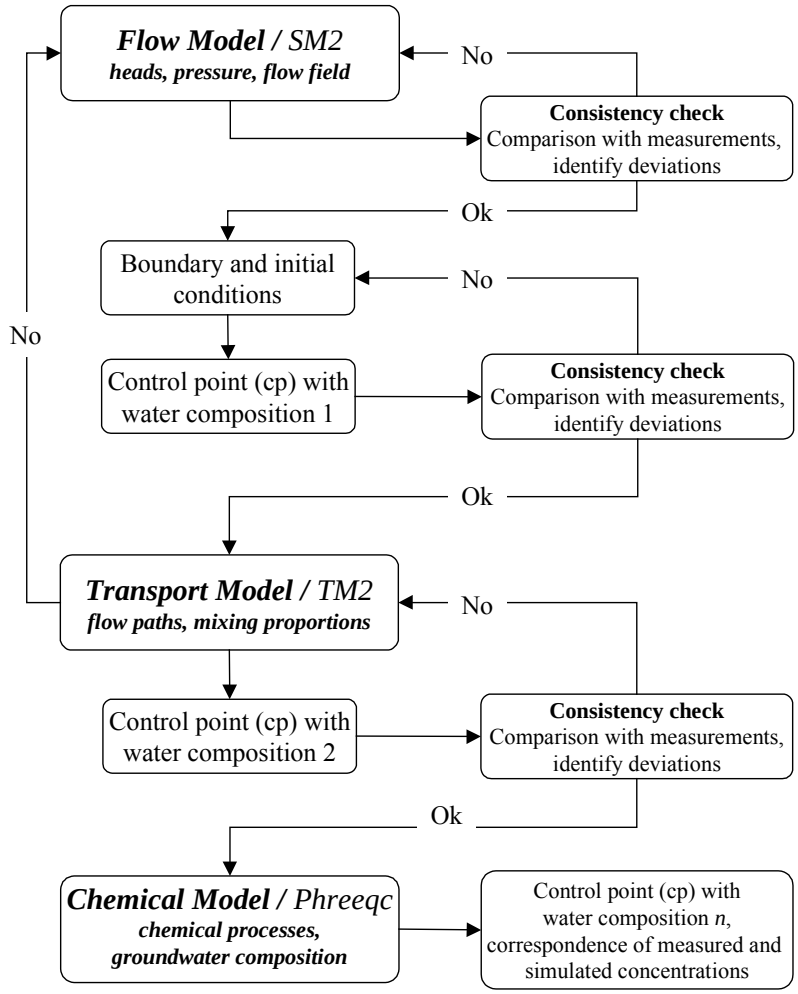

Figure 6-1 *Flow chart of modelling approach.*

The transport model (mixing model) results yielding the simulated water compositions at the control points have to be compared with measurement points. Possible deviations can be identified and explained by applying the chemical methods. Measured groundwater compositions with a time series are used to establish a chemical model which can be used for the simulated compositions at the control points. Hydrogeochemical modelling includes to identify

1.) which processes have the dominant influence on groundwater composition and to what extent, and
2.) which constituents and pure phases participate in the reactions.

In order to be able to characterise the complex hydrochemical system, chemical modelling has to identify and focus on the dominant chemical processes. In this way, it is possible to explain the deviations of mixing modelling in control points and the groundwater compositions of the water samples (measurement points). Different approaches in the chemical modelling can be chosen to achieve a satisfactory match between measured and simulated values.

The difference of mixing modelling results and measured water compositions gives the deviation of the element concentrations that generally shows a decrease of K and Ca and an increase of Na, Mg, HCO_3^- and SO_4^{2-}. This observation corresponds to assumed chemical reactions like redox reactions, ion exchange, silicate alteration etc.

Every water type is characterised by typical chemical reactions that dominate when a special reference water dominates the groundwater composition (>30%). Thus, if we want to indicate which water-rock-interactions are of major importance, we have to look at the dominant water type and its typical processes. This is mostly variable in space. Another important aspect in identifying water-rock interactions is to consider the location of the measurement-points. Different dominating reactions occur e.g. in the saturated and unsaturated zone of groundwater and in the vicinity of the tunnel due to different amounts of oxygen. Especially the spatial classification below Äspö island or the Baltic sea influences the chemical nature of the groundwater.

6.3 Basic Assumptions

The chemical composition of the water samples can largely be explained by mixing processes involving groundwater with different compositions, i.e. the four main water types defined by the M3 - Multivariate Mixing and Mass Balance calculations (LAAKSOHARJU & WALLIN 1997), see Table 6-1. It is assumed, that deviations from analysed non-conservative element concentrations are due to chemical reactions that take place as water-rock interactions, e.g. silicate alteration, solution/dissolution of calcite and gypsum and ion exchange processes.

Table 6-1 Analytical composition of the reference waters (GURBAN et al. 1998).

Constituents [mg/l]	Meteoric	Baltic Sea	Glacial	Brine
Na^+	0.4	1960.0	0.17	8500.0
K^+	0.29	95.0	0.4	45.5
Ca^{2+}	0.24	93.7	0.18	19300.0
Mg^{2+}	0.1	234.0	0.1	2.12
HCO_3^-	12.2	90.0	0.12	14.1
Cl^-	0.23	3760.0	0.5	47200.0
SO_4^{2-}	1.4	325.0	0.5	906.0
$\delta\,^2H$	-80.0	-53.3	-158.0	-44.9
$\delta\,^3H$	100.0	42.0	0.0	4.2
$\delta\,^{18}O$	-10.5	-5.9	-21.0	-8.9

Possible chemical reactions have a different influence on the groundwater composition. This is a criterion to distinguish between important and less important interactions, see below. For example, the potassium content in general is very low, so that processes producing or consuming K have less influence on the total chemical content and are of minor importance. However, the major constituents are consistent with the known mineralogy at the Äspö site whereas chloride acts as a conservative tracer and does not take part in any of the assumed reactions.

- Most important ions in Äspö groundwater:
  Na^+ Cl^-
  Ca^{2+} HCO_3^-
  Mg^{2+} SO_4^{2-}

- Reactions to be taken into account, e.g.:
  - dissolution / precipitation of carbonate: $CaCO_3 \Leftrightarrow Ca^{2+} + CO_3^{2-}$
  - dissolution / precipitation of gypsum: $CaSO_4 \Leftrightarrow Ca^{2+} + SO_4^{2-}$
  - dissolution / precipitation of $Mn(OH)_2$: $Mn(OH)_2 \Leftrightarrow Mn^{2+} + 2OH^-$
  - carbonate chemistry: $H_2CO_3 \Leftrightarrow H^+ + HCO_3^-$
    $HCO_3^- \Leftrightarrow H^+ + CO_3^{2-}$
  - sulphate chemistry: $H_2SO_4 \Leftrightarrow 2H^+ + SO_4^{2-}$

- Reactions, which may be ignored:
  - dissolution / precipitation of salt: $NaCl \Leftrightarrow Na^+ + Cl^-$
    (subsaturated in simulated area)
  - dissolution / precipitation of (iron-)sulphides
    (low concentrations of iron and sulphide)
  - dissolution / precipitation of flourides
    (low concentrations of flouride)
  - dissolution / precipitation of Ba-salts
    (barium not measured)

The mixing ratios of the water samples based on calculations with the M3 approach show significant differences compared to the measured concentrations of conservative elements in the water samples. This requires special caution when working with the data. For a couple of water samples, the chloride concentration shows a deviation of more than 50%. As the initial conditions for transport calculations mainly depend on the M3 data set possible errors must be expected when comparing with real measured concentrations at control points (see chapter 6.1). Additionally, initial deviations must be assumed to increase during the modelling period.

To identify dominating water types without considering absolute ion concentrations, a large number of water samples from the pre-investigation and the construction phase are presented in the Piper plot, see Figure 6-2. The water samples are taken from cored boreholes on Äspö (KAS) and percussion drilled exploration holes in the main tunnel (SA) during the period from 03/1988 to 05/1996 (data base: SKB 1998).

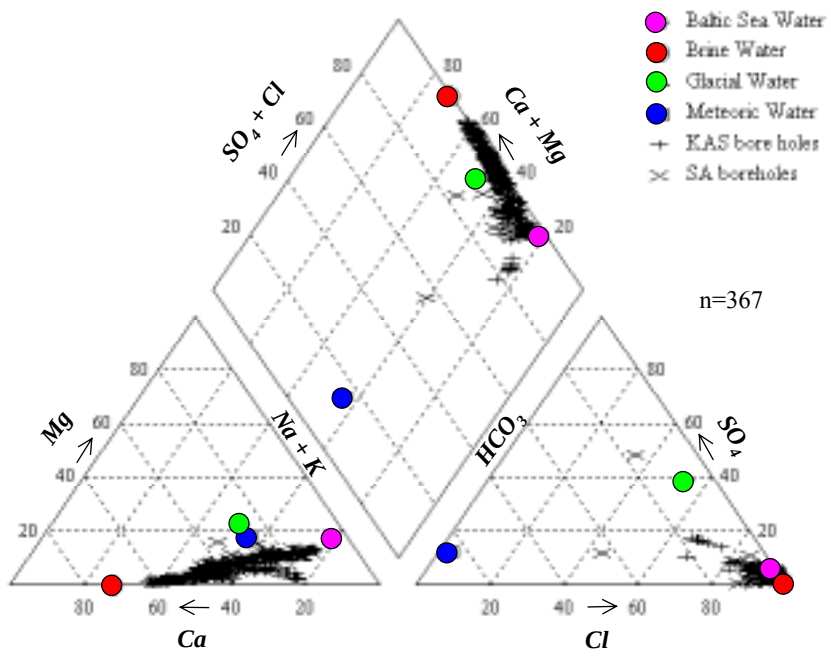

Figure 6-2 *Piper plot showing the distribution of the major anions and cations in Äspö groundwater [mol(eq)%].*

The Piper plot shows a clear clustering indicating sodium and calcium as the dominant cation and chloride as the dominant anion (Na-Ca-Cl or Ca-Na-Cl water type). Only 7% of the water samples have a pure Na-Cl-character, a few belong to Na-Ca-SO_4 and Na-Cl-HCO_3 water types. The total dissolved solids (TDS) of the 367 water samples are between 0.1 - 21.2 g/l and the total ion concentration is 4.2 – 740.9 mmoleq/l. Considering the locations of the four reference waters in the Piper plot, it is obvious that the ion distribution is mainly influenced by Baltic Sea and brine**.** This is due to the fact that both water types are mainly responsible for the higher salinity of a water sample. Nevertheless, the left triangle indicates a difference from the mixing patterns concerning the cations. It shows a change towards a higher sodium content which may result from cation exchange processes.

Additionally, the connection of groundwater flow and electrical conductivity or salinity respectively was investigated (Figure 6-3). The flow rate was measured at the weirs in the tunnel in December 1996 (RHÉN et al. 1998). The electrical conductivity is presented for different dates, but the values are comparable. Although the minimum and maximum conductivities do not coincide the general trend is reflected.

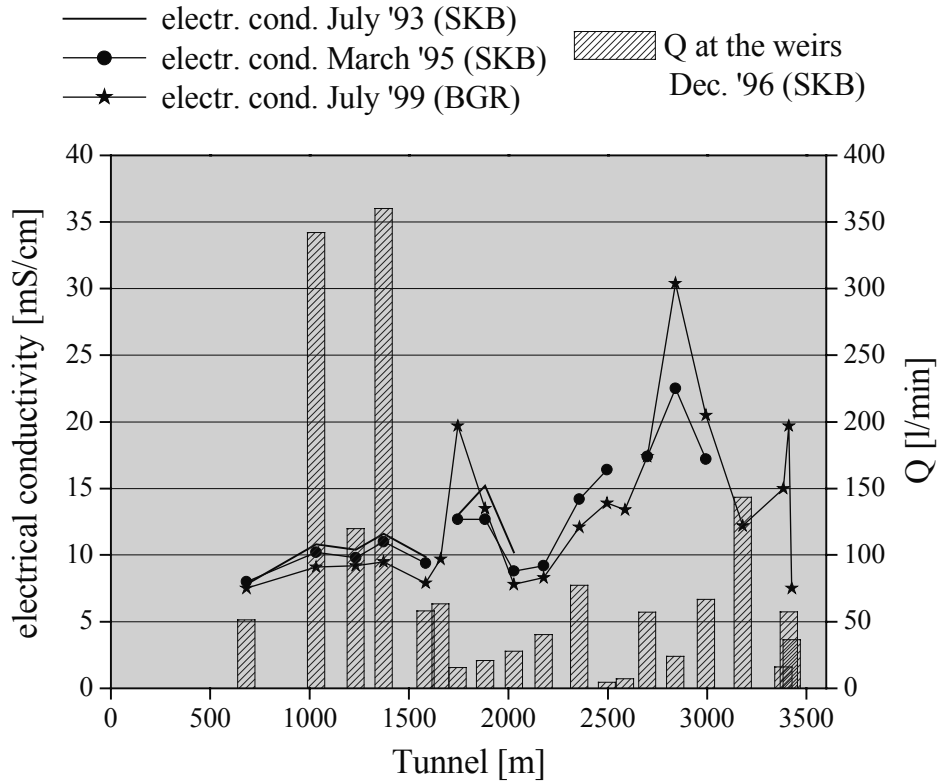

Figure 6-3 *Flow rates and electrical conductivity at the weirs.*

Figure 6-3 shows that minor flow rates are associated with a high content of total mineralisation. One can conclude that salinity not only depends on the vertical depth but also on the residence time, and consequently on the reaction time, that influences the amount of solutes. Nevertheless, the groundwater type remains the same as shown in the Piper plot regardless of the residence time on the pathway. This indicates good connections between the flow paths in the rock mass and almost evenly distributed chemical conditions that are responsible for the main chemical character.

The two main peaks in the electrical conductivity lines that were measured at the weirs MA1745G and MA2840G are assumed to belong to one water conducting fracture or to a conductive zone which may extend up to a few metres in width. Looking at the geometry of the spiral tunnel, these two peaks occur one on top of the other in the NNW part of the facility. One can conclude that the tunnel crossed a water conducting structure twice which typically has a higher salinity because it may transport water from deeper areas below the tunnel to the upper parts.

This assumption would also explain the time-dependent development of the salinity distribution in the tunnel. Comparing the different conductivity measurements in Figure 6-3, it is clear that the amplitudes of the curves tend to more extreme minimum and maximum values. This can be caused by the outflow into the tunnel. The drawdown is associated with an infiltration of fresh water from the surface which leads to a dilution along the fractures near the surface. On the other hand, the contours below the water extraction in the tunnel are directed upwards and thus lead to an increased salinity in the deeper fracture zones which can be measured in weirs MA1745G and MA2840G.

7 Calibration Criteria and Processes

Non-steady-state flow and pressure conditions were calculated – with and without the tunnel – using head measurements to calibrate the model with respect to permeability. The permeability of the fractures was adjusted on the basis of the measured inflow to the tunnel at the intersections of the tunnel with the fractures. The permeability values and fracture widths were varied until flux values were obtained that correspond to the measured values at the weirs downstream from the intersections. The flow rates are from December 1995; see Figure 7-1.

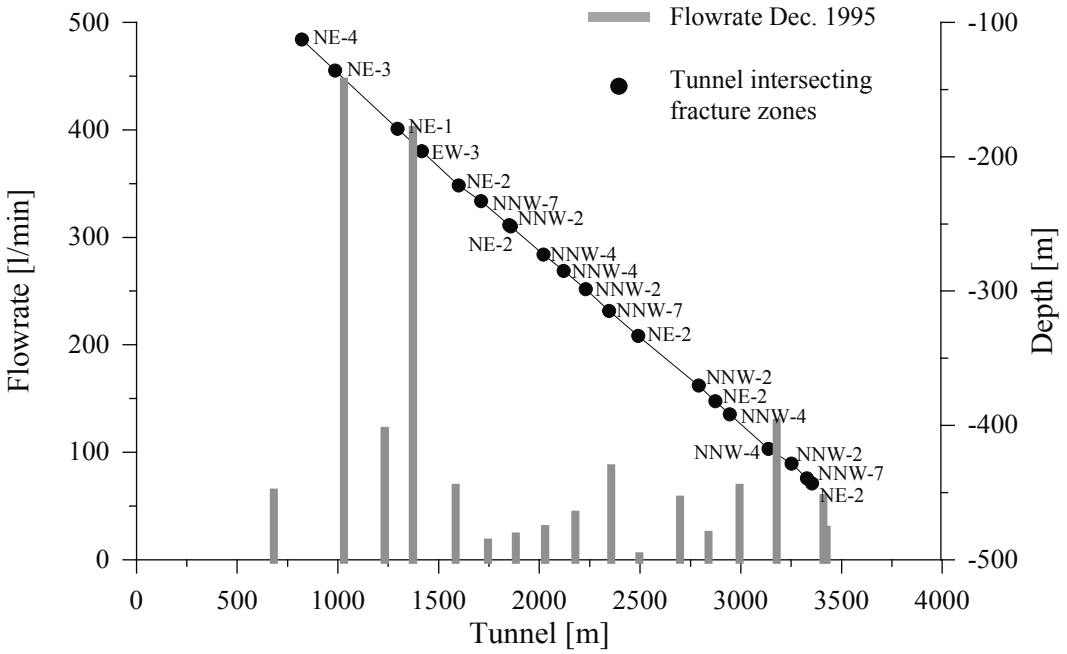

Figure 7-1 *Flow rates at the tunnel weirs in December 1995.*

The storage coefficient was varied until the simulated drawdown values matched the measured ones, see Figures 7-2 and 7-3. The drawdown in the boreholes was compared to model simulations as a function of the specific storage coefficient so that the order of magnitude of the storage capacity could be assessed.

In general, for the numerical calculations, no priority was given to any of the required parameters. Parameter values, e.g., transmissivity, geometry of fractures and storage capacity, were varied iteratively and the calculated drawdown and flow into the tunnel compared with the measured values. The main criterion for calibrating the numerical model is an acceptable agreement between measured and simulated heads or groundwater distributions.

Transport calculations for different types of groundwater were carried out repeatedly to calibrate transport properties using the measured proportions of water types at the control points in the M3 mixing model (LAAKSOHARJU & WALLIN 1997).

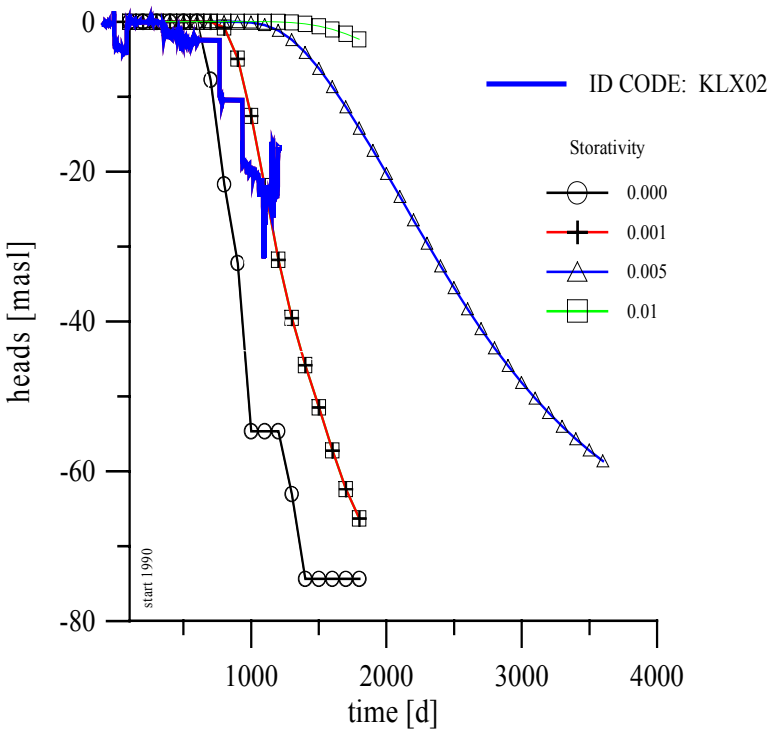

Figure 7-2 *Drawdown versus specific storativity and time at borehole KLX02.*

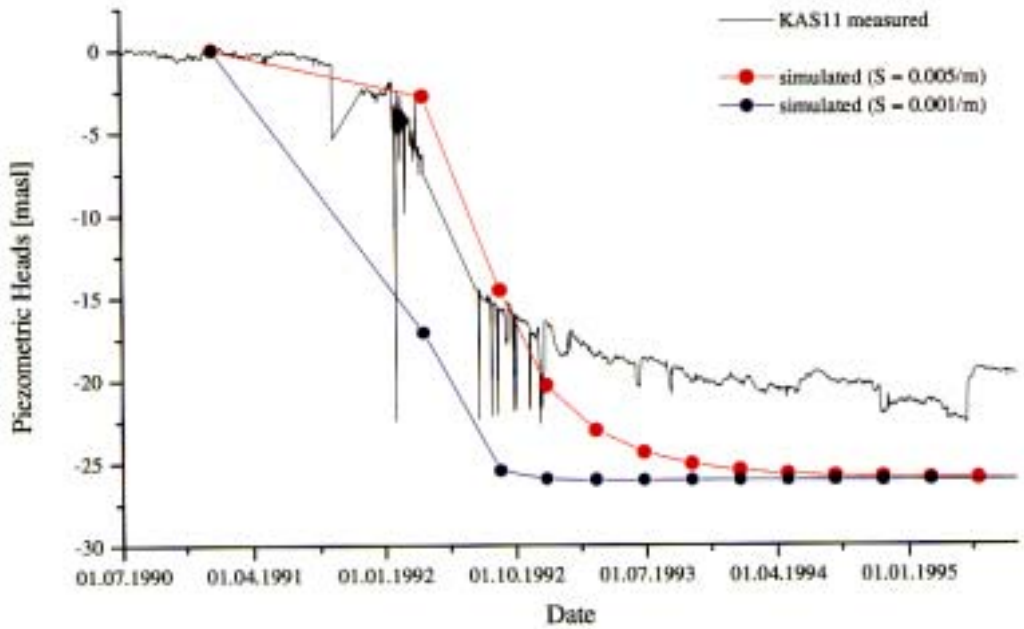

Figure 7-3 *Drawdown versus specific storativity and time at borehole KAS11 in conductive structure NE-2.*

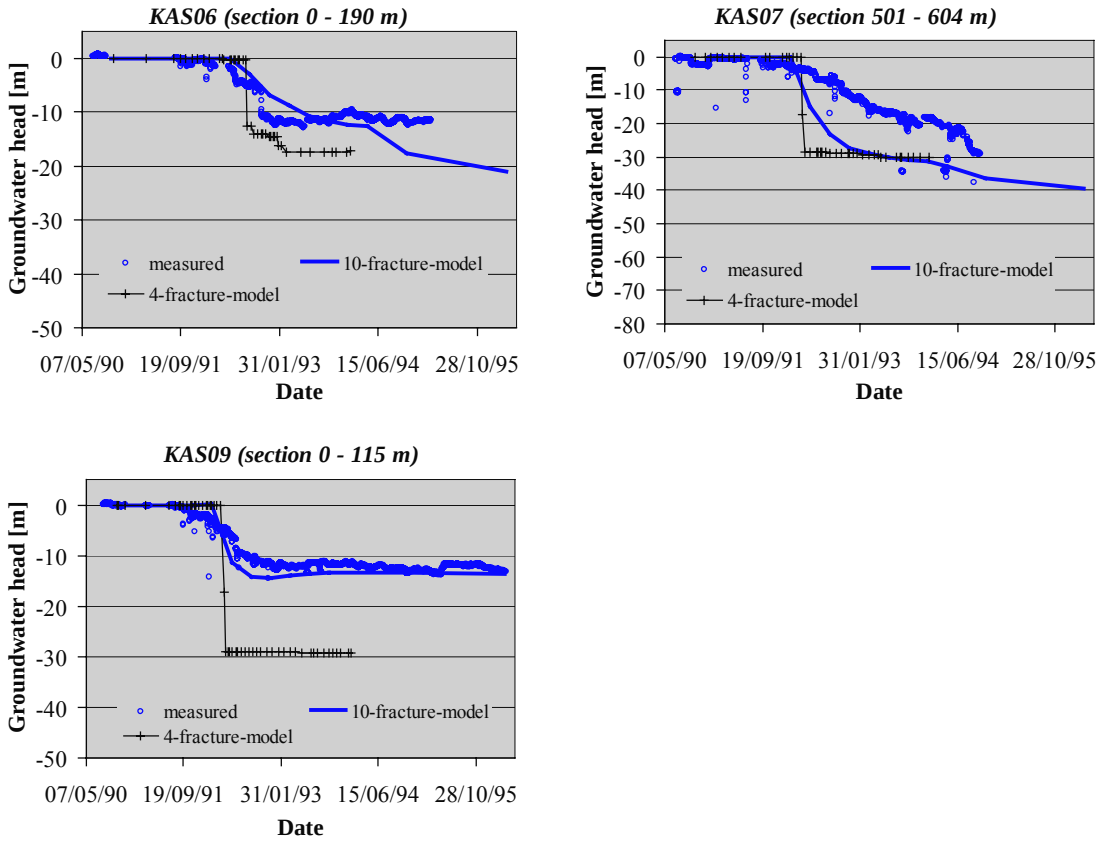

Fig. 7-4 *Comparison of simulated groundwater heads of the 4- and 10-fracture models with the measured values at boreholes KAS06, KAS07, and KAS09.*

Figure 7-4 shows the improvement of the fit of the modelled groundwater heads to the measured ones using the extended 10-fracture model instead of the 4-fracture model. Although the main parameters of the flow model were retained, consideration of additional fracture zones and their intersections with each other and with the tunnel improved the simulation of the regional flow field, especially the reduction and slowdown of the drawdown. Whereas the boundaries of the 4-fracture model, which included only the fracture zones NE-1, EW-3, NE-2, and NNW-4, were inside the drawdown funnel, the 10-fracture model covers a considerable part of the area that is less influenced by the tunnel excavation. By expanding the model, the effect of the change of the conditions at the model boundaries resulting from the tunnel construction was reduced.

The extended transport model contains additional control points for calibration. However, as the interpolation method for assigning the initial distribution of the four water types to the fracture grid was retained, the calculated changes in the proportions of the mixing fractions as a function of time were improved less than in the flow model. Part of the discrepancies between the modelled and measured mixing fractions is due to inadequate initial conditions. Although the transport model gives very satisfactory results and describes the tendency of the measured mixing fractions well (see section 8.3.2), inappropriate initial conditions cannot be compensated for.

The transformation of the measured water composition into four conservative water types with the M3 approach represents a good basis for characterising the Äspö site with numerical models. This method, however, implies a loss of information. This loss is intensified by the construction of an interpolated data grid as described in chapter Section 5.6 and the transferring of these data by interpolation to the fracture model in this study. The regional flow field is modeled at the expense of very local features and good agreement at the control points. This is assumed to be the main reason for the discrepancies between measured and modelled values.

8 Main Results

8.1 Introduction

The rsults of the numerical flow model include the groundwater pressure in the fractures (at every node of the FE mesh) and the inflow to the tunnel. Different stages during tunnel construction were considered so that main flow directions can be derived from the contours or from flow paths.

The transport calculations give the distribution of the four types of groundwater at different control points which is supported by borehole data. In this way, measured values can be compared with the simulated results of the mixing proportions. Mass balances were checked for specific stages of the excavation work.

Deviations of the mixing model compared to measured concentrations were used to apply some chemical approaches. Water conditions concerning the saturation indices of several minerals as well as possible water-rock-interactions were considered to compensate for these deviations. This was done applying the PHREEQC computer program– Version 2 (PARKHURST 1999). Apart from the chemical modelling approaches some general aspects were discussed that look at the chemical environment at the site, e.g. the salinity distribution.

8.2 Natural Conditions

The initial conditions before tunnel excavation are characterised by an undisturbed dynamic system valid for completely water filled fractures. The piezometric heads amount to zero, except in the recharge areas of the islands where positive values are present corresponding to an assumed freshwater lens following the topography. Due to this, the very small hydraulic gradients have very little influence on the distribution of groundwaters of different origin. Furthermore, the chemical environment is assumed to be in balance and to be mainly controlled by long-term water-rock interactions.

8.3 Completed Tunnel

8.3.1 Flow Model

The numerical model shows that since the beginning of the HRL excavation a distinct change can be observed in the groundwater system. A drawdown in the modelled area, that has also been measured as a decrease of the hydraulic pressure in the boreholes, corresponds to the leakage rate into the tunnel (MÉSZÁROS 1996). The intersections of the tunnel with the fractures cause an increase in the hydraulic gradients in the vicinity of the tunnel. The disturbed area around the extraction points extends with time as the tunnel progresses and the total inflow to the tunnel increases. The observed drawdown goes down to a maximum depth of 80 to 90 m below sea level in the central area of the HRL. The results of the simulated drawdown in several boreholes were compared with measurements (Figure 8-1). Ths includes the surface drilled boreholes KAS04, KAS06, KAS07, KAS08, KAS09, and KAS14.

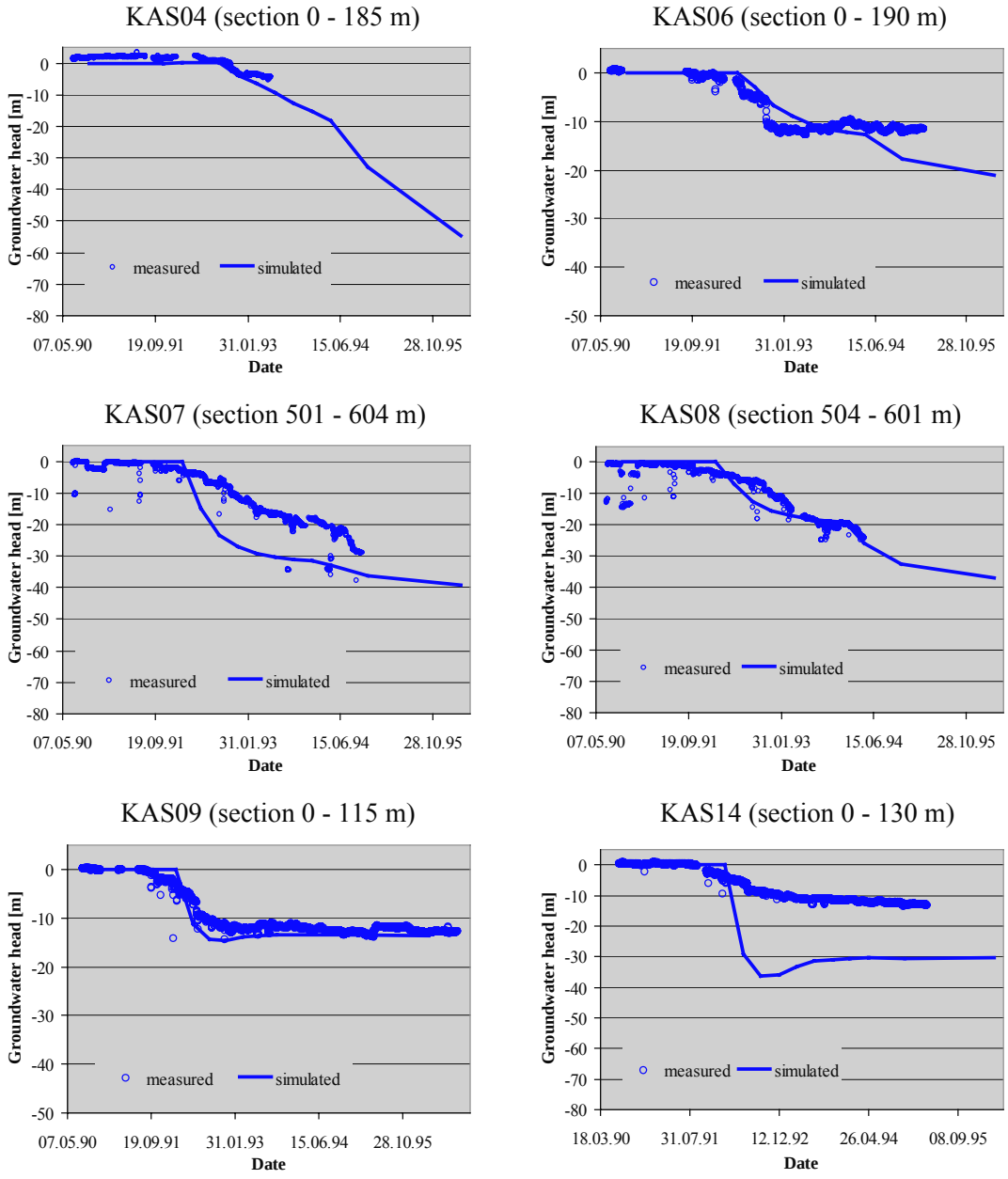

Figure 8-1 *Measured and simulated groundwater heads at selected control points.*

The modelled results at the control points show a good fit compared to the measurements. Nevertheless, the general trend of the computed heads indicates a drawdown that is too deep. This is partly due to the inner boundary conditions where the tunnel penetrates the fractures (Dirichlet conditions). In this area, the hydraulic gradient is very high and a control point that is very near to the inflow in the model is strongly influenced by the pressure heads assigned to the extraction node.
Figure 8-2 shows the comparison of calculated flow rates in the tunnel and measured values that were also used for calibration. Although the single flow rate of every weir deviates more or less from the modelled inflow, the total amount corresponds to the measurements.

Table 8-1 shows the calculated flow rates at the tunnel penetration points using a specific storativity coefficient of 0.0001/m. They were calibrated using the measured flow rates at the weirs in the tunnel.

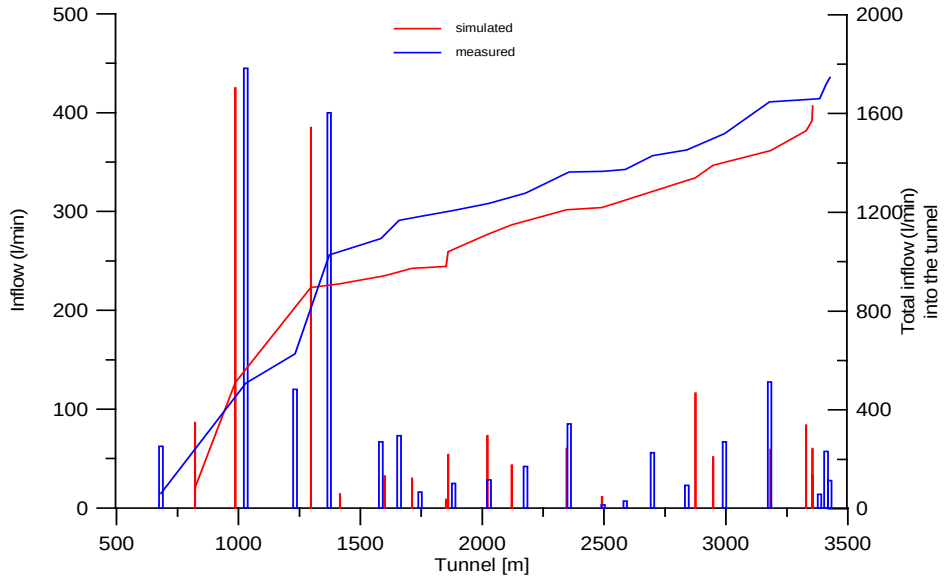

Figure 8-2 *Simulated and measured inflow to the tunnel and flow rates at the weirs.*

Table 8-1 Calculated flow rates at the tunnel intersection points.

Fracture	Q_1 [l/min]	Q_2 [l/min]	Q_3 [l/min]	Q_4 [l/min]	Q_5 [l/min]
NE-4	86.4	-	-	-	-
NE-3	426.0	-	-	-	-
NE-1	385.2	-	-	-	-
EW-3	13.8	-	-	-	-
NE-2	32.4	53.9	11.2	11.6	83.4
NNW-7	30.0	60.0	60.0	-	-
NNW-2	107.4	-	-	34.2	-
NNW-4	73.0	43.2	51.7	58.8	-

The modelled drawdown in the fracture network is presented for the time steps of 1000 days (TFP at 2600 m in June 1993) and 2000 days (after tunnel construction in March 1996), see Figure 8-3. The pictures show the groundwater heads interpolated for a surface plane around the island of Äspö. In this way, a clear increase in the drawdown cone can be observed that reaches a maximum depth of –100 masl in the central area above the tunnel after construction. The extension of the sphere of influence tends to the northwestern part of the island and reflects the orientation of the water conducting structures. Although e.g. the fractures EW-1 were not crossed by the spiral tunnel, they are also affected by the drawdown as they have a good connection with the NNW-oriented fractures. The NNW-fractures serve as pathways for the groundwater flowing from the north to the extraction points.

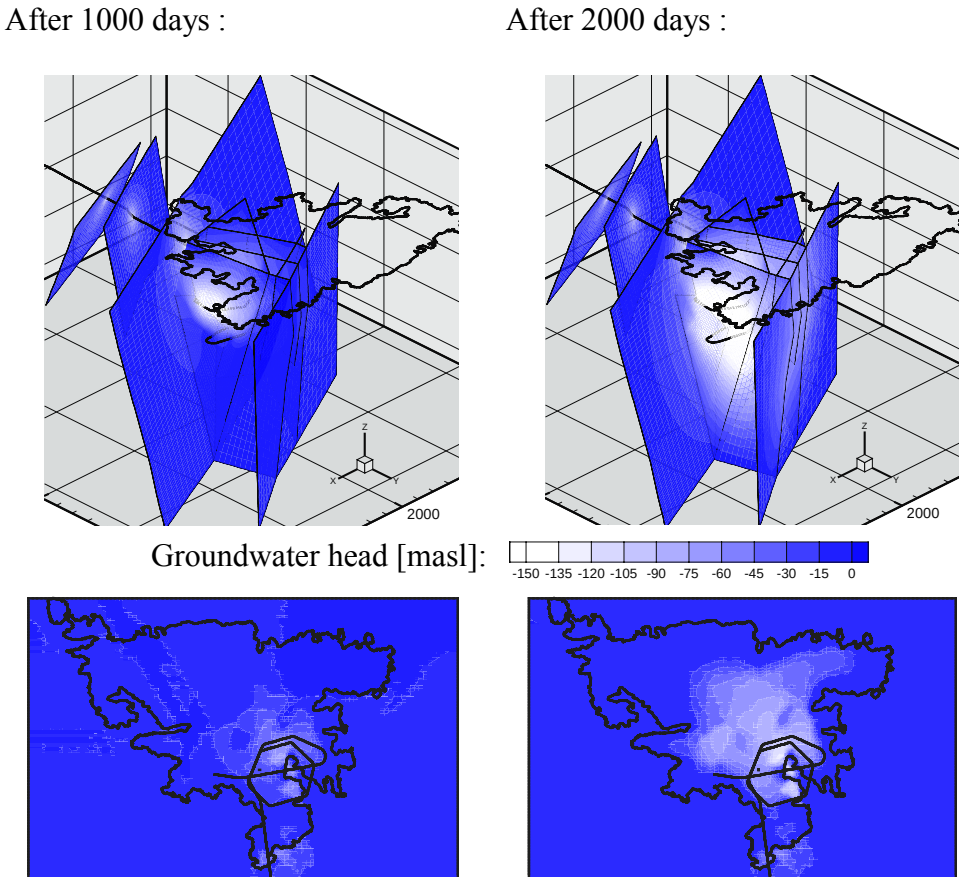

Figure 8-3 *Groundwater heads in the fractures and for an interpolated surface plane at z = 0 for t = 1000 and 2000 days.*

8.3.2 Transport Model

The initial distribution of the different types of groundwater is disturbed by tunnel excavation. The intersection of the tunnel with the first fracture zones causes a significant change in the initial balance. As a result of the disturbance, an increased inflow of mainly meteoric and Baltic Sea water can be observed, which reflects the orientation of the flow lines. They extend downwards to the points in the tunnel where water is constantly extracted. Simultaneously, a rise in the contours below the intersections of the tunnel with the fractures is apparent, even if it is only of secondary importance. However, this leads to an increase in the proportion of glacial water and brine above the tunnel. Nevertheless, the proportion of glacial water in general decreases with time. This effect can be explained by a glacial water lens which is slowly bleeding out and cannot be refilled because it is relict water.

In Figure 8-4, the positions of the control points that were also selected for calibrating the transport model are shown in relation to the Äspö HRL and the island of Äspö.

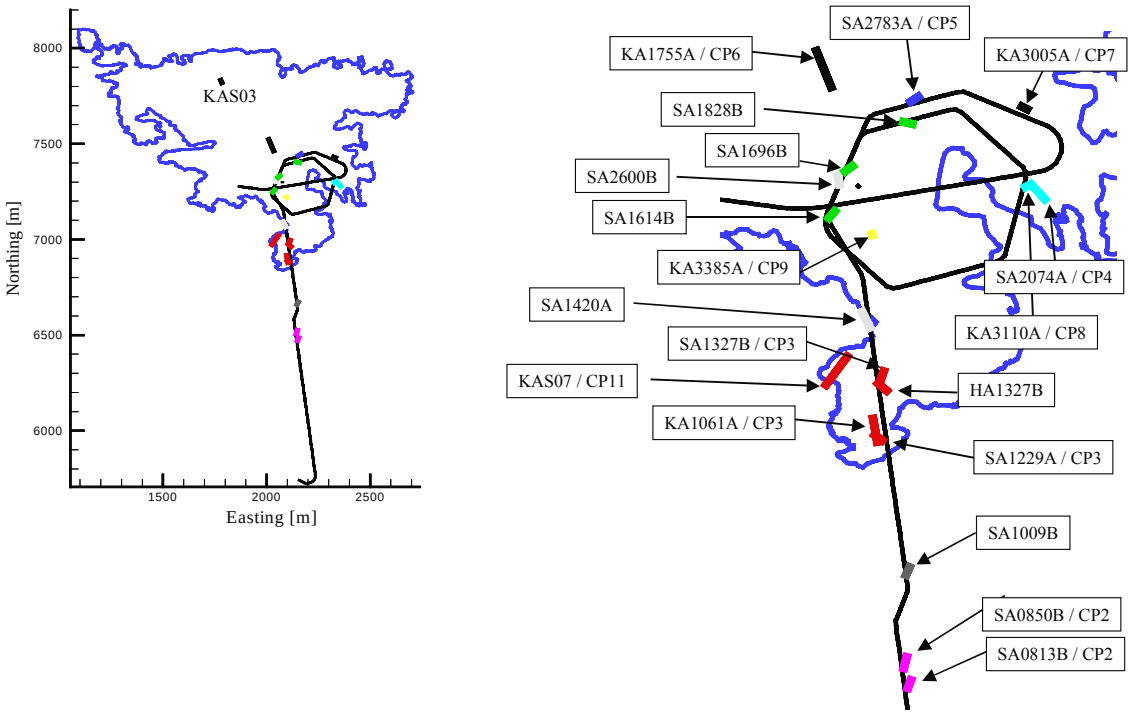

Figure 8-4 *Location of the control points at the HRL.*

Appendix 2 shows the results of the transport calculations: the water proportions for different stages of tunnel construction (TFP = Tunnel face position) and the comparison of measured and simulated values for the selected control points. As the central part of the spiral tunnel is hidden behind the fracture zones, additionally the water distribution in some interpolated zones is presented for a better visualisation. The interpolation was done by using the inverse distance method.

The measured values compared to the outcome of the transport model at the control points refer to the modelled mixing ratios resulting from the M3 approach (LAAKSOHARJU & WALLIN 1997). The different types of groundwater (brine, glacial, meteoric and Baltic Sea water) were considered separately and treated as conservative tracers. The conservative species Cl and ^{18}O at the control points were calculated according to the proportion of every water type and its chemical composition (see Table 6-1).

In order to check the modelled water distribution, the mass balance was calculated for different time steps. The sum of the four water types at every node should be 100 %. The deviation generally amounts to ± 2 % which lies at an acceptable level.

The distribution of the groundwater types in the fractures comprises the time period from the beginning till the end of the tunnel construction. As the disturbance of the flow field increases with the continuation of the excavation, the most significant changes in the water distribution can be observed after one or two years. After this time, the tunnel

crossed several water conducting fractures and caused the most distinctive mixing processes in the central part of the spiral tunnel. This can be observed by looking at the interpolated horizontal planes at a depth of –300 m. For the most part, the sphere of influence does not extend to the model boundaries, neither concerning the drawdown nor the mixing of the water types.

The effect of the induced mixing processes can easily be observed by looking at specific control points. The boreholes are each located in typical environments with respect to water composition. For this, a time dependent influence of the natural conditions is more significant than for a whole area, e.g. a fracture zone.

In general, the computed water ratios reflect the order of magnitude of the M3 values. Several control points show a very good fit according to the measurements, e.g. SA1229A, HA1327B, KAS07, KA3385A. Others, such as KA3005A and KA3110A, correspond very well to two of the four water types, whereas the distribution does not match the other two types. This effect can also be observed at control point SA1009A and is largely due to inappropriate initial conditions. Nevertheless, the trend could be reproduced. In a similar way, a significant anomalous initial condition for meteoric water was found at borehole SA1696B. The initial conditions differ by about 30%, which corresponds with the deviation in the chloride concentration. The initial conditions are inconsistent with a proportion of meteoric water exceeding 60% at a depth of -230 masl.

Considering the conservative species chloride, it is obvious that a small deviation in the brine proportion leads to a significant difference in the chloride content compared to the measured values. This effect is clearly shown at control point SA2783A even though the water types show a very good agreement. The same effect considering ^{18}O is caused by an anomalous proportion of glacial water in borehole SA2074A. This fact raises the question of the degree of agreement between the conservative mixing approach with different water types and the content of a measured conservative species in the analysis. Furthermore, the acceptable discrepancy of 10% between the mixing proportions and the analysed elements is exceeded, possibly due to the grid interpolation. An improvement in the simulated data could be achieved by directly modelling the transport of chloride and ^{18}O on the basis of the measured concentrations at the boreholes. Nevertheless, this approach demands a close grid of measured data for the modelling domain to adjust the initial and boundary conditions.

8.3.3 Calculation of Flow Velocity as a Function of Tracer Concentration

In addition to the method described above (particle tracing) to determine the transport velocities of substances dissolved in water, a second method was used that is based on the calculation of the flow field and a finite-element tracer calculation. Seven fractures, some of them connected, were included in the model. All but one (EW-1) is crossed by the spiral tunnel. Fracture EW-1 is connected to EW-3, NE-1 and NE-2 via NNW-4. NE-3 and NE-4 are not connected to the fracture system owing to their dip, strike and limited extent; see Figure 8-5. The geometrical, hydraulic, and transport parameters are given in chapter 5.

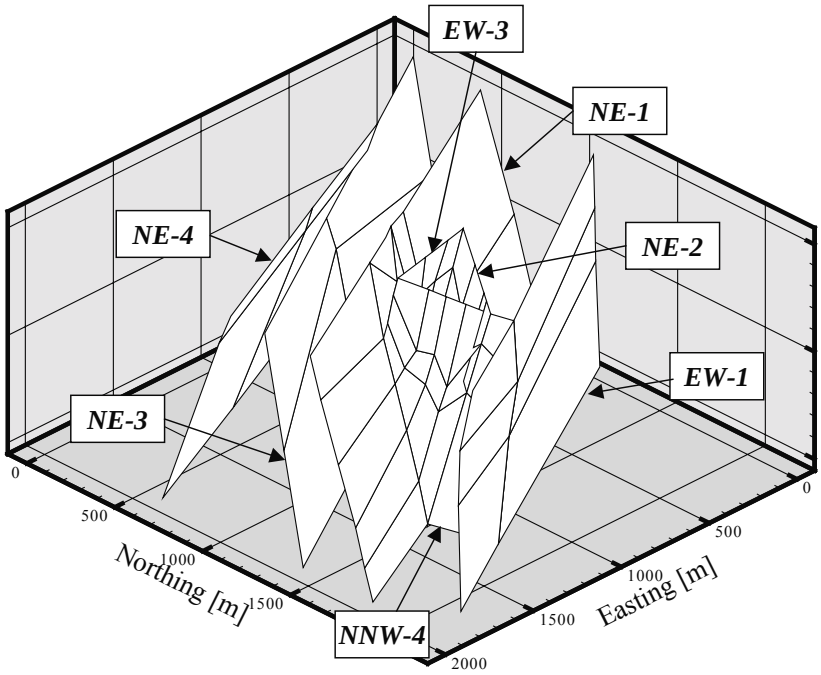

Figure 8-5 *Structural model including fracture zones NE-1, NE-2, NE-3, NE-4, EW-1, EW-3, and NNW-4.*

The flow field was calculated for a period of 10,000 days after construction of the tunnel (Appendix 3.1 to 3.5). The level of the Baltic Sea and infiltration of meteoric water were boundary conditions. The flow velocity is determined mainly by the permeability, the locally variable fracture aperture, and the storage coefficient. The parameter values were obtained by iteration, taking into consideration the amount of water entering the tunnel and the proportions of meteoric, Baltic Sea, glacial water and brine. The initial values for the hydraulic parameters were those determined in the TRUE project (LIEDTKE & SHAO 1997) ($K=1 \cdot 10^{-4}$ ... $6 \cdot 10^{-4}$ m/s) and the projects in the Grimsel Rock Laboratory (LIEDTKE et al. 1999), which yielded velocities that were too large. Comparison of the concentrations of the four types of water, and comparison with the in situ measurements, yielded plausible results that are two orders of magnitude lower than the initial values.

The transport model has the following boundary conditions:

1. non-stationary flow field ($S_o = 0.001$ (1/m))
2. infiltration of meteoric water as a function of fracture aperture and drawdown in the fractures
3. completed tunnel construction
4. permeability $K = 8 \cdot 10^{-7}$ .... $1 \cdot 10^{-7}$ m/s (Tab. 5.4)
5. variable width of the fracture or fracture system of 0.1 – 100 m
6. dispersion coefficients of $\alpha_L = 2.5$ m and $\alpha_T = 2.5$ m
7. diffusion $d_o = 10^{-9}$ m^2/s
8. constant concentration of the conservative tracer at 7 injection points

9. seven injection points at ground level
10. two injection points above the tunnel in fractures NE-3 and NE-4
11. two injection points 150 and 200 m from the tunnel walls in fracture NE-1
12. one injection point on each of the intersection lines between fractures EW-3 and NE-2, EW-3 and NNW-4, and EW-1 and NNW-4
13. one injection point at 1000 m depth at the point of intersection of fractures NNW-4, NE-2, and NE-1
14. a period of 11,000 days
15. Δt = 1 day for the first 1000 days
16. Δt = 10 days from day 1000 to day 11,000

The flow velocities were calculated from the distance of the injection points (Appendix 3.1) from the tunnel and the length of time for the first arrival of tracer, and the arrival of a 5 %, 10 %, and 50 % concentration of the tracer (Appendix 3.6). The results for fractures NE-3 and NE-4 are not reliable owing to the lack of connections in the model. The simulations predict that the tracer will reach the tunnel within the 30 year modelled period with a very low concentration.

The flow velocities lie between 0.1 (50% concentration arrival time) and 7.1 m/day (first arrival time). A concentration of 50 % is reached after 30 years only in fracture NE-2. The tracer concentration is plotted in Appendix 3 as a function of mean flow velocity. The travel times of dissolved substances in the fracture system can be predicted using the calculated velocities and the distance from the tunnel (Appendix 3.6).

These calculations neither take into account the hydraulic roughness of the fracture, nor the density differences of the fluids, nor the temperature changes in the Earth's mantle. Therefore, a longer travel time of the particles or of the water-bearing materials can be foreseen.

8.3.4 Chemical Model

The chemical model pursued in this study yielded a qualitative picture of the hydrochemical conditions at the Äspö site which is composed of different aspects and approaches. It was aimed at improving the understanding of the regional groundwater flow and transport modelling by consideration of chemical aspects and the knowledge of changing element concentrations being due to chemical processes.To make good use of the available chemical data set, different approaches and calculations were carried out, for a part by applying the PHREEQC program (PARKHURST & APPELO 1999). The different approaches represent different steps in characterising the chemical environment and in identifying chemical reactions, i.e. some deal with general aspects and others refer to details (see chapter 6.1). The following describes the different approaches, their aims and outcomes.

Ideal mixing line

Measured element concentrations at boreholes are compared with concentrations resulting from the mixing model with the aim of highlighting deviations from the ideal mixing line. The plotted data points are located on the ideal mixing line if conservative mixing processes only are responsible for the observed water composition. In this way sources or sinks for specific constituents are identified and it is possible to qualitatively draw conclusions concerning the chemical processes (Figure 8-6).

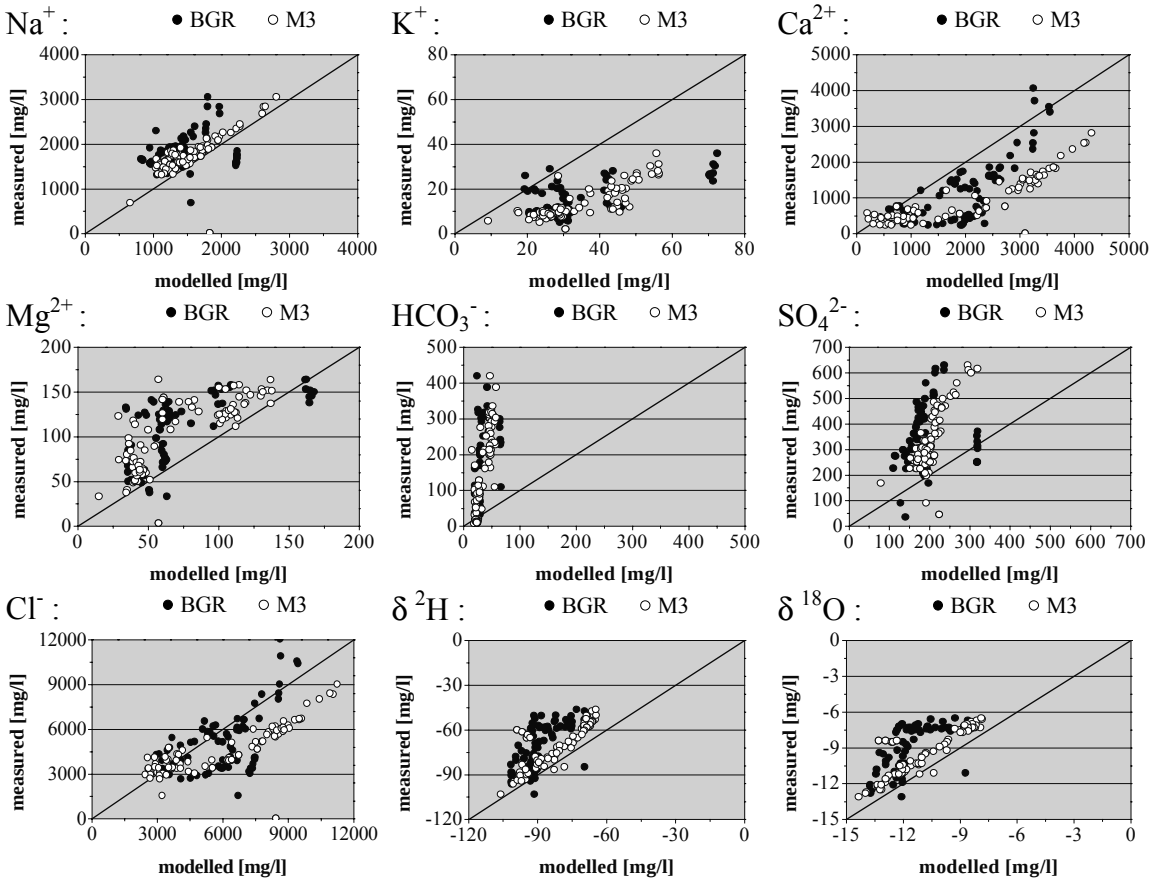

Figure 8-6 *Deviations of element concentrations from the ideal mixing line.*

The measured data refers to water samples taken at different times and places at disturbed conditions (time series at boreholes). This data is compared with the modelled concentrations at the same time and place. Modelled element concentrations are based on the modelled mixing ratio of meteoric, Baltic Sea, glacial, and brine water at the borehole, and the corresponding element concentrations. For comparing the modelled outcome, the mixing results of the M3 approach as well as the transport results of the BGR model are presented. Both data sets show a similar grouping of the data points.

As seen in the diagrams, data points located above the mixing line indicate an element source, a sink is indicated by data points below the line. Thus, a loss of potassium and calcium, and a gain of sodium, magnesium, bicarbonate, and sulphate is apparent.

Cl^-, ^2H, and ^{18}O are assumed to be conservative and therefore should match the ideal mixing line. Nevertheless, deviations are observed and this difference has to be taken as a normal scattering.

The interpretation of the distribution of the data points includes the assumption of potential chemical reactions. The explanation derived from Fig. 8-6 applies to general aspects concerning the Äspö site. Individual water samples or time series may indicate different chemical processes which tend to dominate local areas. Furthermore, a gain or loss of a reactive component only describes the summed up result or dominating effect of a series of chemical reactions a specific element was involved in. Simultaneously with an element-producing process, an element-consuming process can take place that disturbs the equilibrium of the first reaction.

The assumption of cation exchange processes accounts for deviations concerning the alkali and alkaline-earth elements. Potassium and magnesium appear to be more affected than sodium and calcium. However, the calcium concentration is assumed to be mainly influenced by the carbonate and sulphate minerals. Apart from possible influences attributable to ion exchange, the increase in magnesium can also be related to the dissolution of dolomite.

Although sodium may be involved in exchange processes it is assumed to be relatively conservative. Sodium is present in relatively high concentrations which are not affected significantly by small element shifts due to cation exchange. The influence on the relatively high sodium concentration due to exchange processes seems to be negligible compared to other cations, e.g. potassium. Potassium has a lower sorption energy compared to the bivalent alkaline-earth elements. Due to its ionic radius, potassium is preferably bound to the exchange mineral illite and is difficult to displace. This explains the loss and clear deviation from the mixing line in comparison with the other cations.

Nevertheless, considering most of the water analyses the Na/Cl- and Na/Ca-ratios increase with time and indicate the participation of sodium in exchange processes or other chemical reactions. On the other hand, the observed water compositions do not represent a typical exchange water of $NaHCO_3$-type, although the alkaline-earth : hydrogen carbonate ratio decreases with time.

The increased concentration of HCO_3^- can have several reasons, e.g. dissolution of calcite, organic decomposition and redox reactions. Sulphate reduction as a source for HCO_3^- is uncertain because of the simultaneous gain of SO_4^{2-}. However, the dissolution of calcite as a source for bicarbonate is inconsistent with the loss of calcium. Because the reducing conditions at the site are believed to be maintained during the tunnel construction owing to the amount of organic material (RHÉN et al. 1997), the dissolution of gypsum as a SO_4^{2-} source is more realistic than inorganic redox reactions.

Summarising the arguments above, the following reactions are assumed to explain the observed deviations:

Calcite dissolution	➠	gain of HCO_3^-
Calcite precipitation	➠	loss of Ca^{2+}
Gypsum dissolution	➠	gain of SO_4^{2-}
Dolomite dissolution	➠	gain of Mg^{2+}
Cation exchange	➠	loss of K^+
	➠	gain of Mg^{2+}
	➠	gain of Na^+
Organic decomposition	➠	gain of HCO_3^-
Organic redox reactions	➠	gain of HCO_3-
Oxidation of pyrite / organic matter	➠	gain of SO_4^{2-}
Degassing of CO_2(g)	➠	loss of Ca^{2+}
	➠	loss of HCO_3^-.

Batch reaction and equilibrium calculations

Batch reaction calculations with the PHREEQC computer program were carried out by applying a batch program specially developed for this purpose. In this way, a prescribed problem is automatically solved in PHREEQC for the whole computational domain of the fracture network grid. The results, e.g. element concentrations, pH, saturation indices of different minerals, etc. are written in a separate file from which they can be read in and transferred to the fracture grid.

The results of the conservative mixing model (transport) are used for characterising the chemical environment at the site without assuming potential reactions. Equilibrium calculations at every node of the FE grid were carried out considering different times of the tunnel construction. The results of the batch reaction calculations are time-variable chemical conditions at every node in the FE mesh. In addition to the ideal mixing line, this method spatially identifies possible sources and sinks in the fracture network. Figure 8-7 shows the calculated saturation indices of gypsum, calcite and CO_2(g) for initial conditions (0 days) and after completion of the tunnel (2665 days). The saturation index (SI) is the logarithm of the quotient of ion activity product and solubility product Depending on the calculated saturation index, a negative value (SI<0) indicates subsaturation of the phase in question, and thus possible dissolution. In the reverse case, a positive index indicates supersaturation and probable precipitation or degassing. These are possible chemical reactions that may be induced by the drawdown and the mixing of different groundwater types. However, this approach gives no clear evidence of the actual flow or progress of theses reactions.

Initial conditions: **After tunnel construction:**

Calcite:

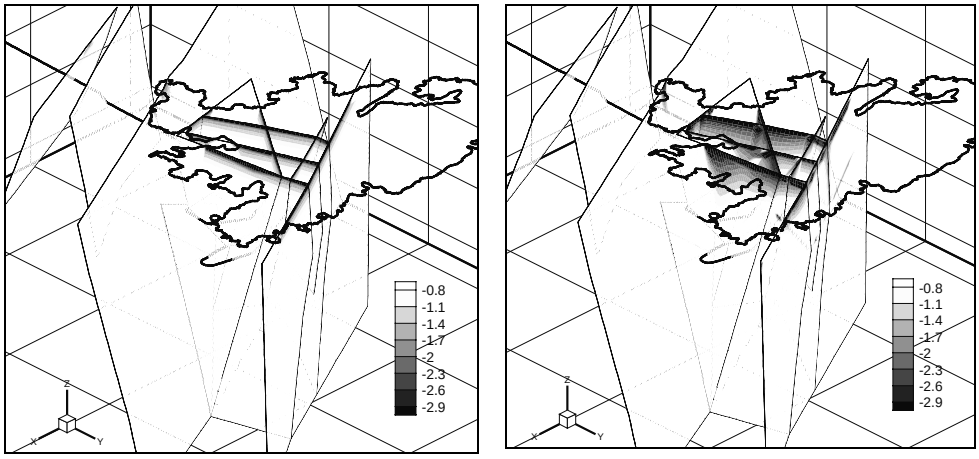

CO2 (g):

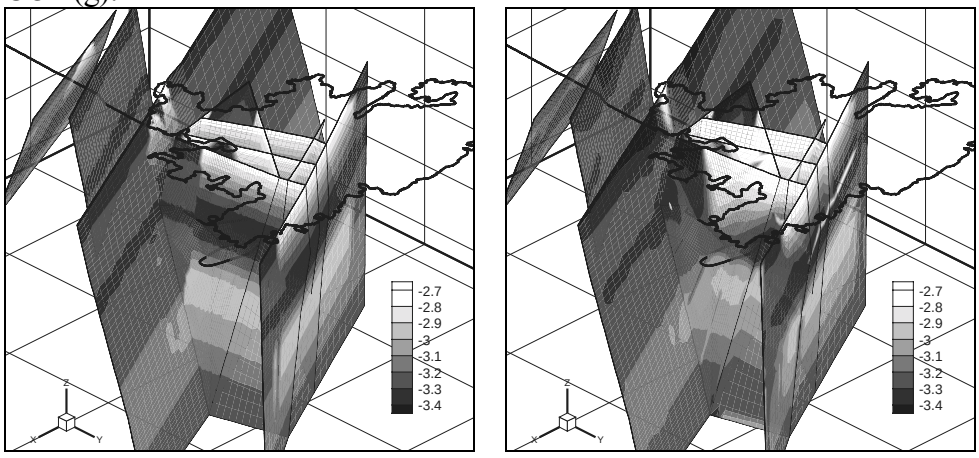

Gypsum:

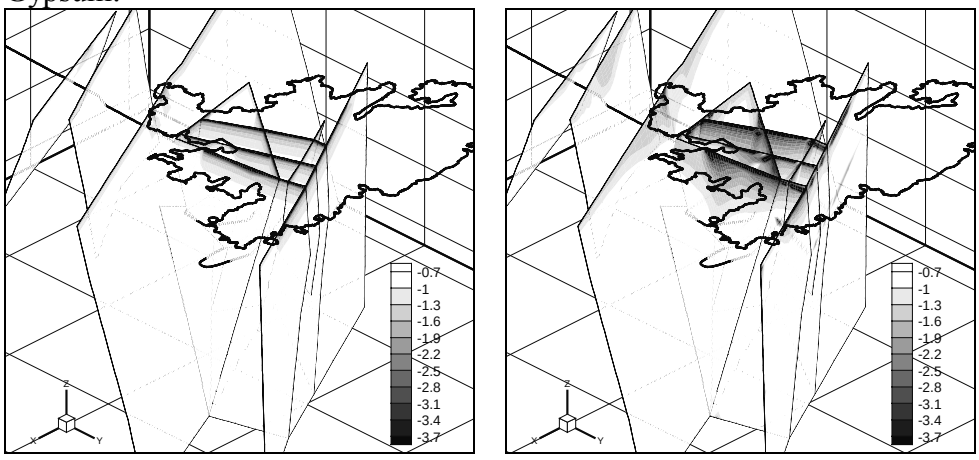

Figure 8-7 *Saturation indices in the 10-fracture model for initial conditions in Oct. 1990 (0 days) and after the tunnel construction in Jan. 1998 (2665 days).*

The variation of the chemical balance for specific mineral species depends on the distribution of the reference waters. Similar to the flow-dependent transport processes, the chemical conditions at one place change with time following the chemical characteristics of the dominating water type. As meteoric water shows a clear subsaturation concerning calcite and gypsum, and the penetration depth of meteoric water increases with time, the general evolution at the site moves towards a higher subsaturation of these minerals. This consequently implies mineral dissolution. In contrast, carbon dioxide is characterised by an increased saturation index resulting from infiltration of meteoric water.

Some additional equilibrium calculations were carried out with the PHREEQC program. Two boreholes were chosen for this purpose: SA1009B and SA1420A. The equilibrium calculations are based on analysed water samples taken at different times during the unnel construction. Chemical reactions controlling the ion content can be identified by pointing out the saturation indices of different minerals in the water samples measured at different times (Figure 8-8). As the saturation state of some specific mineral phases changes significantly with time, these minerals probably are involved in the chemical processes. The selected minerals were chosen on the basis of mapped fracture filling minerals in the laboratory tunnel (LANDSTRÖM & TULLBORG 1995). In accordance with the batch calculations for the fracture network the time series of boreholes SA1009B changes towards a subsaturation of calcite as well as of dolomite. However, the saturation index of CO2(g) shows a clear decrease, too. This may due to a degassing of CO2(g) owing to a decrease in pressure during the tunnel construction.

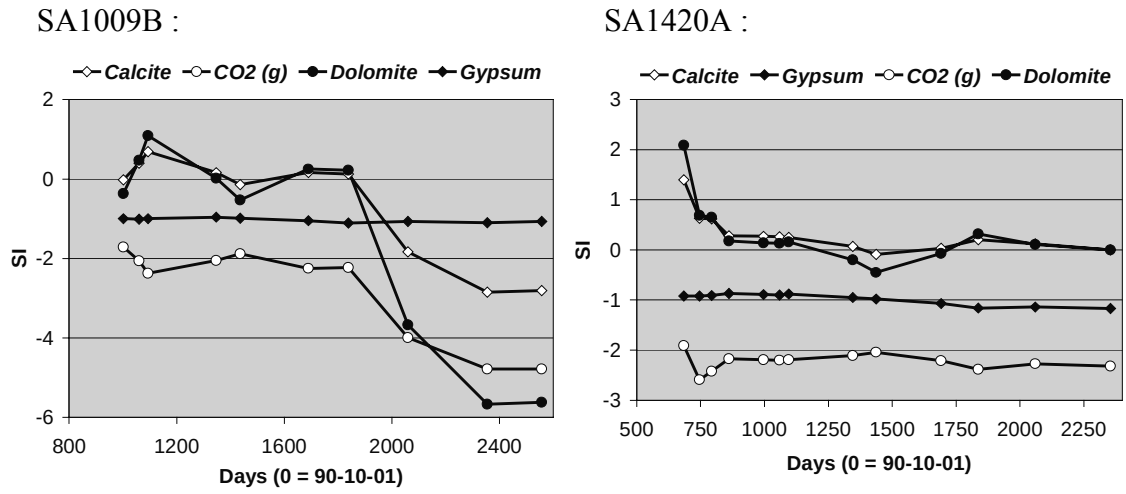

Figure 8-8 *Saturation indices of different minerals with time at boreholes SA1009B and SA1420A.*

Recalculation of mixing proportions

In order to diminish the deviations of the constituents that occur when comparing measured and modelled concentrations, the mixing proportions were recalculated corresponding to the initial composition of the reference waters. Chloride, sodium and ^{18}O were used as conservative tracers.

Exemplarily, the mixing proportions for water samples taken from boreholes SA1614B, SA1696B, and SA1828B were recalculated. The recalculation was done in an attempt to reduce the deviations of a pure mixing model from measured elemental concentrations that exist for conservative elements in the M3 model and to not overestimate chemical reactions which seem to occur due to increased element deviations.

The following describes the procedure for recalculating the water proportions and for carrying out speciation calculations for the water sample, and mixing and equilibrium calculations for the recalculations with PHREEQC. The conservative element analyses of a water sample serve as basis for the calculations. For each water sample, the proportions of the different groundwater types are calculated according to a set of equations, whereby chlorine, sodium and the oxygen isotope ^{18}O act as conservative tracers.

The concentrations of the remaining non-conservative elements can be determined using the recalculated proportions of each reference water. This is done by means of mixing calculations in PHREEQC. The initial compositions of the reference waters are mixed in the determined ratios. The prescribed pH values are 6.5 for glacial and meteoric water, brine has a pH of 7.2 and Baltic Sea water 8.2. The redox potential is constant at -250 mV, the temperature is a constant 13°C.

The mixture calculation leads to a composition for a specific water sample, whereby concentrations of the non-conservative elements still deviate from the measured values. These deviations are to be minimised by equilibrium calculations. This first involves a speciation analysis of the water sample which gives the specific boundary conditions (SI of calcite, gypsum, dolomite, and $CO_2(g)$) for the following equilibration calculations. The elemental concentrations, which resulted from the mixing calculation, are defined as the initial solution for the equilibrium calculation with appropriate pH and Eh values. The boundary conditions are the saturation indices mentioned above as well as equilibrium with albite, K-feldspar and quartz (SI = 0).

The element concentrations for boreholes SA1614B, SA1696B, and SA1828B after the mixing and equilibrium calculations are shown in Figures 8-11 to 8-13. The concentrations of the non-conservative species Ca^{2+}, Mg^{2+}, K^{+}, HCO_3^{-}, and SO_4^{2-} correspond better with the measurements. After the equilibrium simulations, these elements very closely match the measured values at the expense of sodium, which was used for charge balance purposes during the simulation process.

The results prove the usefulness of the four water types classified by the M3 model. Although the M3 grid data deviates more or less from measured values, the composition of the reference waters (Table 6-1) can be used for reproducing the element analysis by summing up the mixing ratios. The correspondence can even be improved by means of the PHREEQC equilibrium calculations.

However, the recalculation of the mixing proportions are done individually for each water sample. Furthermore, they are based on the conservative elements, which in this study include sodium. For this reason, the set of equations does not always solve for one clear solution. If the analysed concentrations of Cl, Na, and ^{18}O are of an unsuitable ratio, the proportion of a water type may result in a negative value. This again leads to a clear error in the mass balance if the negative difference is too high, e.g. exceeds a tolerable deviation of 5 %.

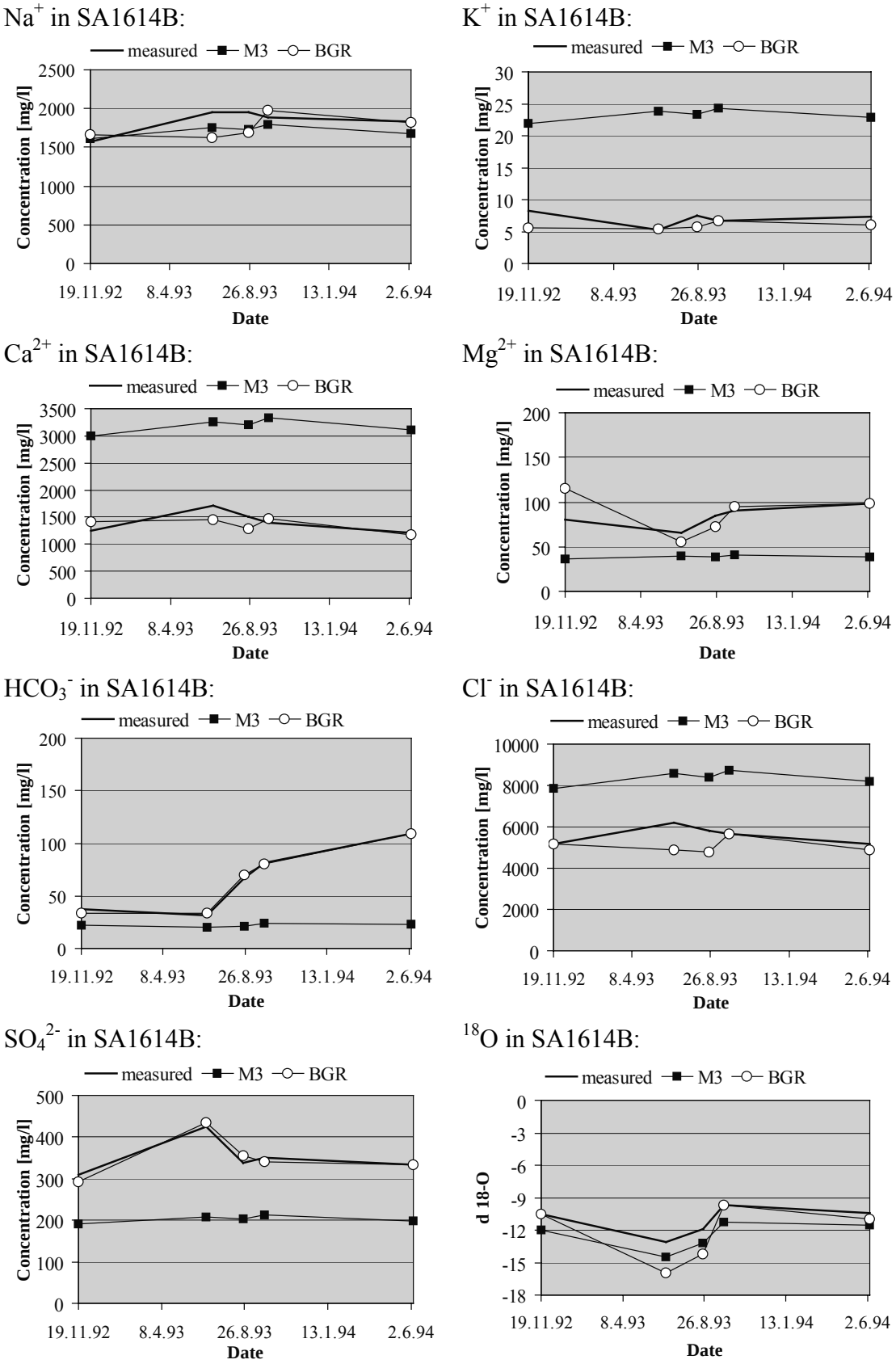

Figure 8-9 *Measured element concentrations in borehole SA1614B compared to a mixing-equilibration approach.*

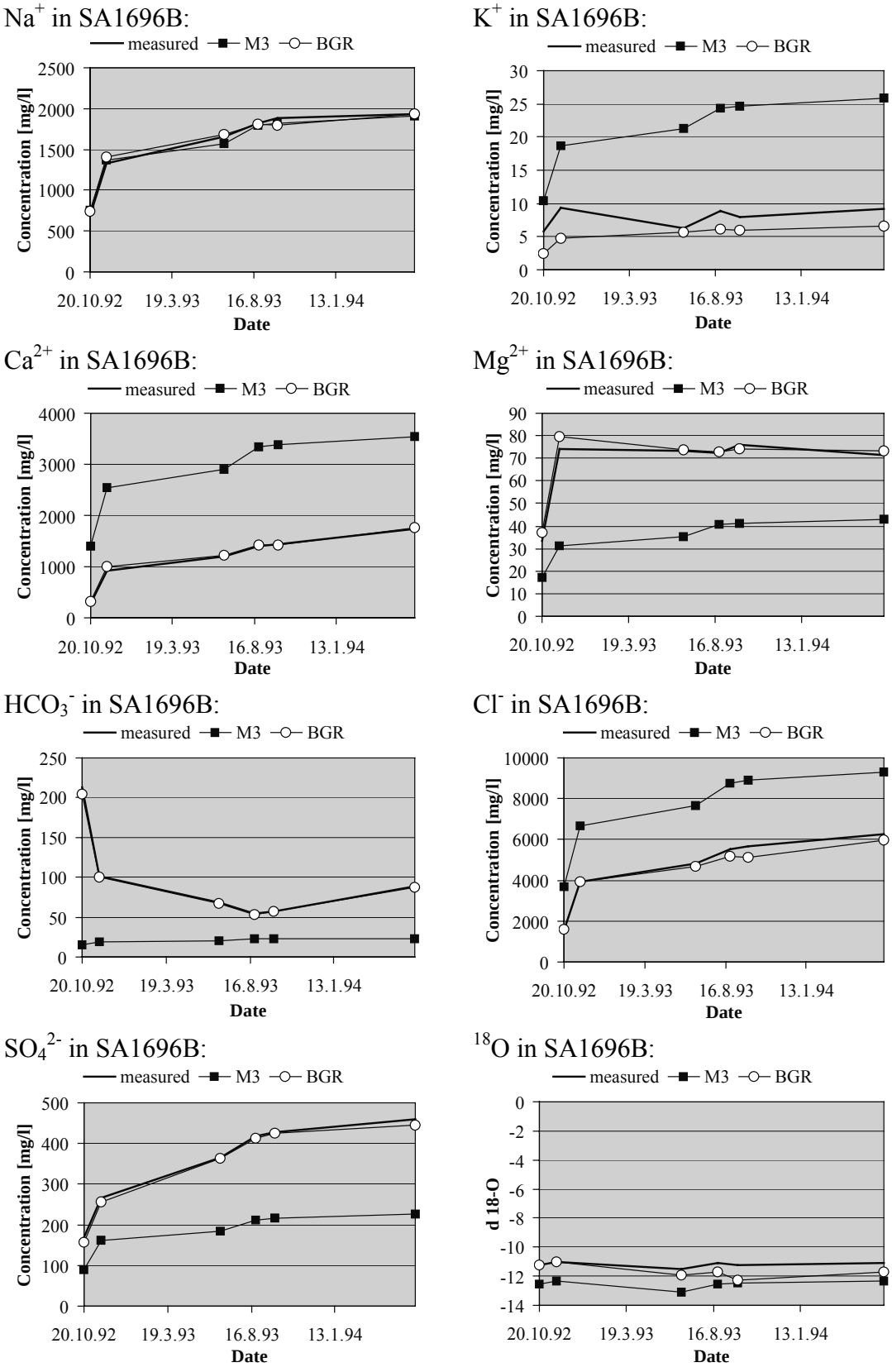

Figure 8-10 *Measured element concentrations in borehole SA1696B compared to a mixing-equilibration approach.*

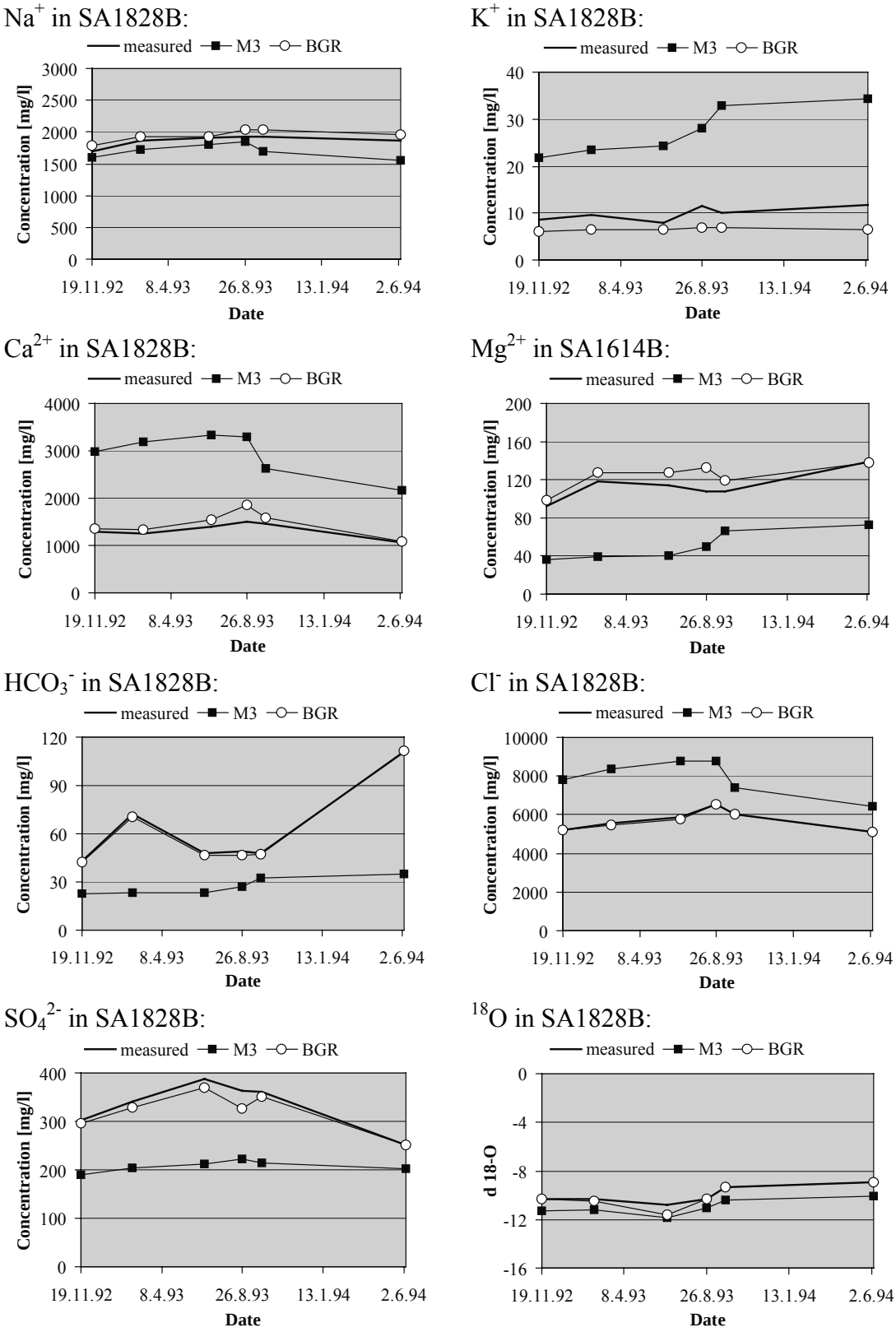

Figure 8-11 *Measured element concentrations in borehole SA1828B compared to a mixing-equilibration approach.*

9 Sensitivity Analysis

9.1 Hydrogeological Model

In order to develop a hydrogeological model, the geometry of the fractures and the complex processes during excavation of the tunnel must be known. The hydraulic and chemical processes are related and they are non-linear. The finite-element mesh and the time steps were varied until numerical hydraulic and transport model was stable. The initial conditions, the changes in the boundary conditions resulting from the driving of the spiral tunnel, and the amount of groundwater recharge were also varied.

The three-dimensional numerical model consists of two-dimensional macro-elements that intersect. At the intersection of any two macro-elements, both elements have the same width so that when the mesh is subdivided, the nodes of the new elements are the same at the intersection of the original macro-elements. The macro-elements are subdivided into elements with an edge length that is 1/11 the edge length of the macro-element.

The stability of the model is decreased by irregularly shaped elements and elements with three edges (which cause oscillation). The more regular the elements are, the more stable the model becomes; uniform quadrilateral elements are preferred. The following criteria had to be observed:

(1) Courant criterion

$$Cr = \left| \frac{v \cdot \Delta t}{\Delta l} \right| \leq 1$$

Observance of the Courant criterion should guarantee that the change in concentration in a finite element cannot become larger during a time step than the concentration change caused by advective transport. Δl is the length of the element.

(2) Neumann criterion

$$Fo = \frac{D}{\Delta l^2} \Delta t \leq \frac{1}{2}$$

Observance of the Neumann criterion should prevent the concentration gradient in a finite element from being reversed during a time step Δt only by diffusive or dispersive transport.

(3) A third criterion

Another criterion deals with sources and sinks: Within a time step Δt no more substance should leave a finite element than was in that element originally. Correspondingly, no more substance should enter the finite element than that element can contain without raising the concentration above the initial concentration.

(4) The Peclet criterion

$$Pg = \left| \frac{v \cdot \Delta l}{D} \right|$$

The Peclet grid number has a physical, a mathematical, and a numerical meaning. Physically, it is the ratio between advective and dispersive transport. Mathematically, it characterizes the differential equation for transport. Numerically, it guarantees the stability of the numerical solution for a one-dimensional, stationary transport equation with no sinks or sources. Oscillation can occur only where there is a large change in gradient, e.g., at boundaries.

physical	the ratio between advective and dispersive transport	Pe < 1 Pe > 1	more dispersive more advective
mathematical	characterizes the differential equation for transport	Pe < 1 Pe > 1	more parabolic more hyperbolic
numerical	stability criterion	Pe < 2 Pe < 4	linear elements quadratic elements

When the velocities in the flow field have been calculated, the transport velocities of the solutes are then calculated as a function of the flow field. This is done iteratively until the deviations from the measured heads, the amount of groundwater recharge, and measured solute concentrations have been reduced to an acceptable amount.

Three or four fracture zones are then added to the fracture network. First, the fractures with the highest permeabilities were included in the model. At present, 10 fractures which are hydraulically connected have been examined. The proportion of water from each of the four sources is calculated from the solute concentrations, the amount of water, and the flow velocity. An interpretation of the hydrogeological conditions can be made on the basis of the proportions of water from the four sources.

9.2 Hydrochemical Model

The sensitivity of the chemical model depends on the approach used for the modelling. As the chemical model represents a picture of the hydrochemical environment for a better understanding of possible hydrochemical processes, the quality of water analyses and of conservative transport models, a numerical sensitivity has less effect on the results of the hydrochemical model pursued in this study. It is rather the general composition of different aspects and manifold approaches that yield a conclusive qualitative model.

However, if only single calculations for each water sample or for a time series are made with the PHREEQC program, the modelled results largely depend on the concentrations of conservative elements. These simulations are for specific water samples and are based on the measured values of the non-reactive elements. Thus, it is always necessary to know roughly the intrinsic element concentrations, especially the conservative ones. Additionally, the conservative elements are important because the proportions calculated for the four types of water are based on these elements. Errors in the initial and boundary conditions also affect the calculated concentrations of the non-conservative elements and consequently the assumed chemical reactions and chemical equilibrium in the chemical model.

The environmental parameters temperature, redox potentials and pH have less effect on the simulations because the same starting point was to be used for the different approaches. As mentioned in RHÉN et al. (1997), it is assumed that biological oxygen consumption leads to reducing conditions. Thus, chemical simulations were carried out assuming constant reducing conditions with an Eh (redox potential) of -250 mV.

10 Methodology and Implications for Model Integration

Flow and transport calculations were carried out for a fracture network on a site scale with the DURST/Rockflow program. A conservative mixing model was then developed using the M3 reference waters. The M3 groundwater classes facilitated the general characterisation of the site and improved the quality of the transport model.

A module specially developed to carry out batch calculations with PHREEQC was then used for speciation and equilibrium calculations for the entire fracture network resulting from the mixing model. This provided a qualitative assessment of the chemical changes at the site, from which possible chemical reactions could be derived.

Chemical calculations carried out with PHREEQC are for selected control points. Chemical reactions are assumed to account for changes in the chemical water composition throughout the site (identified, for example, by the batch calculations and the ideal mixing line). The results of the mixing model were compared with the measured element concentrations. Deviations could be explained by assuming specific chemical reactions.

The hydrogeological and hydrochemical data were integrated into the program in separate steps. The inclusion of hydrological and chemical processes can be improved by developing a method for directly coupling conservative transport and chemical reactions to a reactive transport model. The changes in the concentrations of non-conservative elements due to reactions can directly influence the transport calculations and the characteristics of the chemical environment.

11 Concluding Remarks

Corresponding to the objectives for Task 5, the procedure described in Section 1.3 was used to characterize the regional hydraulic system. This characterization has helped to understand the influence of tunnel construction on the groundwater regime. The numerical results of this study help to understand the processes taking place during groundwater flow, which is governed by the main fracture zones. The computer program DURST/Rockflow (KRÖHN 1991; LIEDTKE et al. 1994) was validated and used for the flow and transport simulations carried out within the Task 5 project. The modelling results justify the application of the software and the development of a discrete fracture model.

The chemical data helped to assess the quality and consistency of the flow and transport model results and to show where improvements of the model are necessary. The hydrochemistry data is mainly derived from the M3 approach (LAAKSOHARJU & WALLIN 1997). This data was provided by SKB and made a significant contribution to the success of the modelling.

The integration of hydrological and hydrochemical data into the model is based on the four main sources of water identified at the Äspö site and their distribution in the groundwater system at Äspö prior to tunnel construction. Thus, four conservative tracers were available for fitting the model to the measured values. Each of the groundwater types represents one characteristic part of the groundwater system: meteoric water and Baltic sea water in the upper part of the system, glacial water in the middle part, and brine water at the lower part. This data was sufficient to develop a regional model.

However, it is important to be aware of the strong influence of the boundary and initial conditions on the modelling results, especially as these conditions are derived from grid data. Adjustment of the sum of the different groundwater types to 100 % may also affect the results. There is some difficulty to determine the initial water concentrations in the offshore parts of the model. However, a sensitivity analysis is necessary to confirm the input and output values of the flow and groundwater mixing models, because the results depend mainly on the material properties and boundary conditions.

Additionally, refinement of the model fracture network and an adjustment to the natural conditions would be useful in order to account for the spatial variability of the hydraulic and transport parameters as well as the boundary and initial conditions. Moreover, it would be very helpful if both the hydraulic and the chemical results were available at the control points. The modelling results would be more accurate and the agreement of the modelled and measured values at the calibration points could be improved.

References

Gurban I, Laaksoharju M, Andersson C, 1998. Influences of the Tunnel Construction on the Groundwater Chemistry at Äspö – Hydrochemical Initial and Boundary Conditions: WP D1, WP D2.- IPR-02-59, Stockholm. (in press)

Ittner T, Gustafsson E, 1995. Groundwater Chemical Composition and Transport of Solutes. Evaluation of the Fracture Zones NE-1, NE-2 and NNW-4 during Preinvestigation and Tunnel Construction.- SKB PR HRL-96-03, Stockholm.

Kolditz O, Habbar A, Kaiser R, Thorenz C, 1998. ROCKFLOW User's Manual Release 3.3, November 1998.- Institut für Strömungsmechanik und Elektronisches Rechnen im Bauwesen, Universität Hannover.

Kolditz O, 1997. Strömung, Stoff- und Wärmetransport im Kluftgestein – Berlin; Stuttgart; Bornträger

Kröhn KP, 1991. Simulation von Strömungs- und Transportvorgängen im klüftigen Gestein mit der Methode der Finiten Elemente. Dissertation, Institute für Strömungsmechanik und Elektronisches Rechnen im Bauwesen, Universität Hannover, Bericht Nr. 29

Lege T, Kolditz O, Zielke W, 1996. Strömungs- und Transportmodellierung – Handbuch zur Erkundung des Untergrundes von Deponien und Altlasten – Band 2; Bundesanstalt für Geowissenschaften und Rohstoffe. ISBN 3-540-59140-0 Springer, Berlin, Heidelberg, New York.

Laaksoharju M, Skårman C, 1995. Groundwater Sampling and Chemical Characterisation of the Äspö HRL Tunnel in Sweden.- SKB PR 25-95-29, Stockholm.

Laaksoharju M, Wallin B, 1997. Evolution of the Groundwater Chemistry at the Äspö Hard Rock Laboratory.- Proceedings of the Second Äspö International Geochemistry Workshop, June 6-7, 1995. SKB ICR 97-04, Stockholm.

Landström O, Tullborg E-L, 1995. Interactions of Trace Elements with Fracture Filling Minerals from the Äspö Hard Rock Laboratory.- SKB TR 95-13, Stockholm.

Liedtke L, Götschenberg A, Jobmann M, Siemering W, 1994. Fracture System Flow Test; Experimental and Numerical Investigations of Mass Transport in Fracrured Rock – Grimsel Test Site; NAGRA – Wettingen Switzerland.

Liedtke L, Shao H, 1997. Modelling of the Tracer Experiments in Feature A at ÄSPÖ HRL, SKB – international Cooperation Report 98-02, Stockholm - Sweden

Liedtke L, Shao H, Alheid H J, Sönnke J, 1999. Material Transport in Fractured Rock – Rock Characterisation in the Proximal Tunnel Zone.- Federal Institute for Geosciences and Natural Resources, Hannover.

Markström I, Erlström M, 1996. Äspö Hard Rock Laboratory. Overview of Documentation of Tunnel, Niches and Core Boreholes.- SKB PR HRL-96-19, Stockholm.

Mészaros F, 1996. Simulation of the Transient Hydraulic Effect of the Access Tunnel at Äspö.- SKB ICR 96-06, Stockholm.

Nilsson, A-C, 1995. Compilation of Groundwater Chemistry Data from Äspö 1990 – 1994.- SKB PR 25-95-02, Stockholm.

Parkhurst D L, Appelo C A J, 1999. User's Guide to Phreeqc (Version 2) – A Computer Program for Speciation, Batch-Reaction, one-dimensional Transport, and Inverse Geochemical Calculations.- U.S. Geol. Surv. Water Res. Inv. 99-4259, 312 pp; Denver, Colorado.

Rhén I, Stanfors R, 1993. Passage through Water-Bearing Fracture Zones. Evaluation of Investigations in Fracture Zones NE-1, EW-7 and NE-3.- SKB PR 25-92-18, Stockholm.

Rhén I, Stanfors R, 1995. Supplementary Investigations of Fracture Zones in Äspö Tunnel.- SKB PR 25-95-20, Stockholm.

Rhén I, Gustafson G, R Stanfors, P Wikberg, 1997. ÄSPÖ HRL - Geoscientific Evaluation 1997/5. Models Based on Site Characterisation 1986 - 1995.- SKB TR 97-06, Stockholm.

Rhén I, Magnusson J, Forsmark T, 1998. Äspö Task Force on Modelling of Groundwater Flow and Transport of Solutes - Task #5. Data Compilation: WP A3, WP A 4.- SKB IPR-02-57, Stockholm. (in press)

Wikberg P, 1998. Äspö Task Force on Modelling of Groundwater Flow and Transport of Solutes. Plan for Modelling Task # 5: Impact of the Tunnel Construction on the Groundwater System at Äspö, a Hydrological-Hydrochemical Model Assessment Exercise.- SKB PR HRL-98-07, Stockholm.

Appendix 1

Initial Conditions of Transport Calculations

Meteoric water :

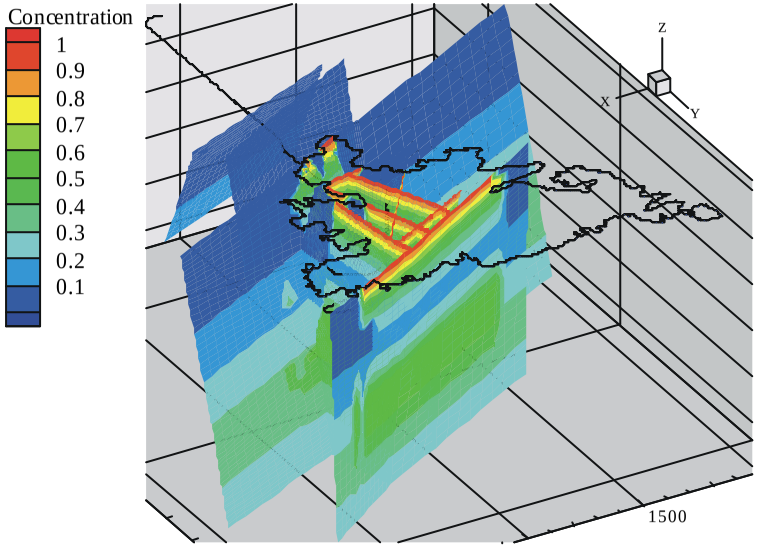

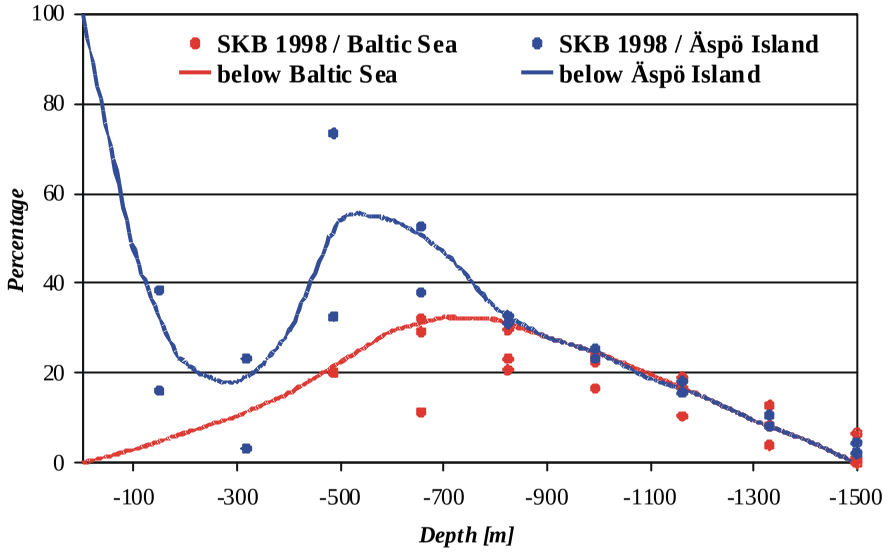

Baltic sea water :

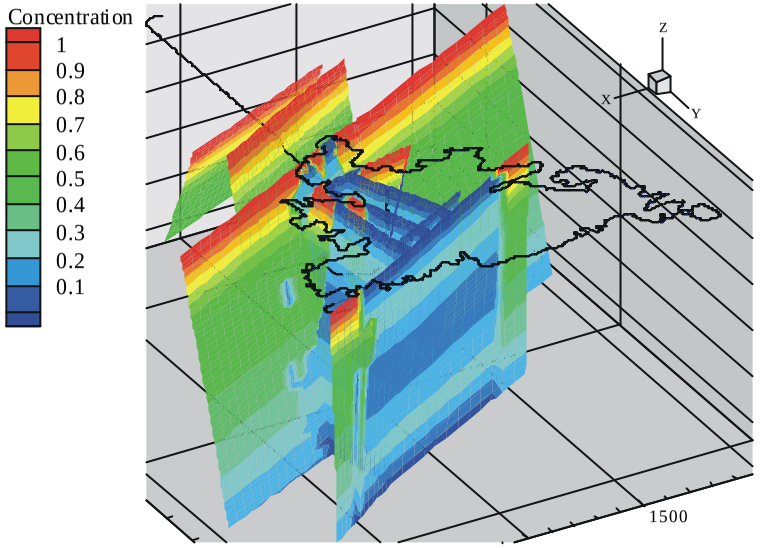

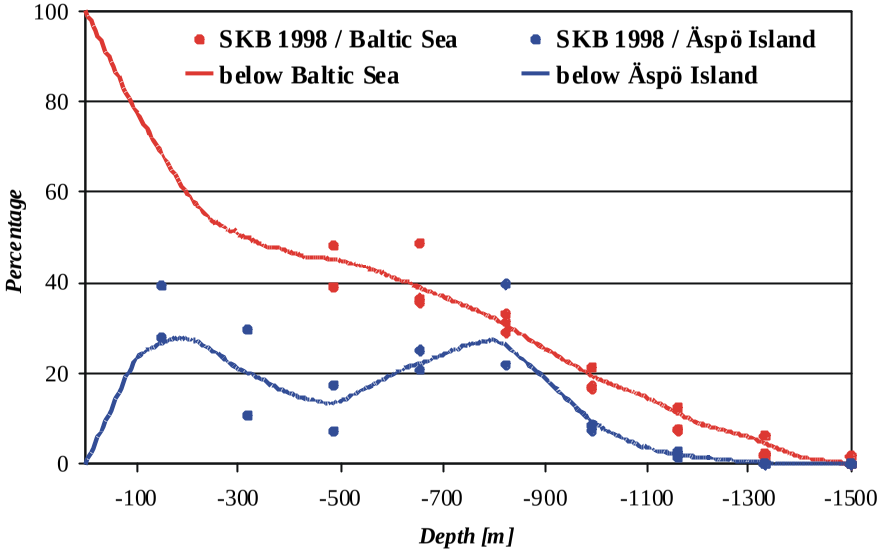

Glacial water :

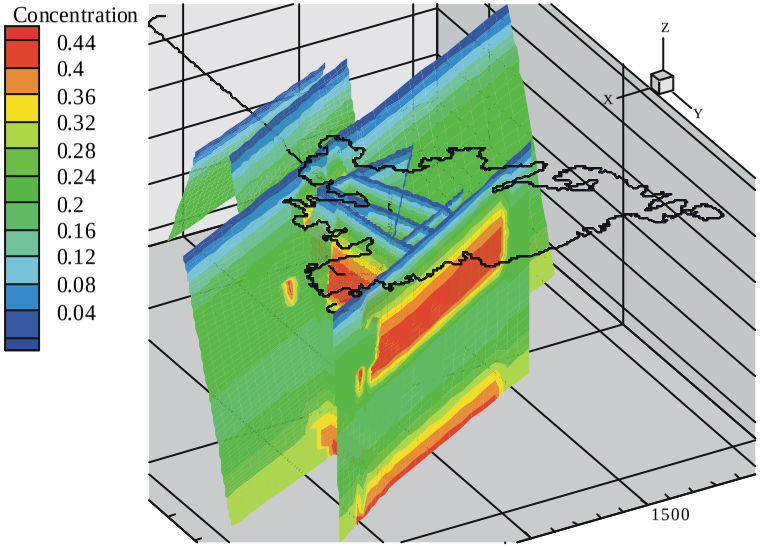

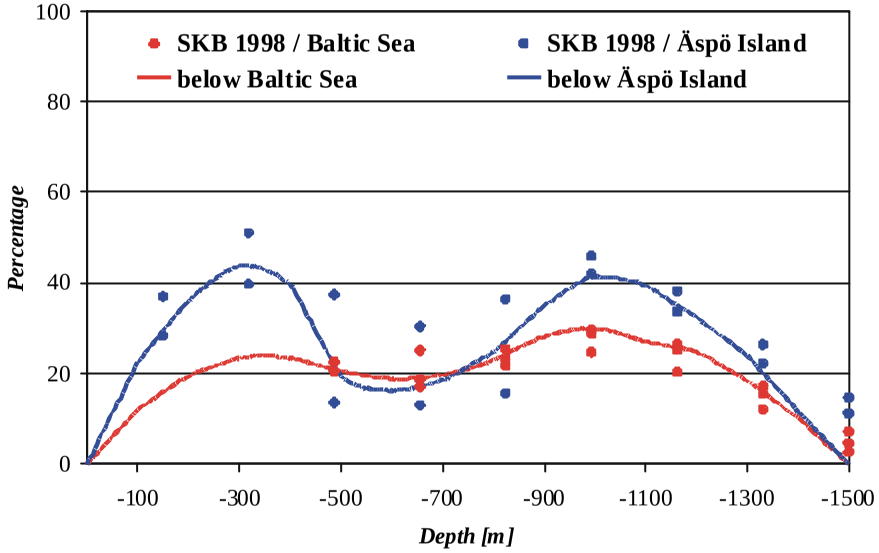

Brine water :

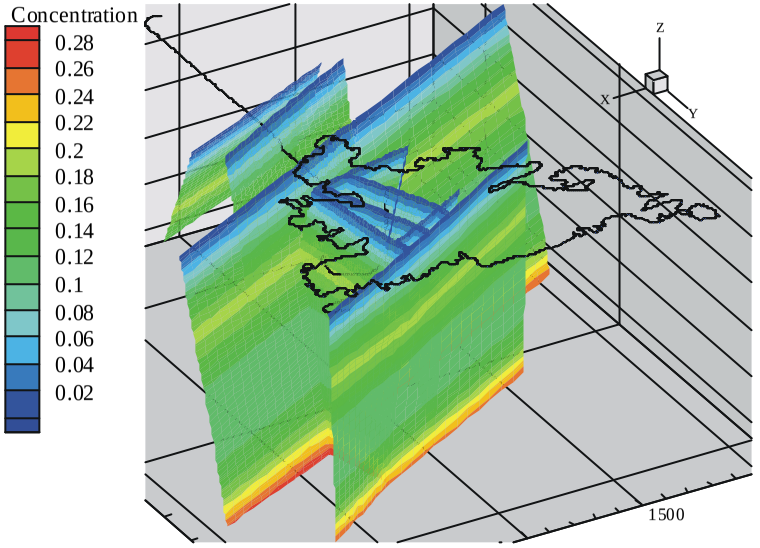

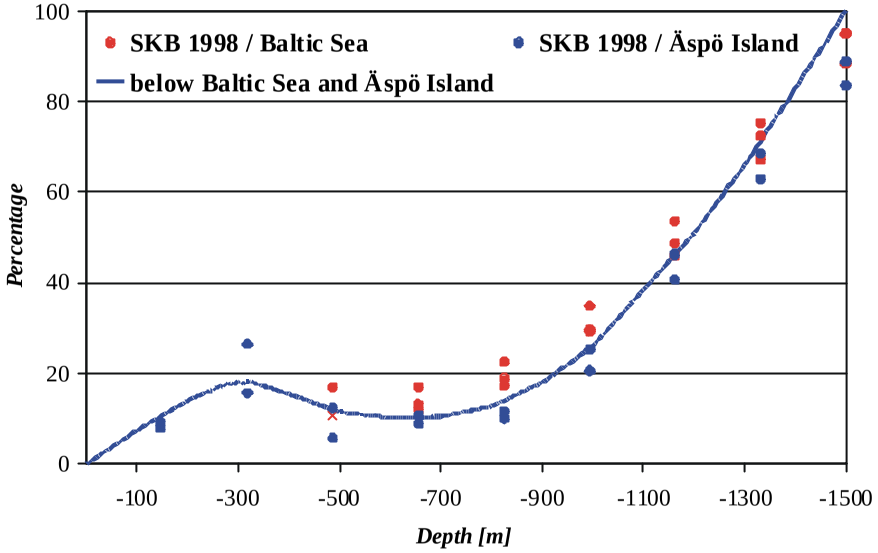

Appendix 2

Results of Transport Calculations

TFP at 1400 m:

TFP at 2100 m:

TFP at 3000 m:

TFP at 3600 m:

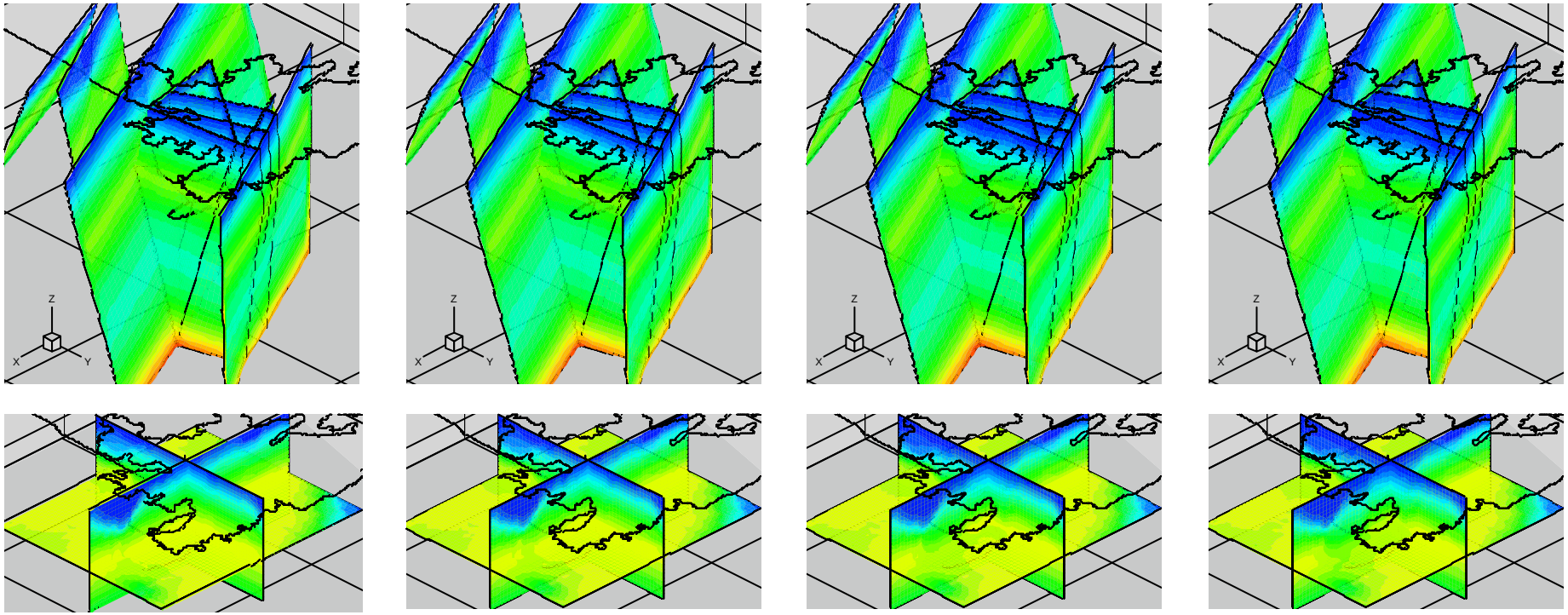

Distribution of Brine water for the tunnel face positions (TFP): 1400 m (680 days), 2100 m (865 days), 3000 m (1235 days), and 3600 m (1447 days) in the fracture network and for interpolated planes (x=2100 m, y=7350 m, z=-300 masl).

TFP at 1400 m: **TFP at 2100 m:** **TFP at 3000 m:** **TFP at 3600 m:**

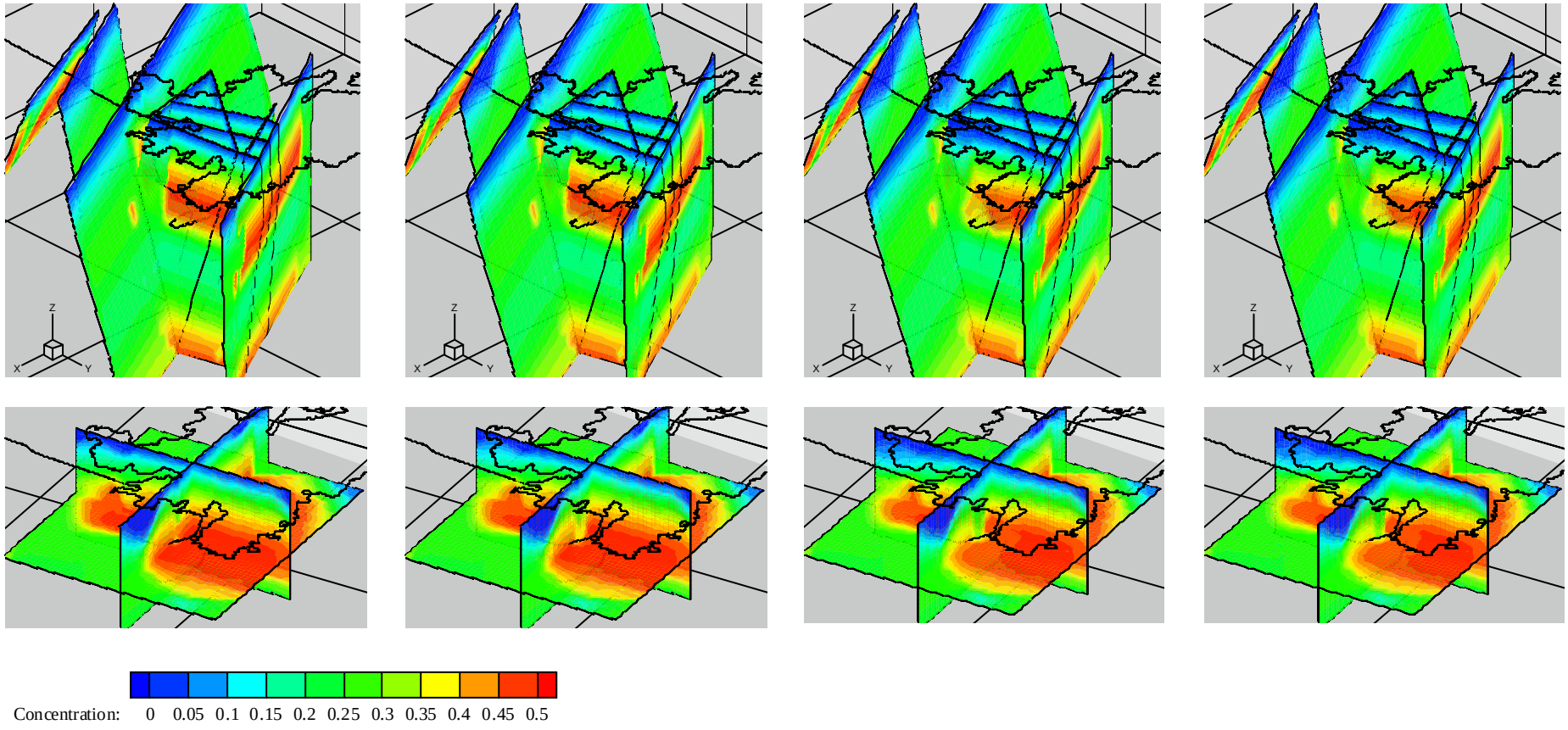

Distribution of Glacial water for the tunnel face positions (TFP): 1400 m (680 days), 2100 m (865 days), 3000 m (1235 days), and 3600 m (1447 days) in the fracture network and for interpolated planes (x=2100 m, y=7350 m, z=-300 masl.

TFP at 1400 m: **TFP at 2100 m:** **TFP at 3000 m:** **TFP at 3600 m:**

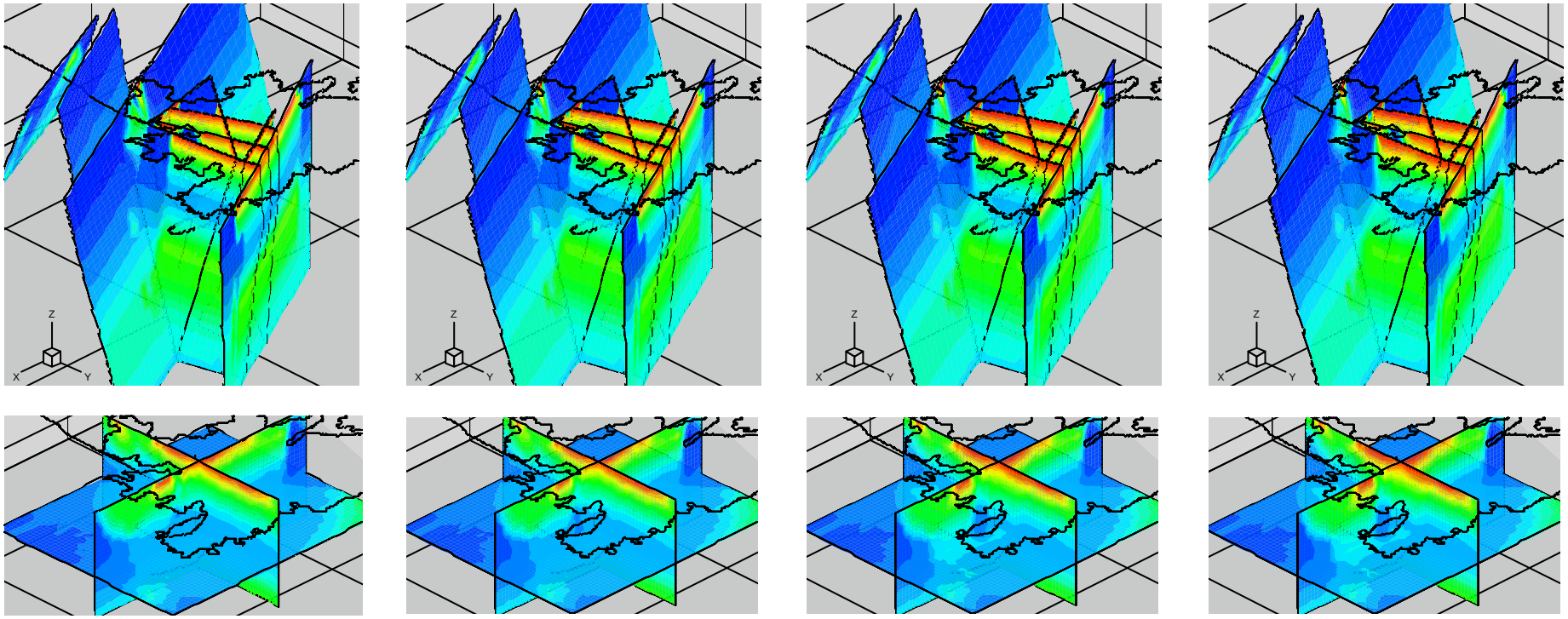

Distribution of Meteoric water for the tunnel face positions (TFP): 1400 m (680 days), 2100 m (865 days), 3000 m (1235 days,) and 3600 m (1447 days) in the fracture network and for interpolated planes (x=2100 m, y=7350 m, z=-300 masl).

TFP at 1400 m:

TFP at 2100 m:

TFP at 3000 m:

TFP at 3600 m:

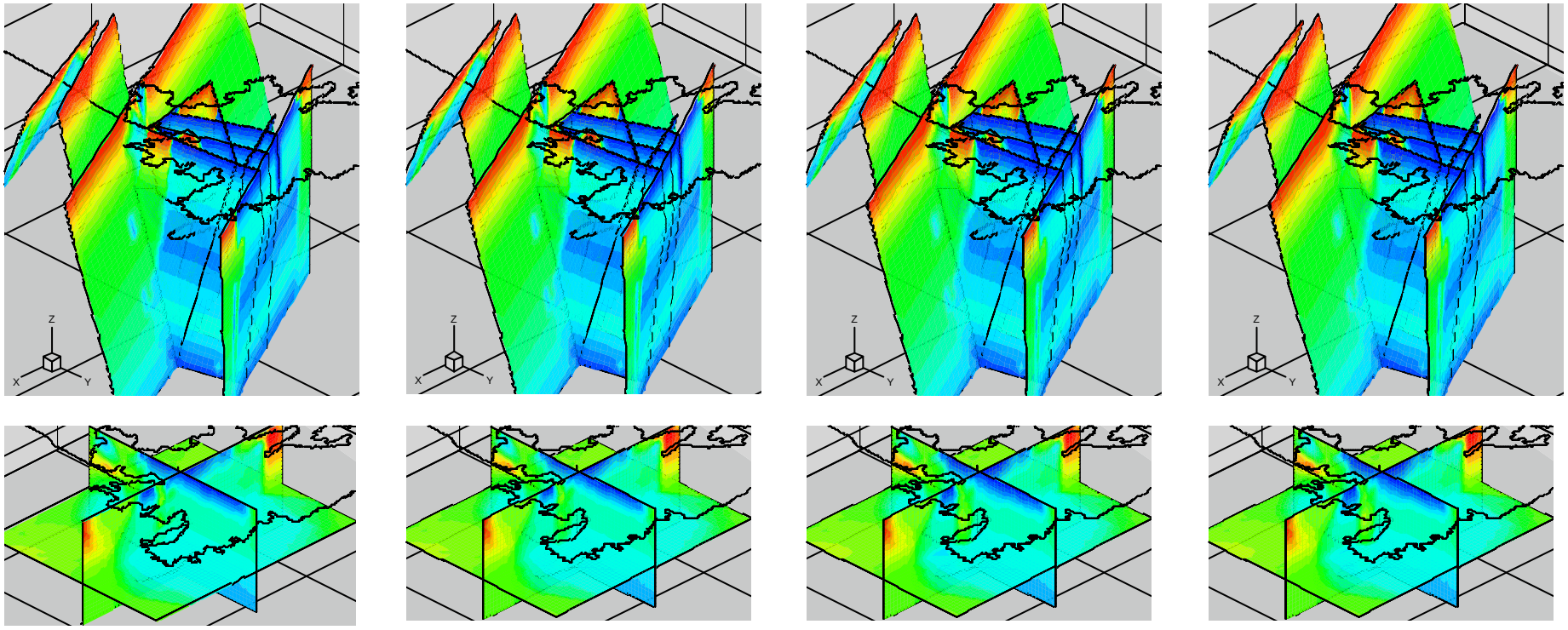

Distribution of Baltic Sea water for the tunnel face positions (TFP): 1400 m (680 days), 2100 m (865 days), 3000 m (1235 days), and 3600 m (1447 days) in the fracture network and for interpolated planes (x=2100 m, y=7350 m, z=-300 masl).

TFP at 1400 m:

TFP at 2100 m:

TFP at 3000 m:

TFP at 3600 m:

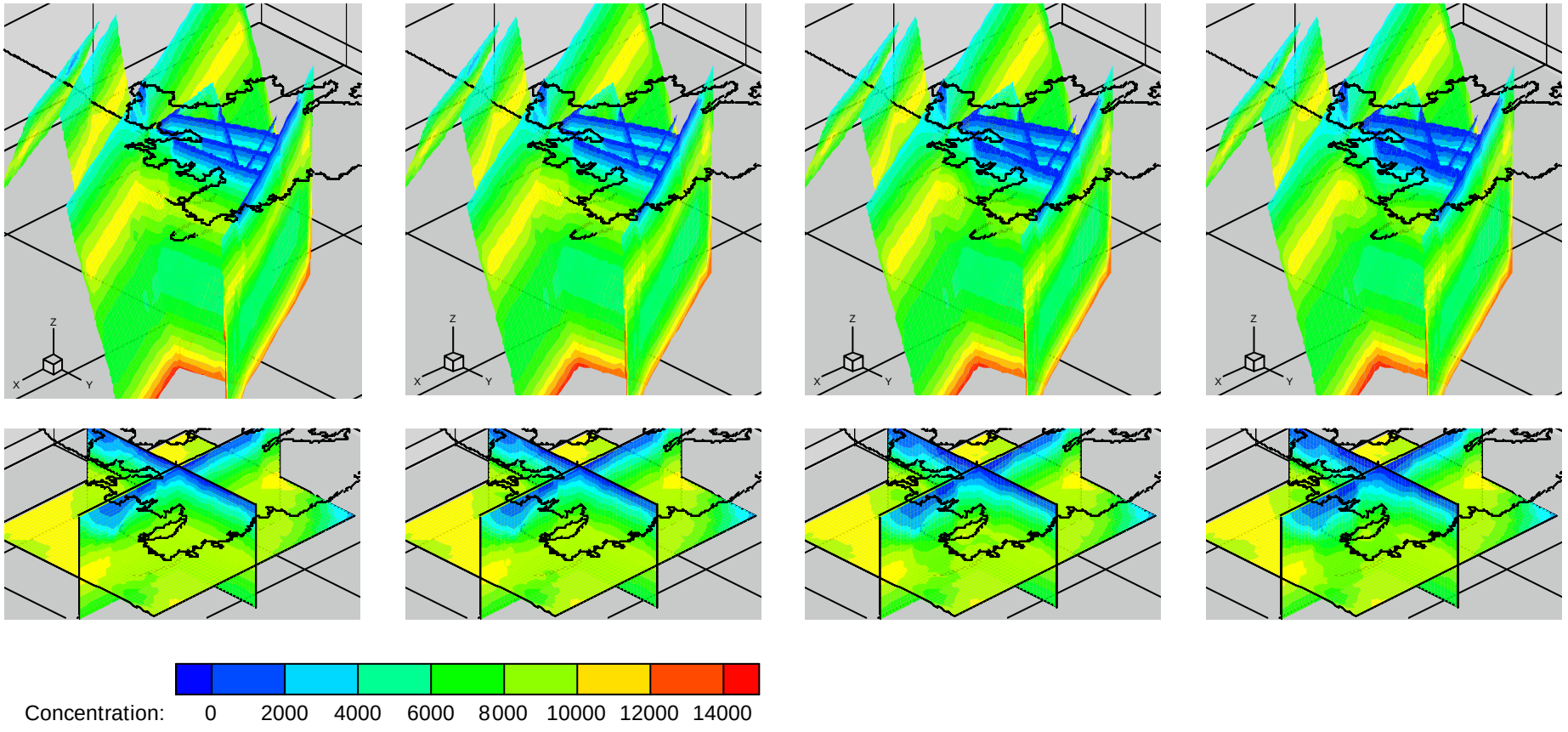

Distribution of Chloride for the tunnel face positions (TFP): 1400 m (680 days), 2100 m (865 days), 3000 m (1235 days), and 3600 m (1447 days) in the fracture network and for interpolated planes (x=2100 m, y=7350 m, z=-300 masl).

TFP at 1400 m: **TFP at 2100 m:** **TFP at 3000 m:** **TFP at 3600 m:**

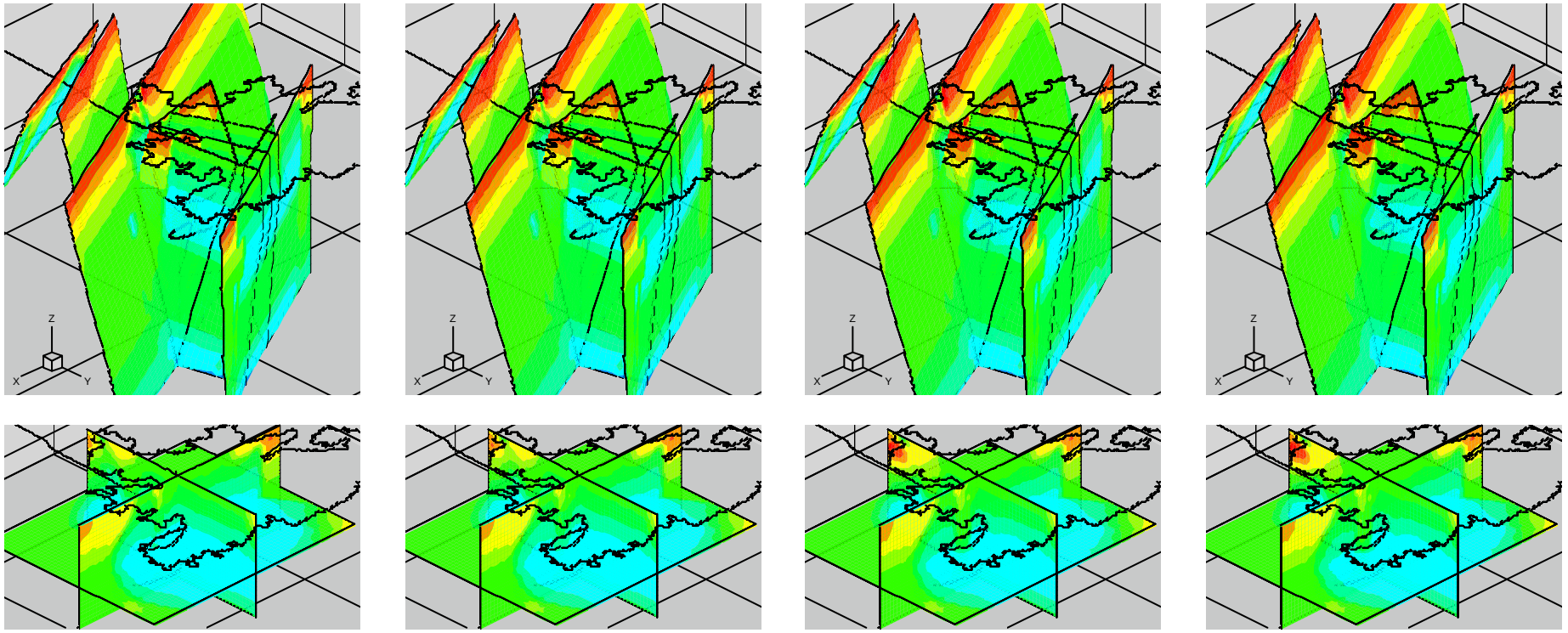

Distribution of 18 O for the tunnel face positions (TFP): 1400 m (680 days), 2100 m (865 days), 3000 m (1235 days), and 3600 m (1447 days) in the fracture network and for interpolated planes (x=2100 m, y=7350 m, z=-300 masl).

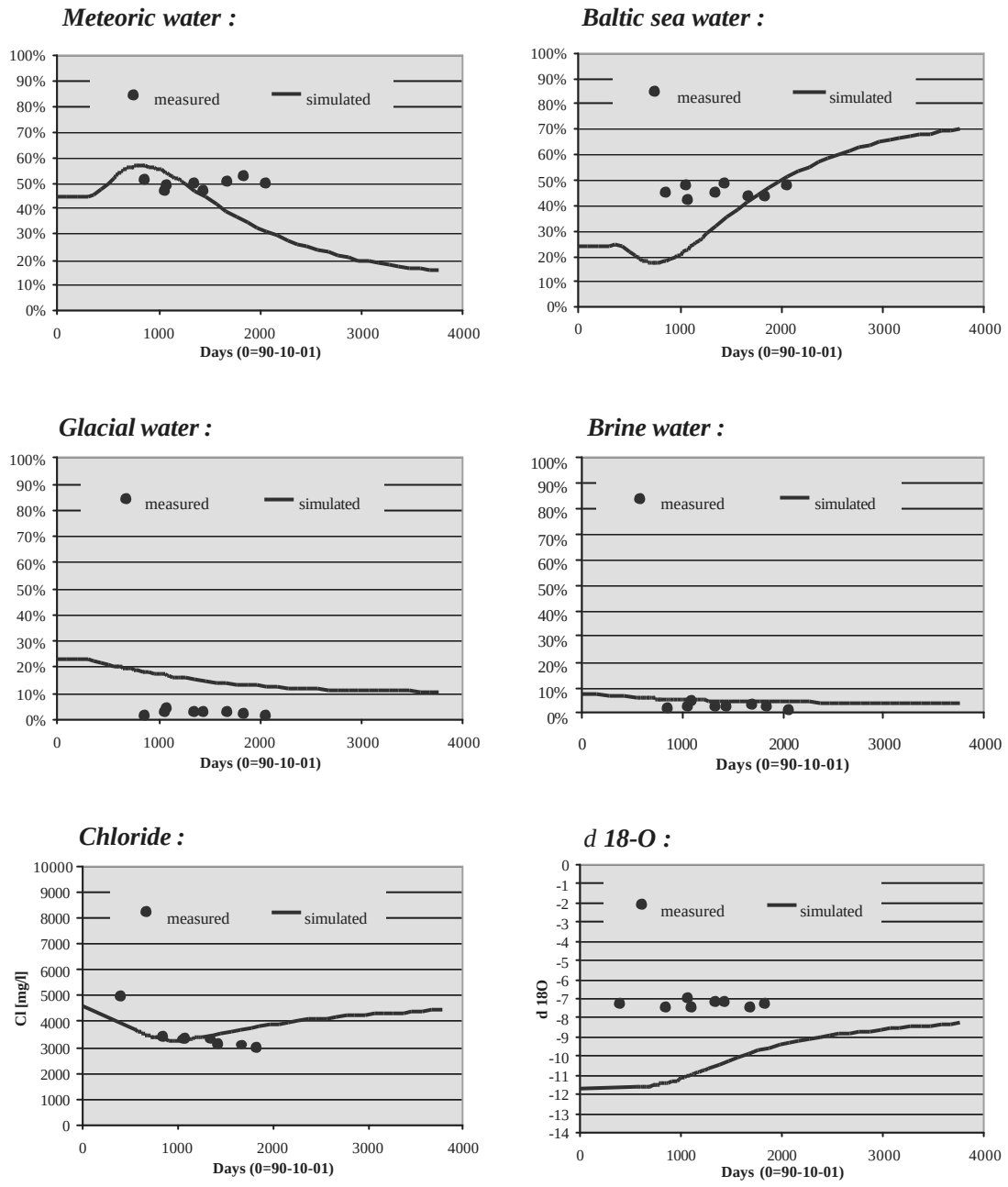

Measured and simulated values of meteoric, Baltic sea, glacial, and brine water, chloride content, and d 18-O at borehole SA0813B (CP 2).

Meteoric water :

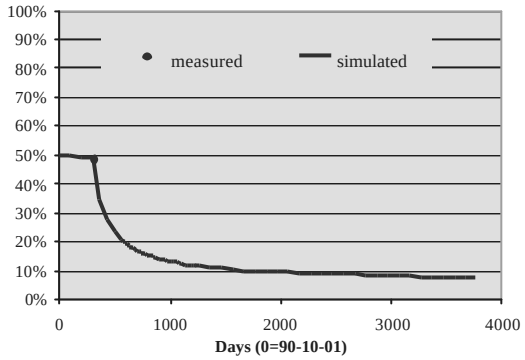

Baltic sea water :

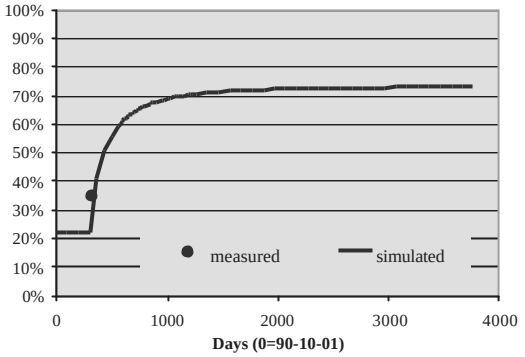

Glacial water :

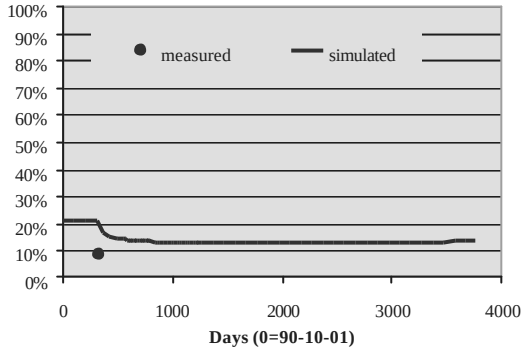

Brine water :

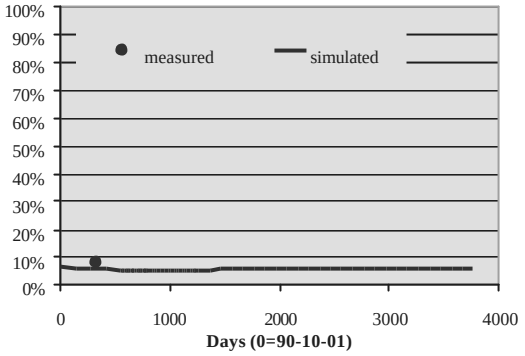

Chloride :

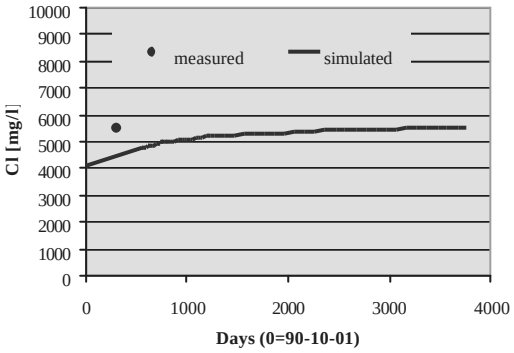

d ***18-O :***

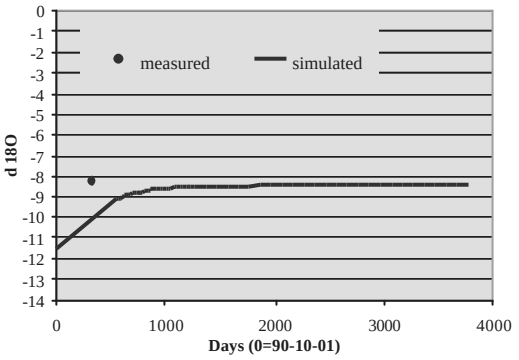

Measured and simulated values of meteoric, Baltic sea, glacial, and brine water, chloride content, and d 18-O at borehole SA0850B (CP 2).

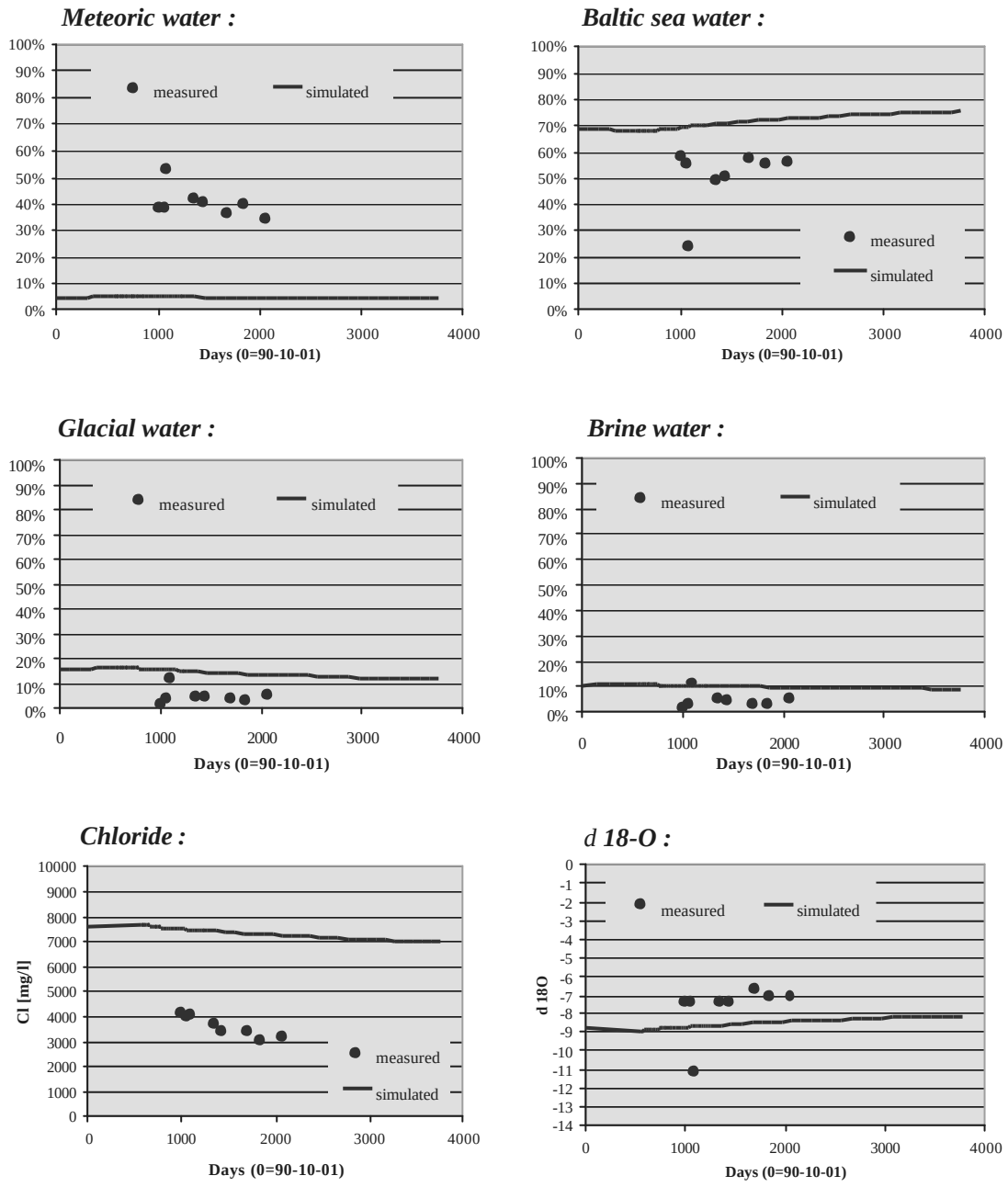

Measured and simulated values of meteoric, Baltic sea, glacial, and brine water, chloride content, and d 18-O at borehole SA1009B.

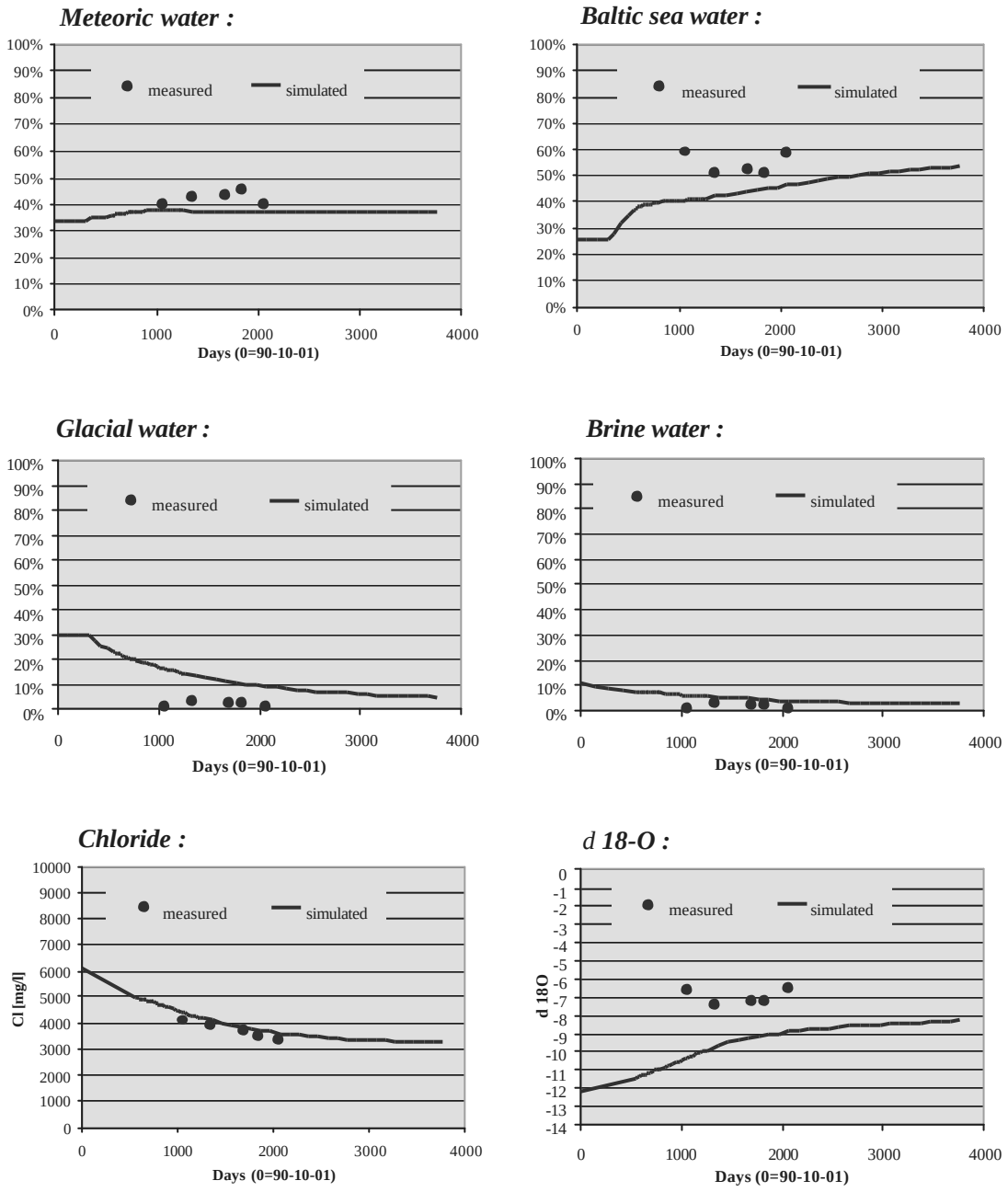

Measured and simulated values of meteoric, Baltic sea, glacial, and brine water, chloride content, and d 18-O at borehole SA1229A (CP 3).

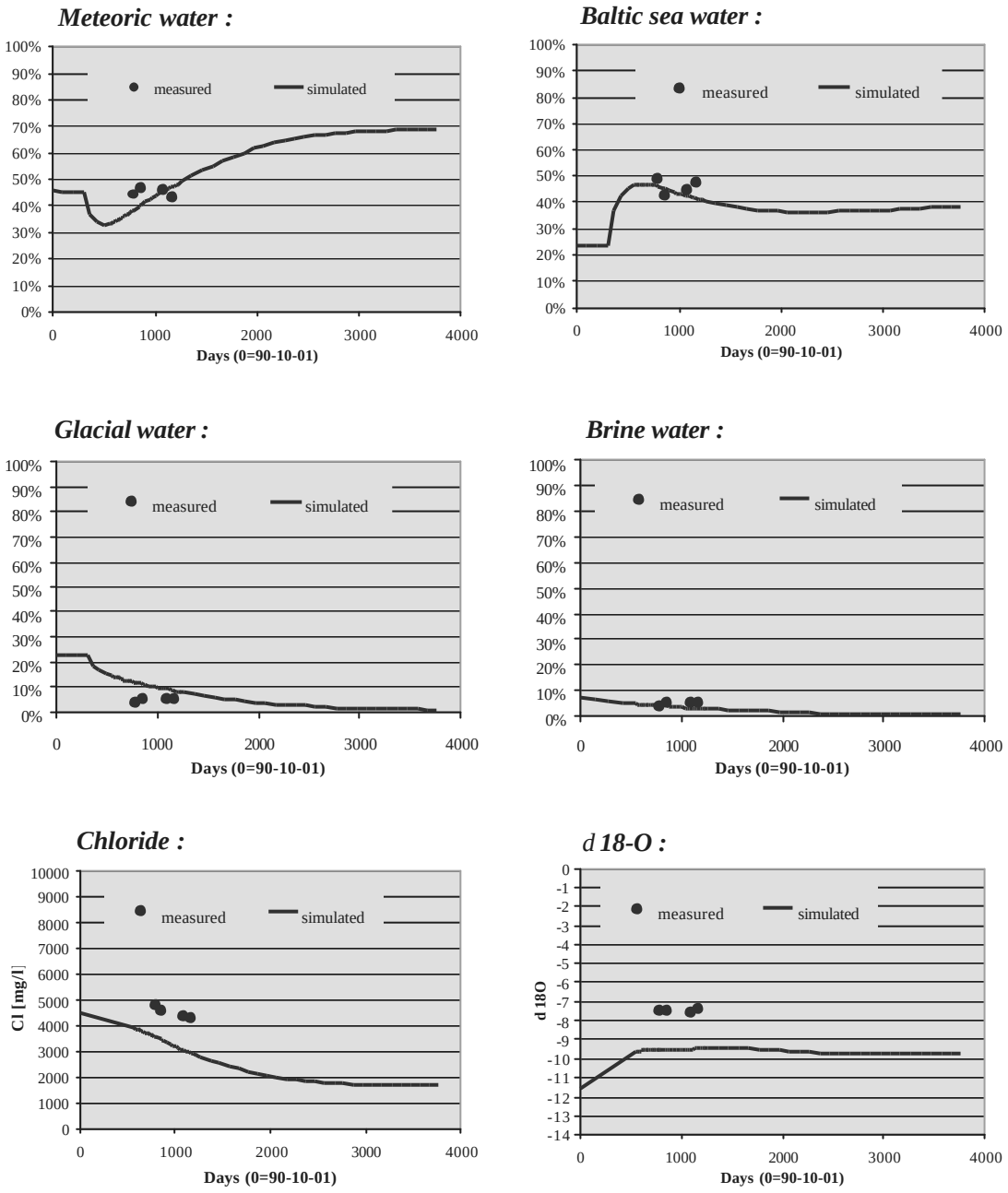

Measured and simulated values of meteoric, Baltic sea, glacial, and brine water, chloride content, and d 18-O at borehole HA1327B.

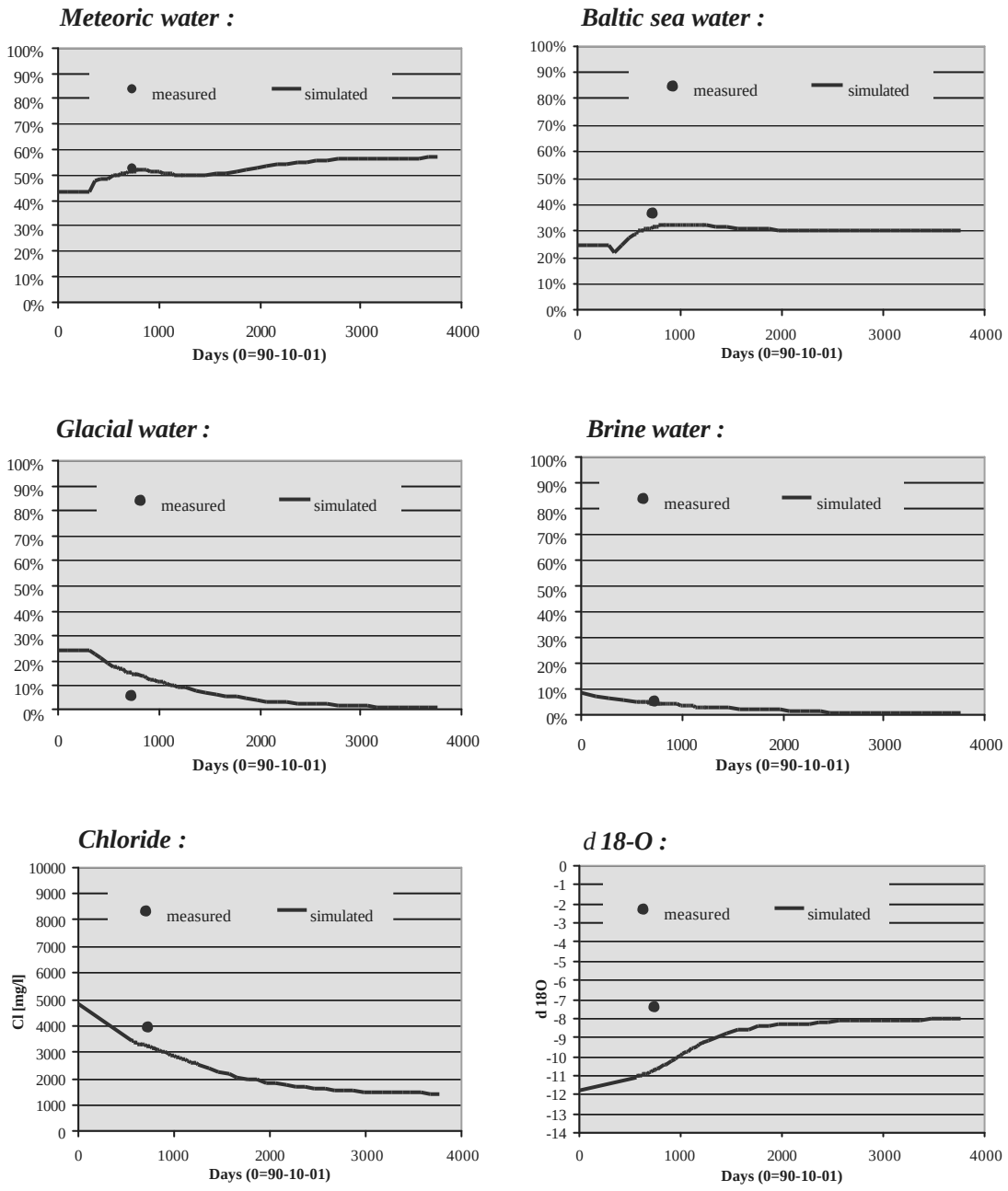

Measured and simulated values of meteoric, Baltic sea, glacial, and brine water, chloride content, and d 18-O at borehole SA1327B (CP 3).

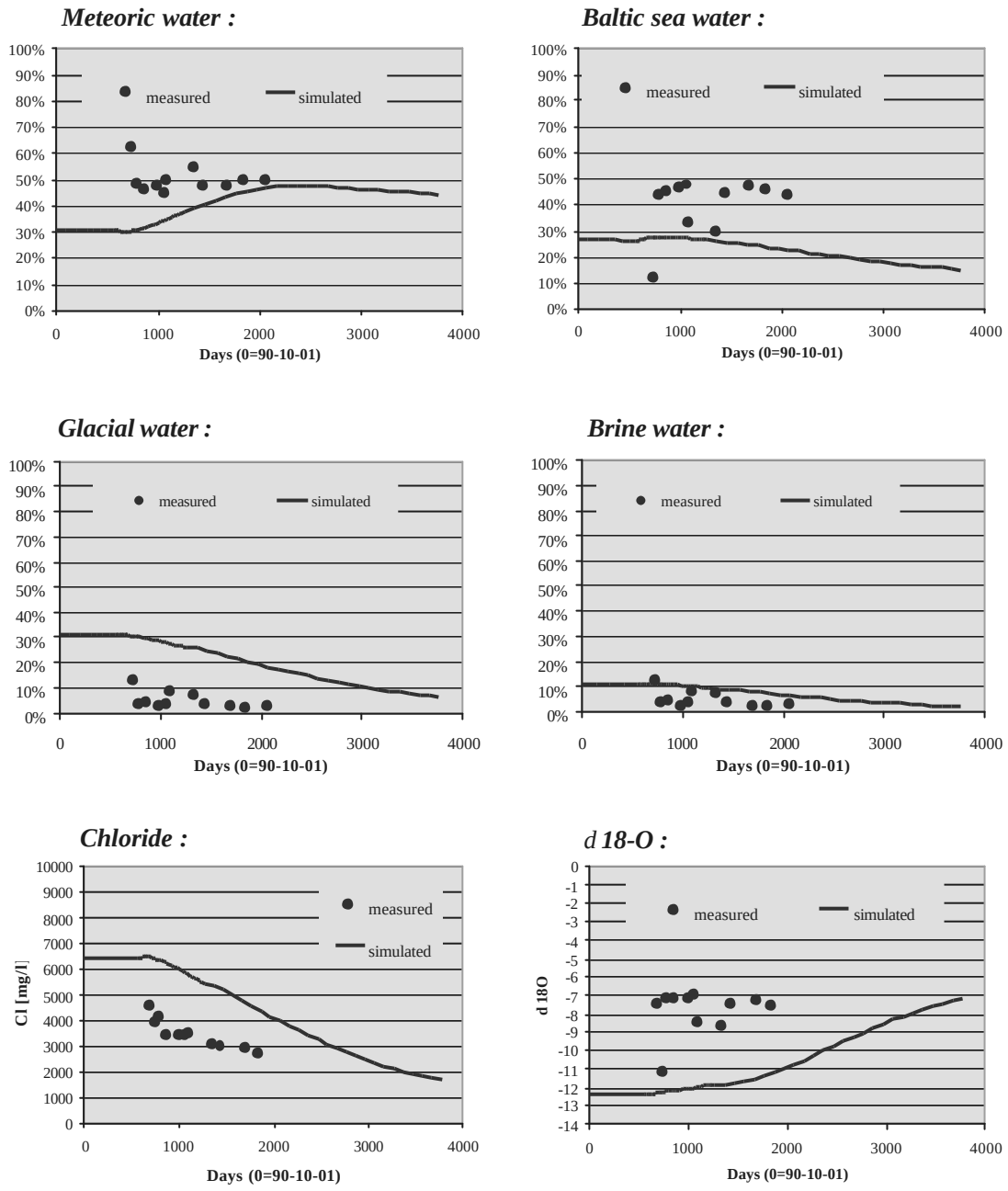

Measured and simulated values of meteoric, Baltic sea, glacial, and brine water, chloride content, and d 18-O at borehole SA1420A.

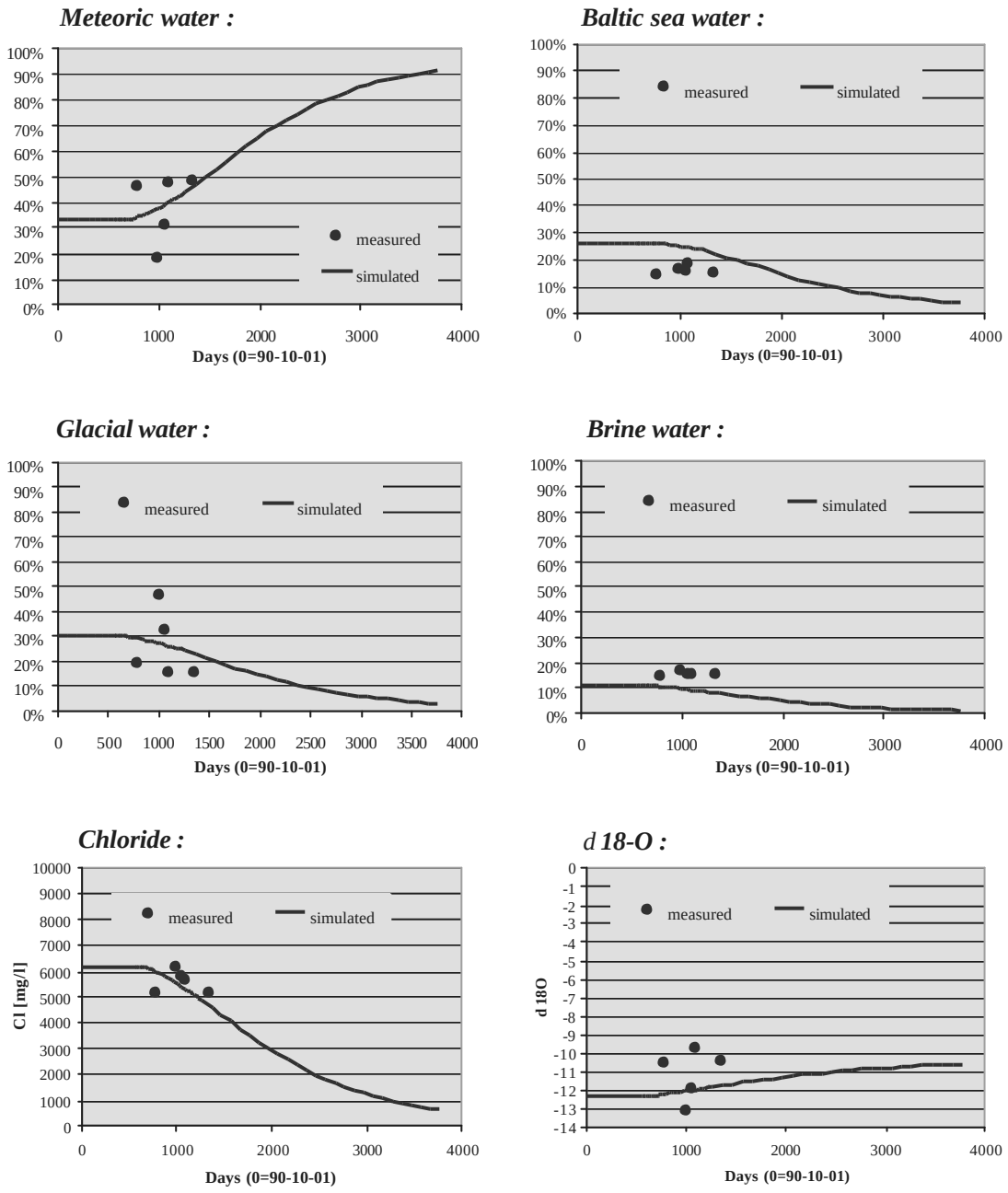

Measured and simulated values of meteoric, Baltic sea, glacial, and brine water, chloride content, and d 18-O at borehole SA1614B.

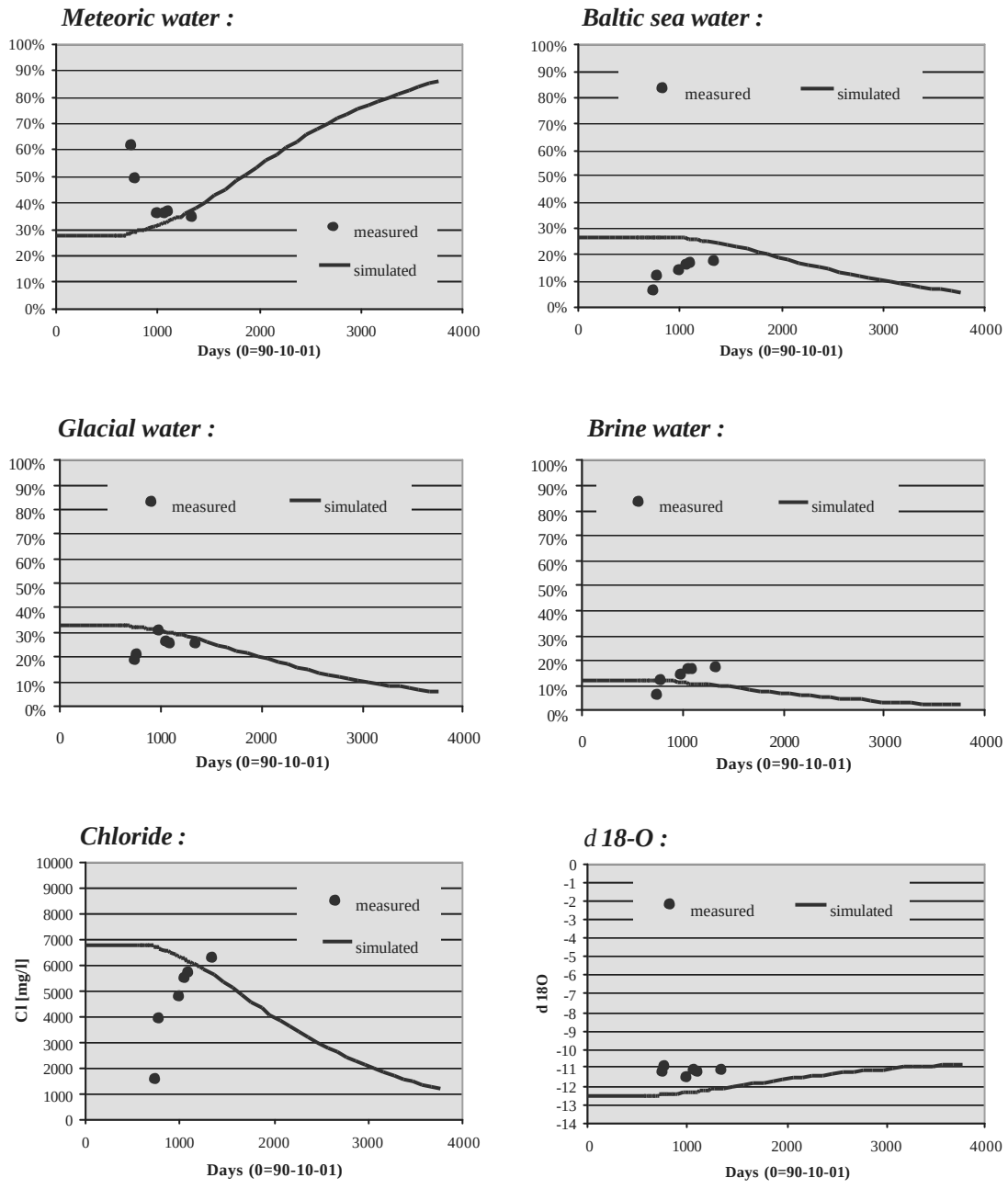

Measured and simulated values of meteoric, Baltic sea, glacial, and brine water, chloride content, and d 18-O at borehole SA1696B.

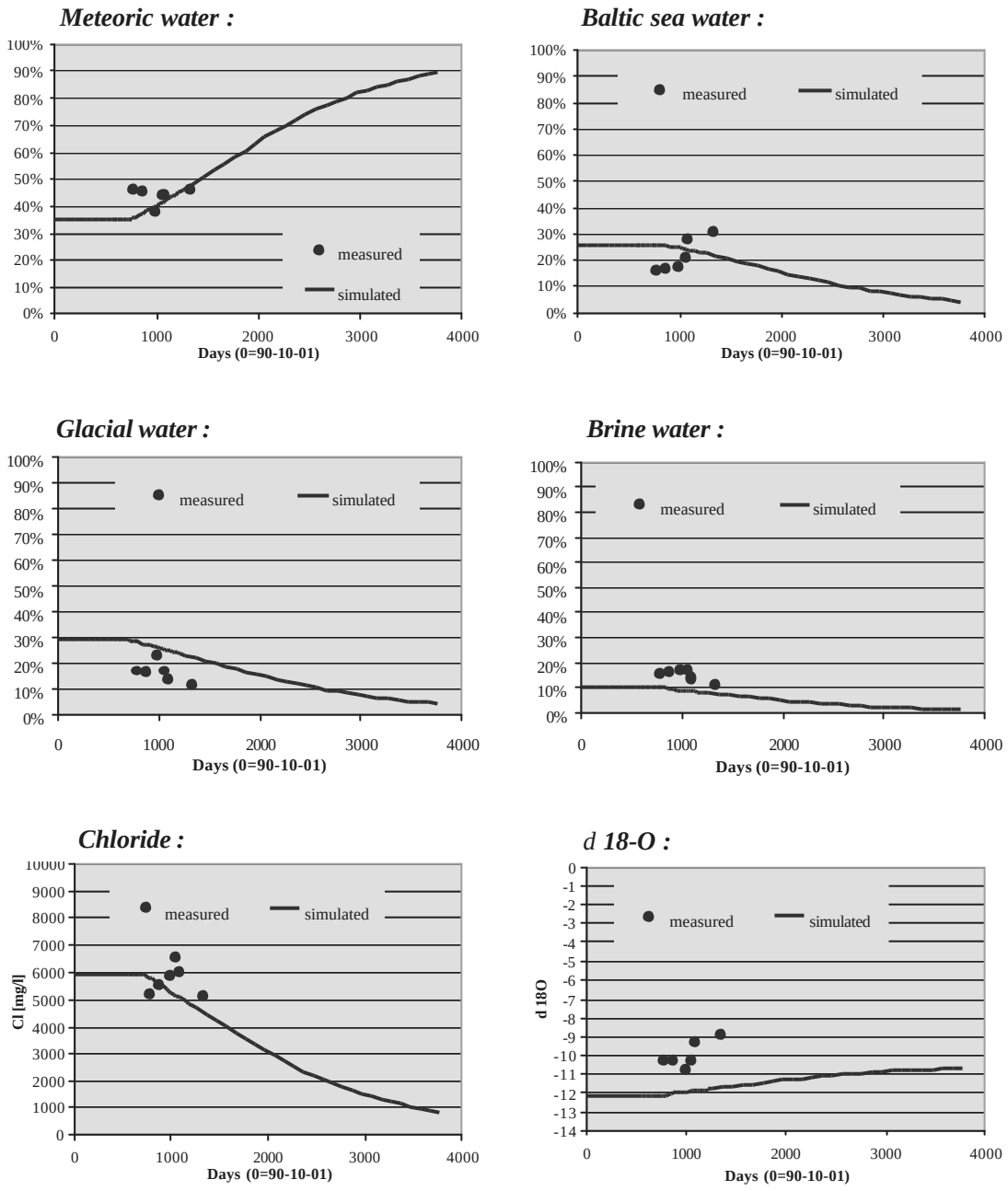

Measured and simulated values of meteoric, Baltic sea, glacial, and brine water, chloride content, and d 18-O at borehole SA1828B.

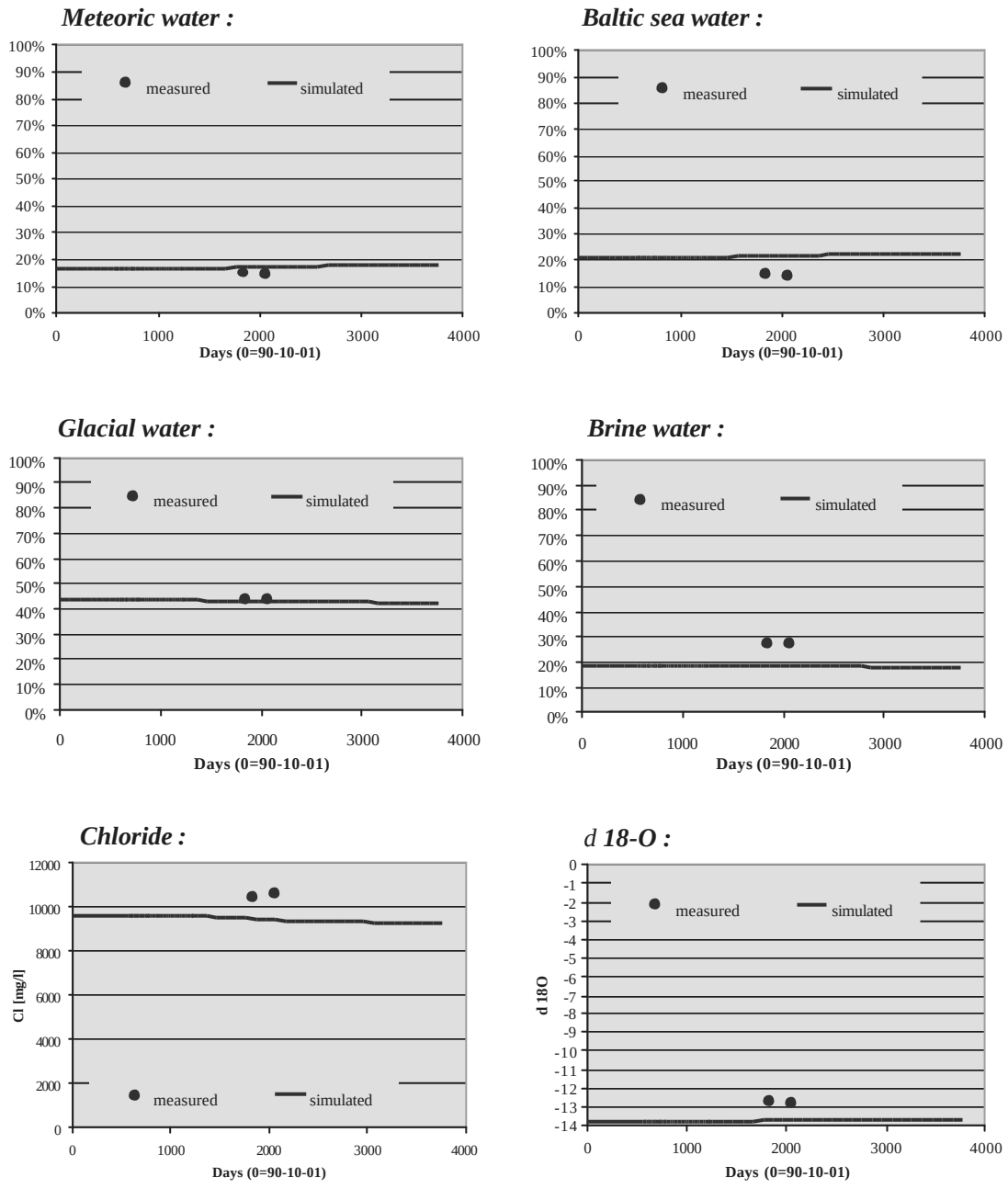

Measured and simulated values of meteoric, Baltic sea, glacial, and brine water, chloride content, and d 18-O at borehole KA1755A (CP 6).

Meteoric water :

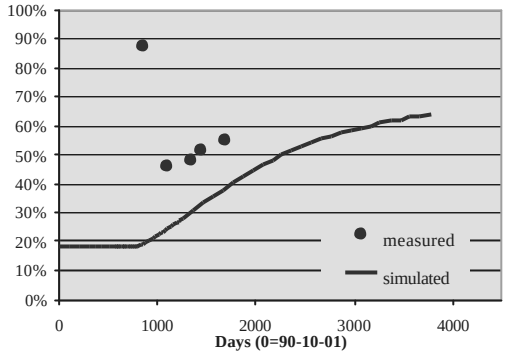

Baltic sea water :

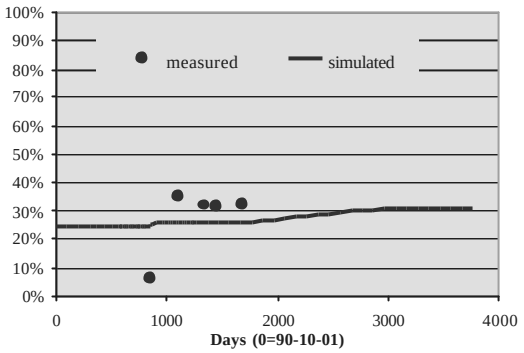

Glacial water :

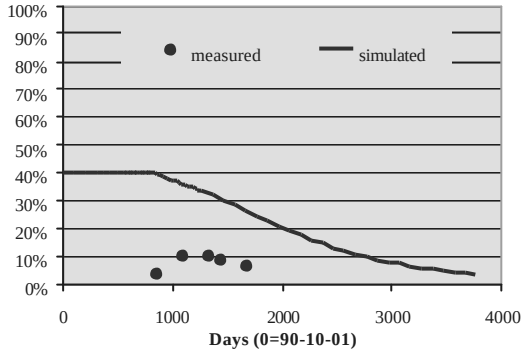

Brine water :

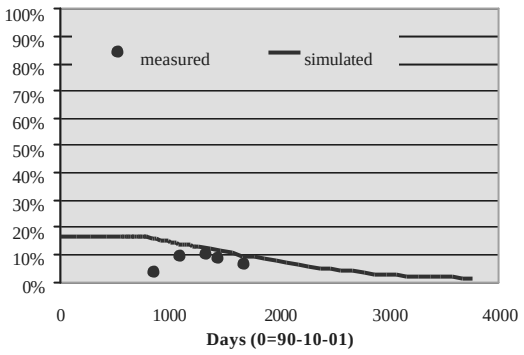

Chloride :

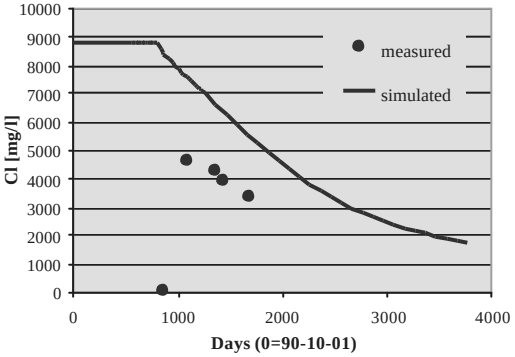

d 18-O :

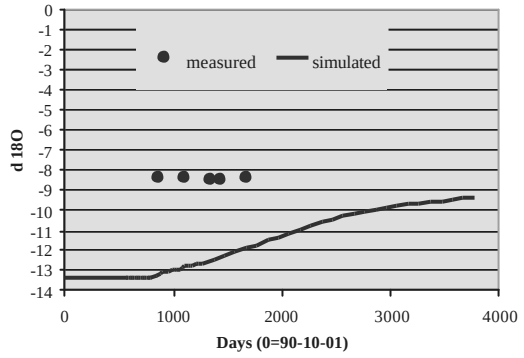

Measured and simulated values of meteoric, Baltic sea, glacial, and brine water, chloride content, and d 18-O at borehole SA2074A (CP 4).

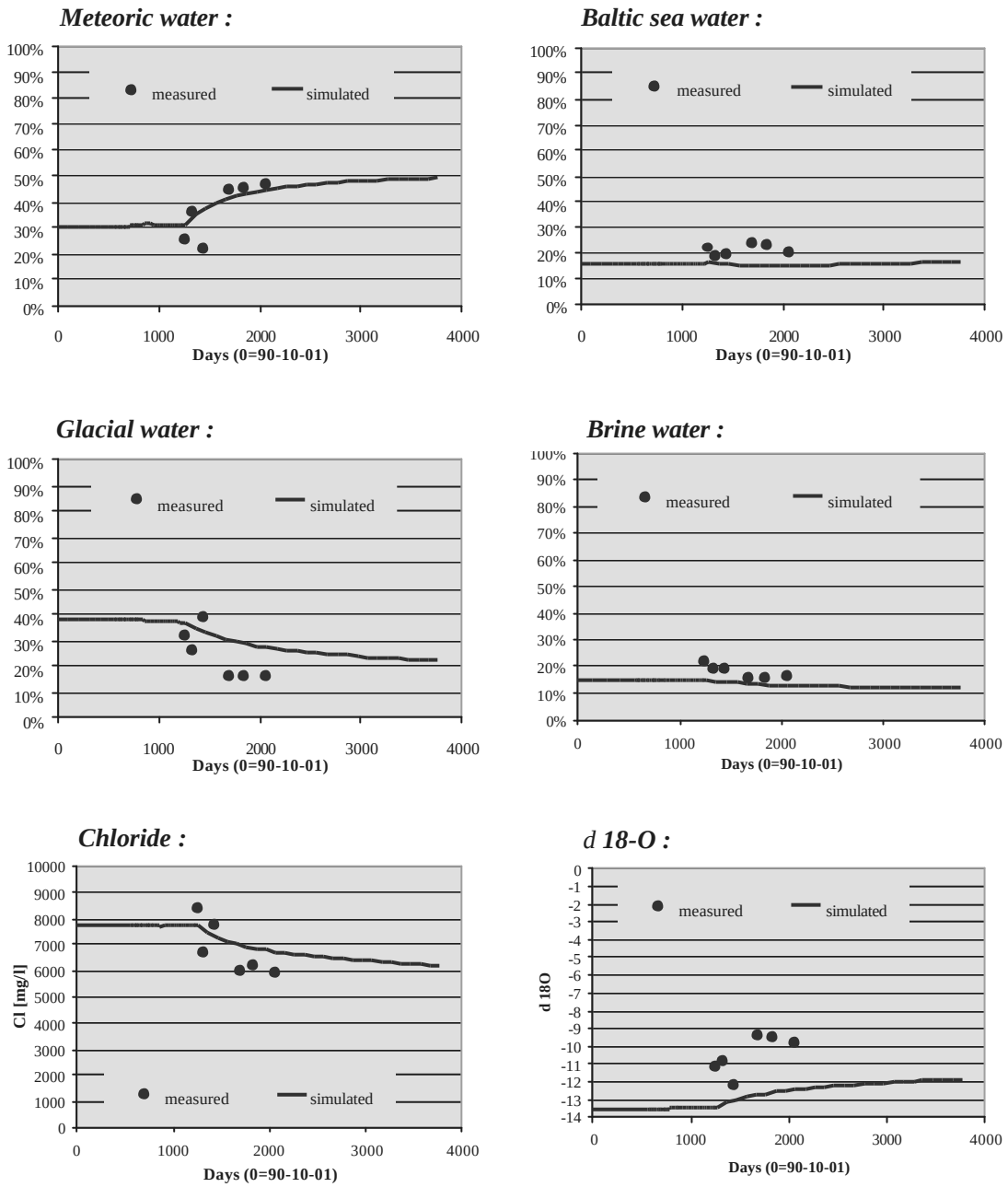

Measured and simulated values of meteoric, Baltic sea, glacial, and brine water, chloride content, and d 18-O at borehole SA2600A.

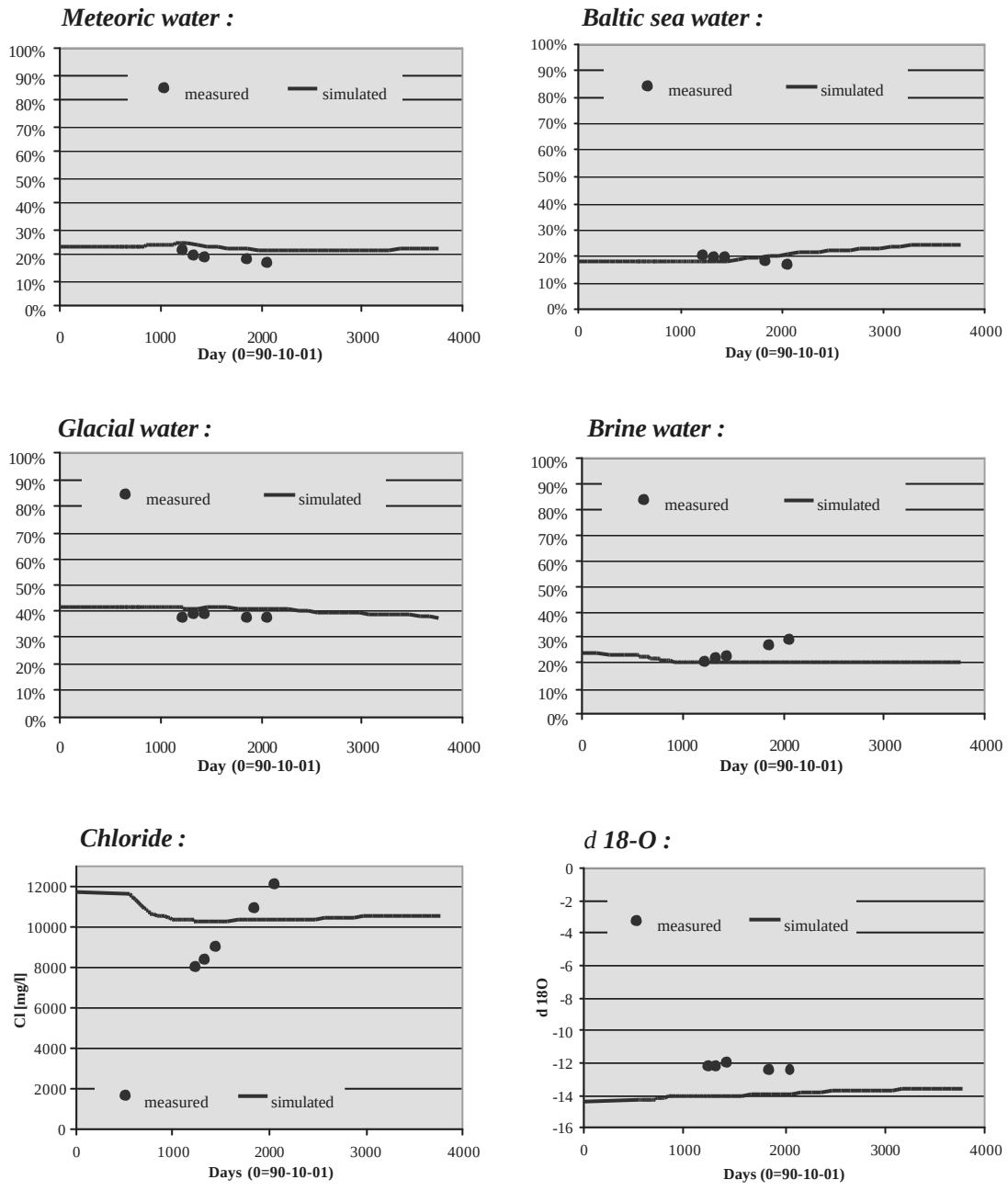

Measured and simulated values of meteoric, Baltic sea, glacial, and brine water, chloride content, and d 18-O at borehole SA2783A (CP 5).

Meteoric water :

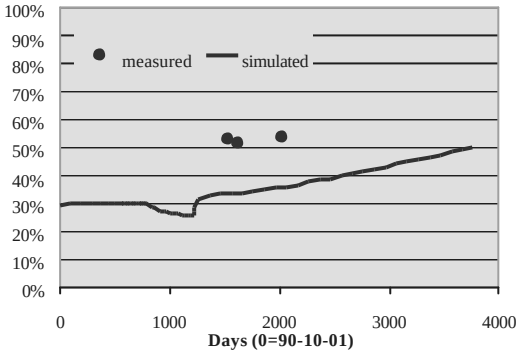

Baltic sea water :

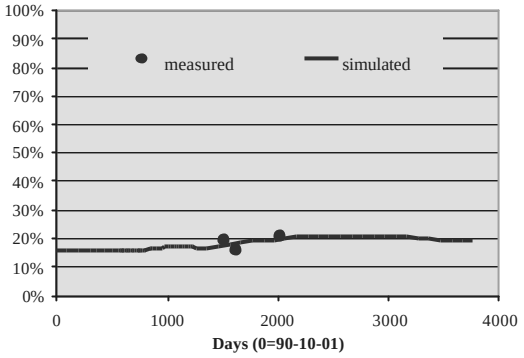

Glacial water :

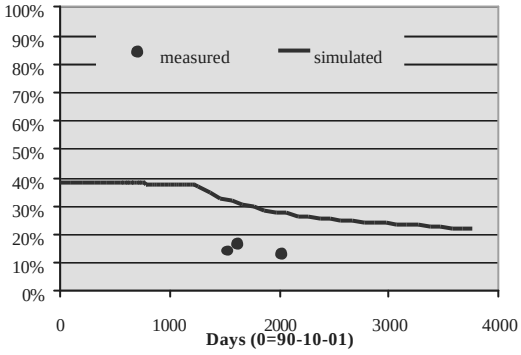

Brine water :

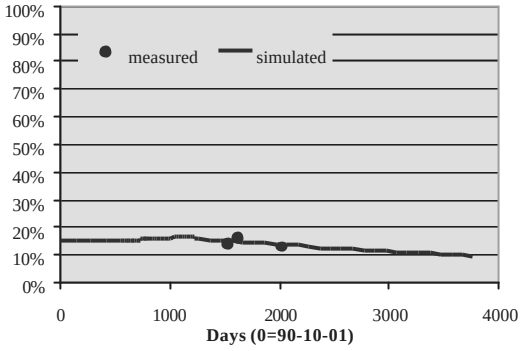

Chloride :

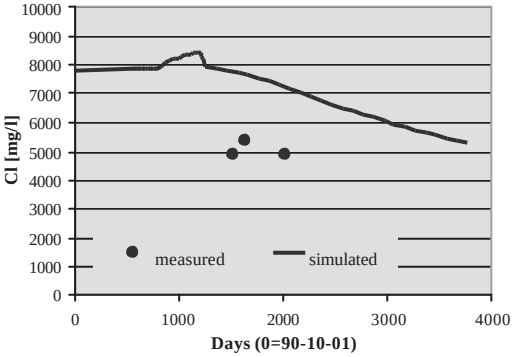

d 18-O :

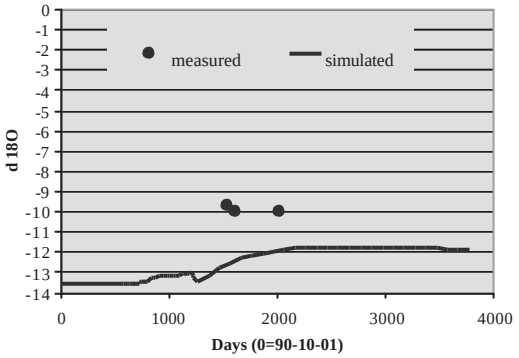

Measured and simulated values of meteoric, Baltic sea, glacial, and brine water, chloride content, and d 18-O at borehole KA3005A (CP 7).

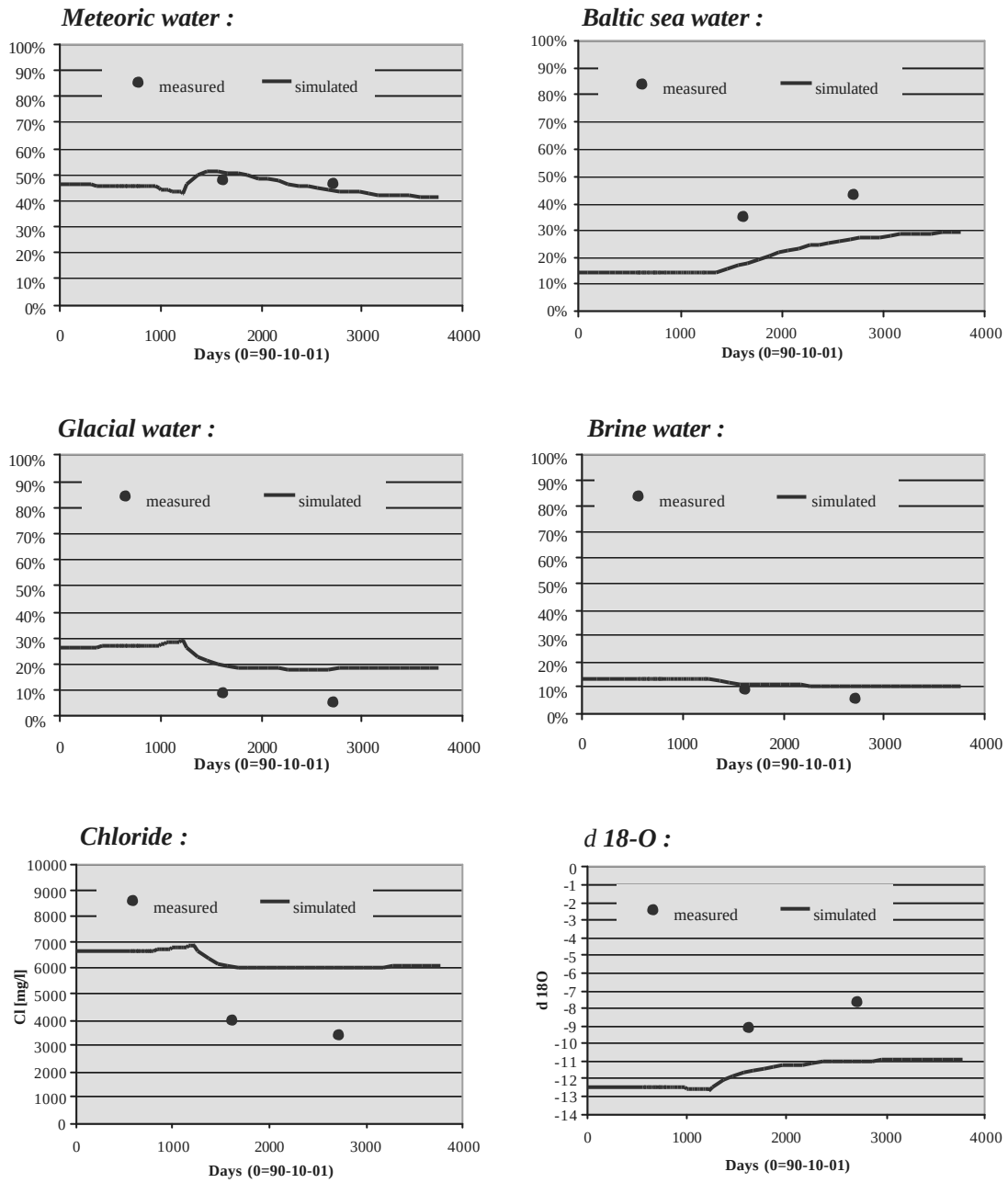

Measured and simulated values of meteoric, Baltic sea, glacial, and brine water, chloride content, and d 18-O at borehole KA3110A (CP 8).

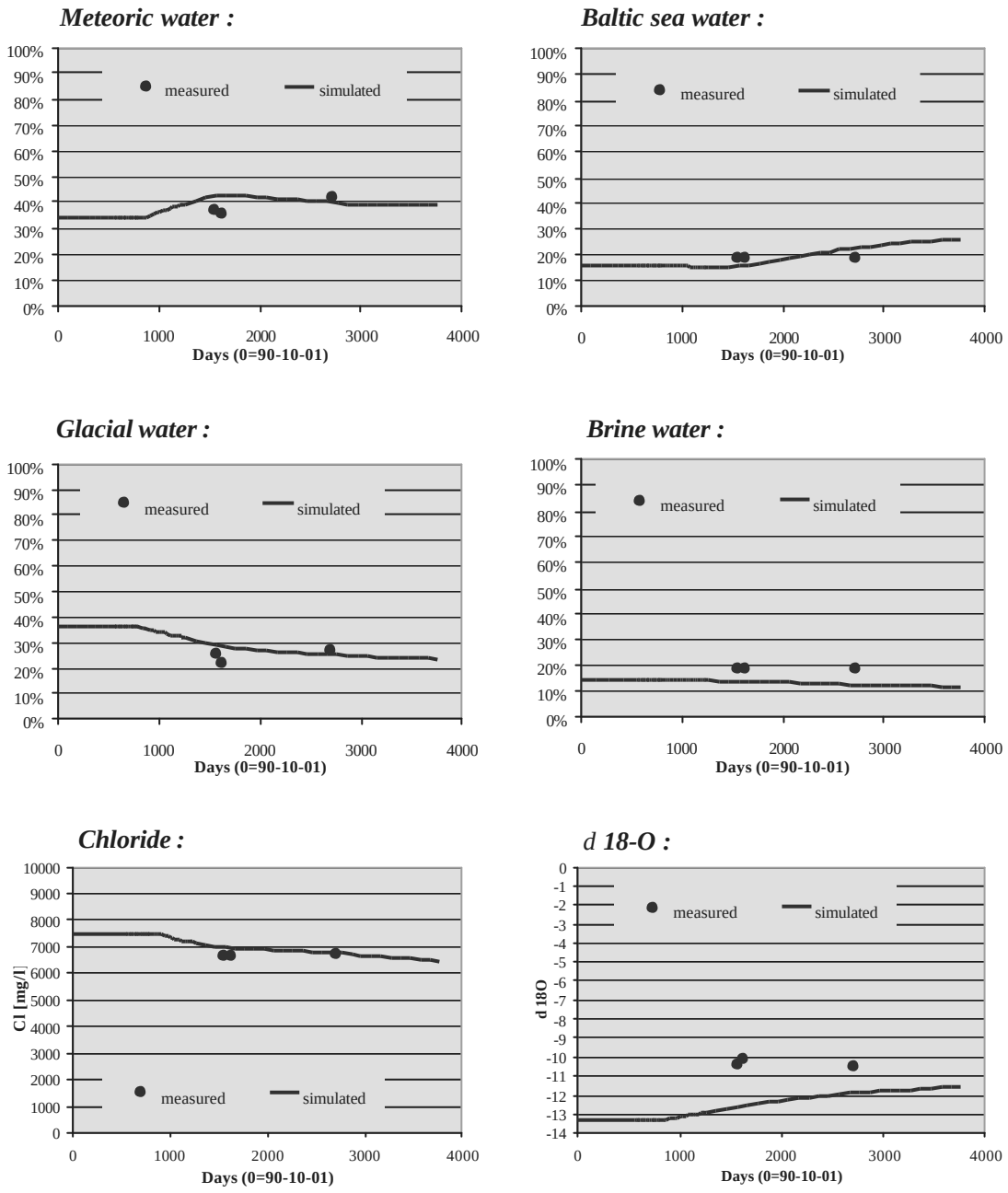

Measured and simulated values of meteoric, Baltic sea, glacial, and brine water, chloride content, and d 18-O at borehole KA3385 (CP 9).

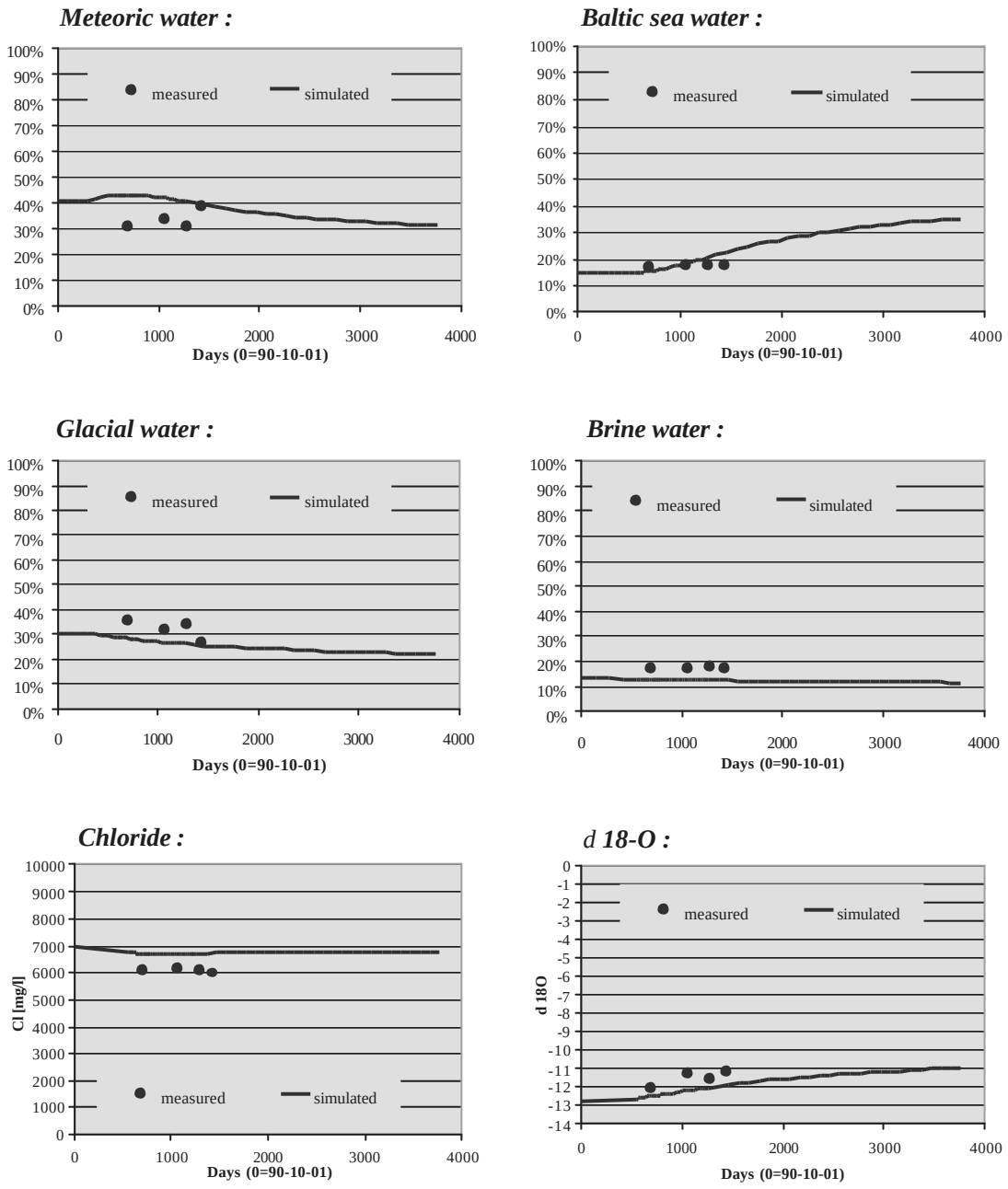

Measured and simulated values of meteoric, Baltic sea, glacial, and brine water, chloride content, and d 18-O at borehole KAS07 (CP 11).

Appendix 3

Calculation of Flow Velocity as a Function of Tracer Concentration

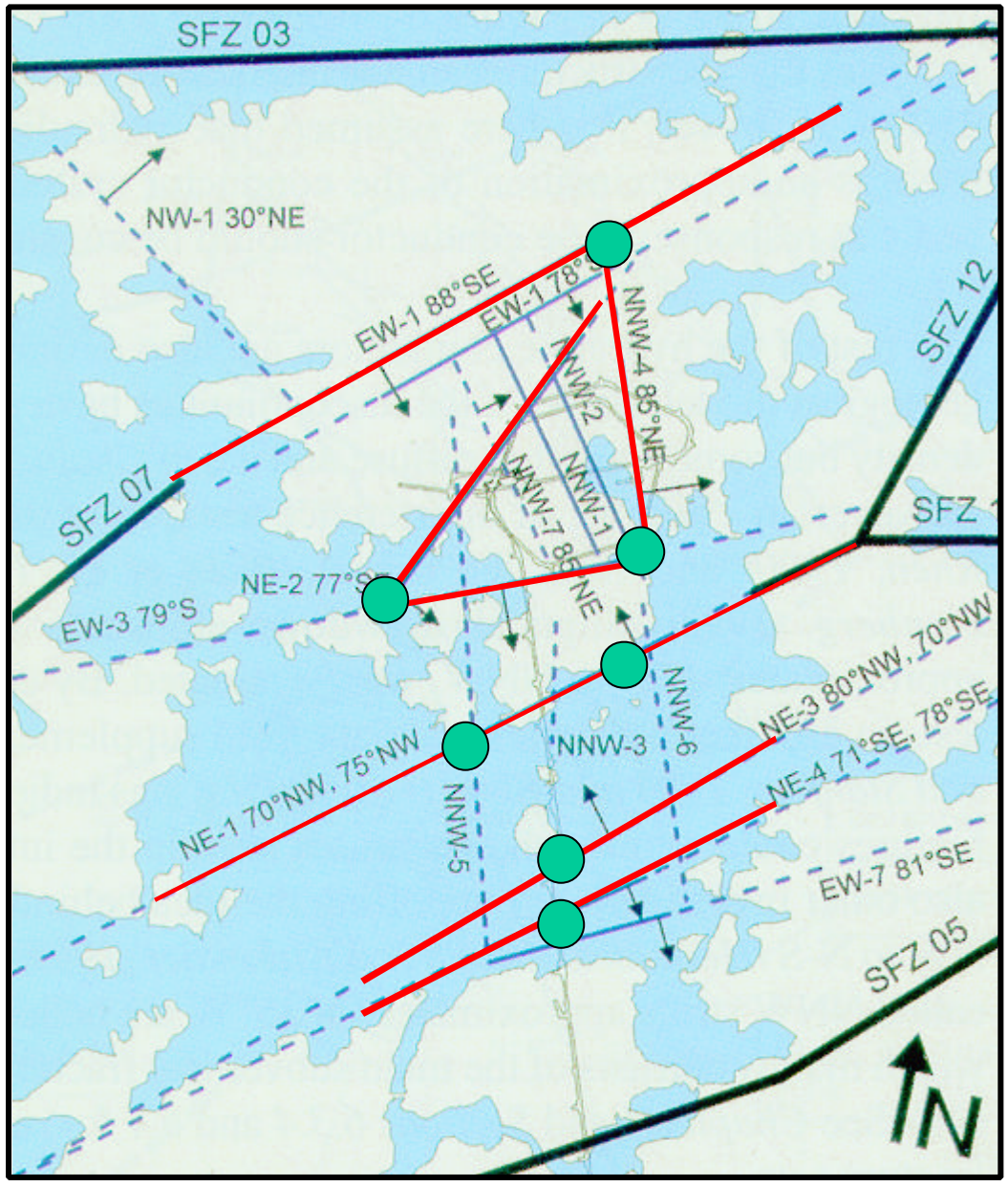

Flow ways in fractures

fracture model

injection point

Appendix 3.1

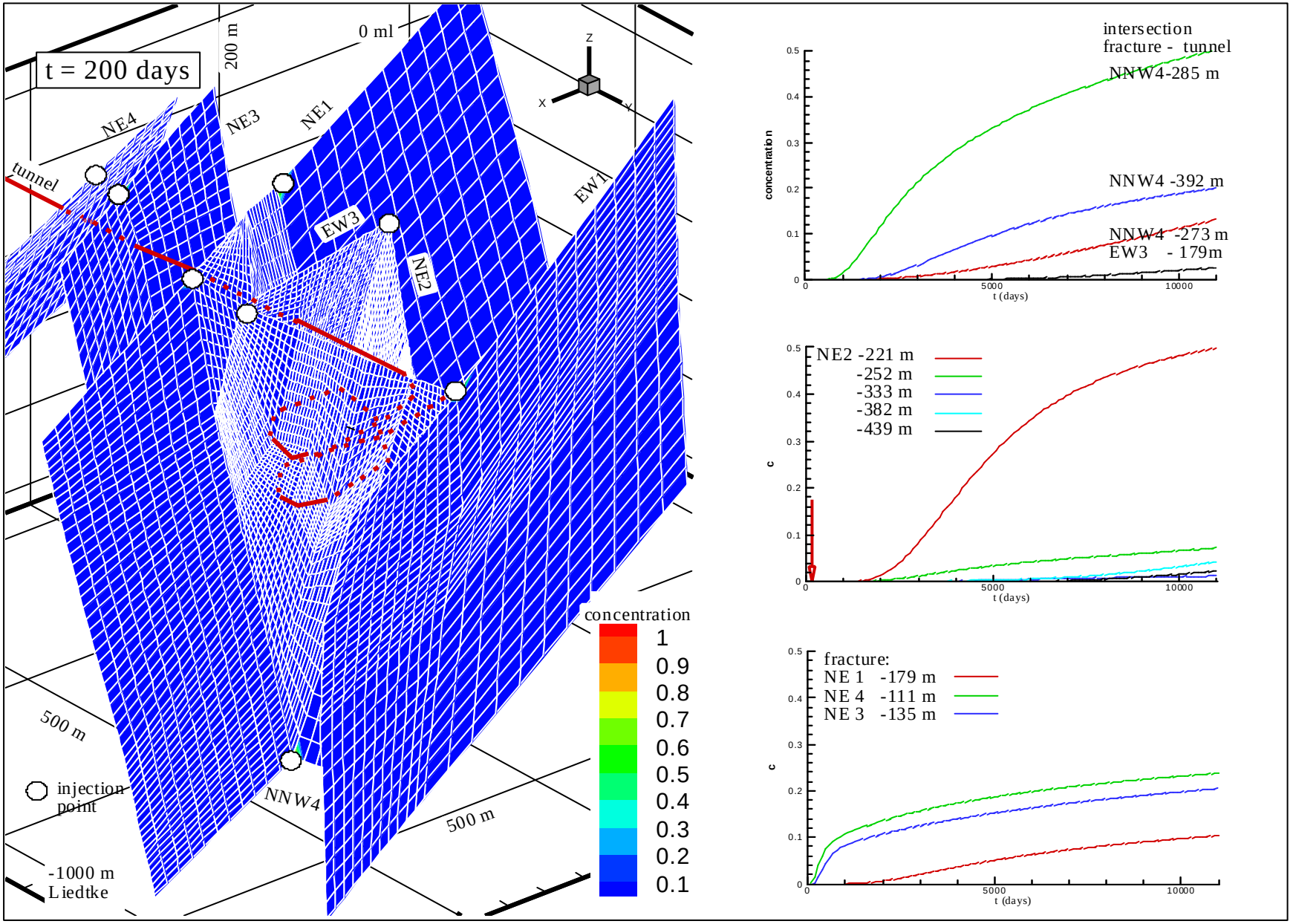
t = 200 days
200 m
0 ml
NE4
NE3
NE1
EW1
EW3
NE2
tunnel
z
x
y
concentration
1
0.9
0.8
0.7
0.6
0.5
0.4
0.3
0.2
0.1
500 m
500 m
injection point
NNW4
-1000 m
Liedtke
intersection
fracture - tunnel
NNW4-285 m
NNW4 -392 m
NNW4 -273 m
EW3 - 179m
concentration
t (days)
NE2 -221 m
-252 m
-333 m
-382 m
-439 m
c
t (days)
fracture:
NE 1 -179 m
NE 4 -111 m
NE 3 -135 m
c
t (days)

Appendix 3.2

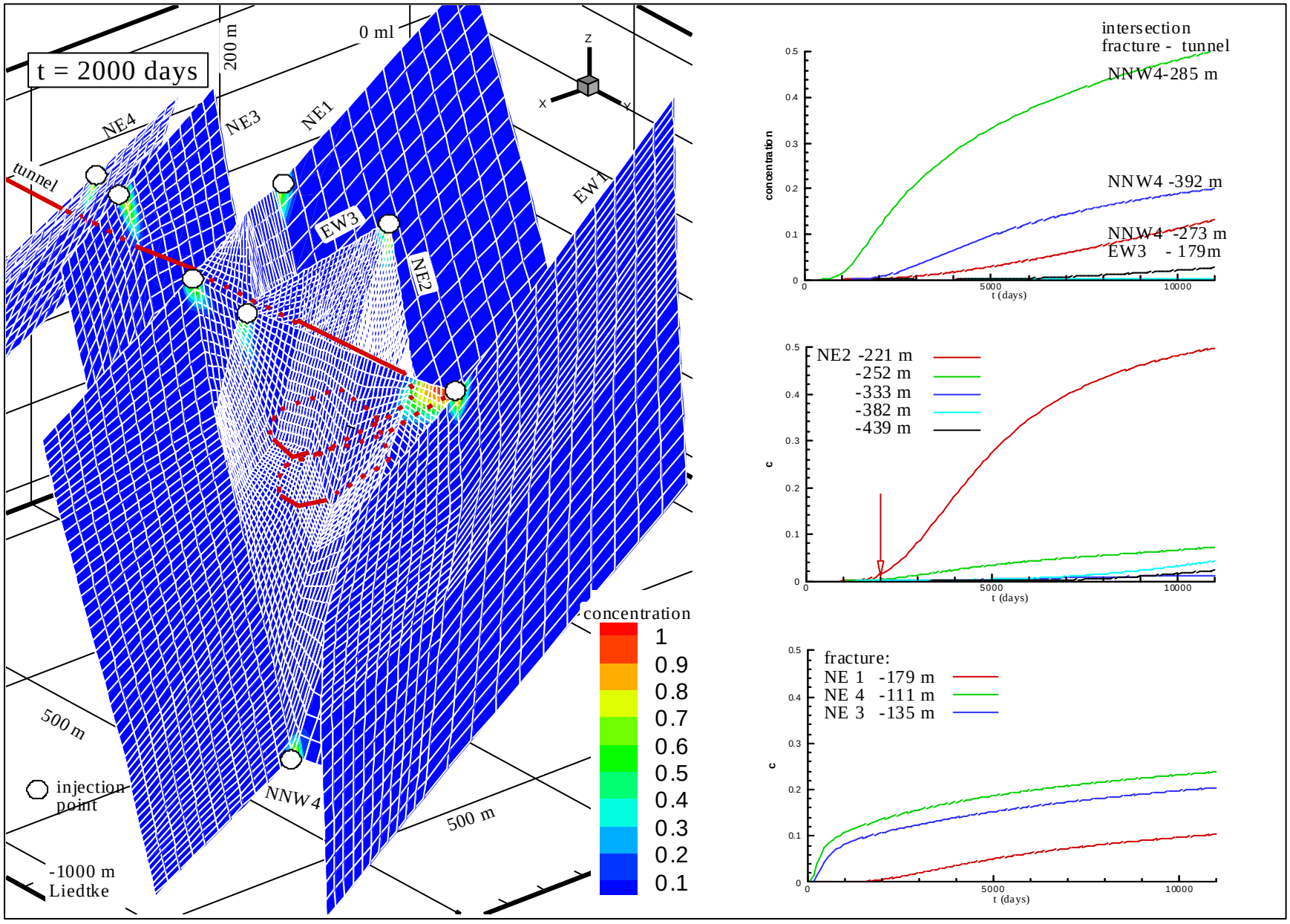
t = 2000 days
200 m
0 ml
NE4
NE3
NE1
tunnel
EW3
NE2
EW1
NNW4
injection point
500 m
500 m
-1000 m
Liedtke
concentration
1
0.9
0.8
0.7
0.6
0.5
0.4
0.3
0.2
0.1
intersection
fracture - tunnel
NNW4-285 m
NNW4 -392 m
NNW4 -273 m
EW3 - 179m
concentration
t (days)
NE2 -221 m
-252 m
-333 m
-382 m
-439 m
c
t (days)
fracture:
NE 1 -179 m
NE 4 -111 m
NE 3 -135 m
c
t (days)

Appendix 3.3

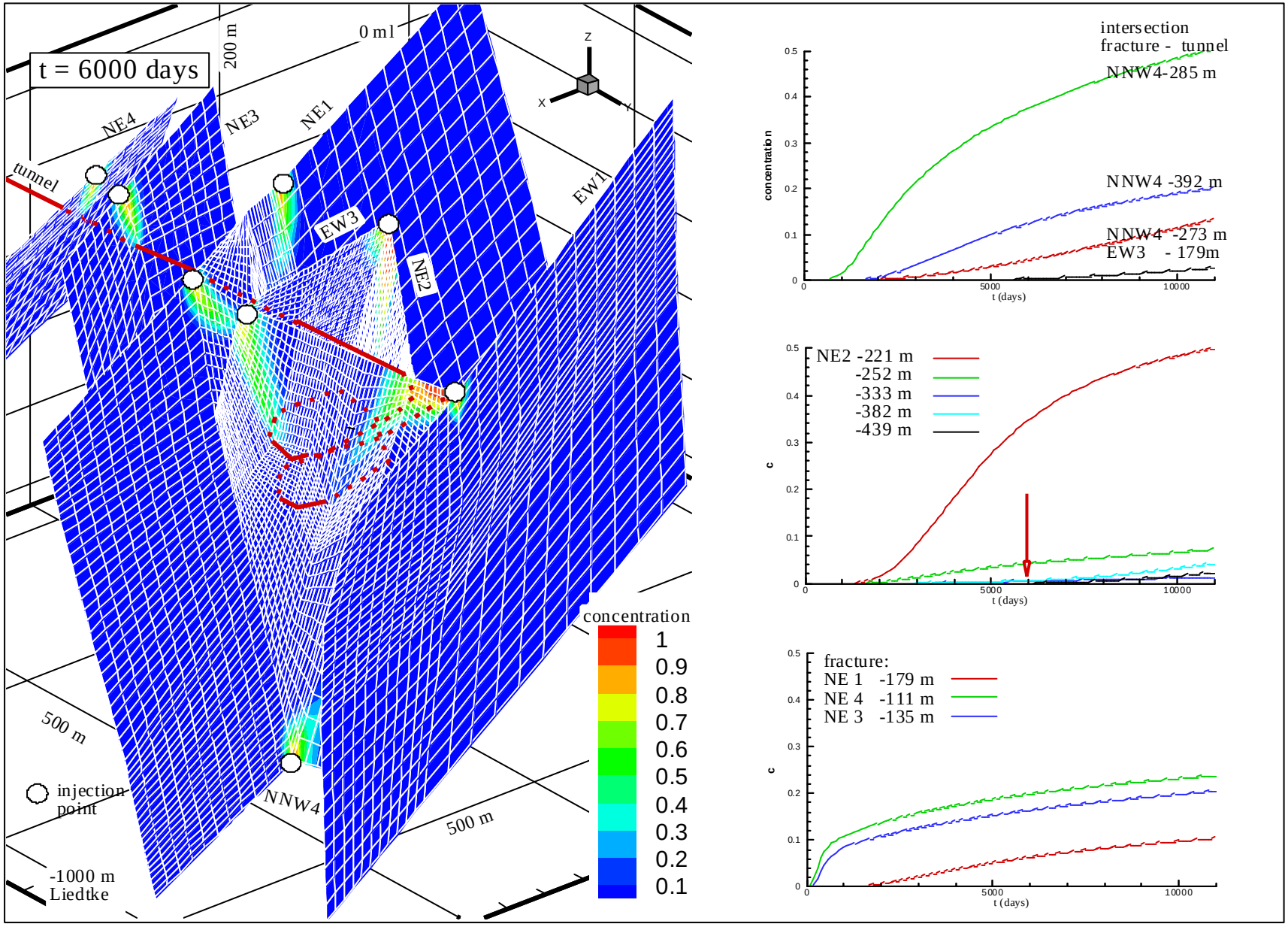
t = 6000 days
200 m
0 ml
NE4
NE3
NE1
EW1
EW3
NE2
tunnel
z
x
y
concentration
1
0.9
0.8
0.7
0.6
0.5
0.4
0.3
0.2
0.1
500 m
500 m
injection point
NNW4
-1000 m
Liedtke
intersection
fracture - tunnel
NNW4-285 m
NNW4 -392 m
NNW4 -273 m
EW3 - 179m
concentration
t (days)
NE2 -221 m
-252 m
-333 m
-382 m
-439 m
c
t (days)
fracture:
NE 1 -179 m
NE 4 -111 m
NE 3 -135 m
c
t (days)

Appendix 3.4

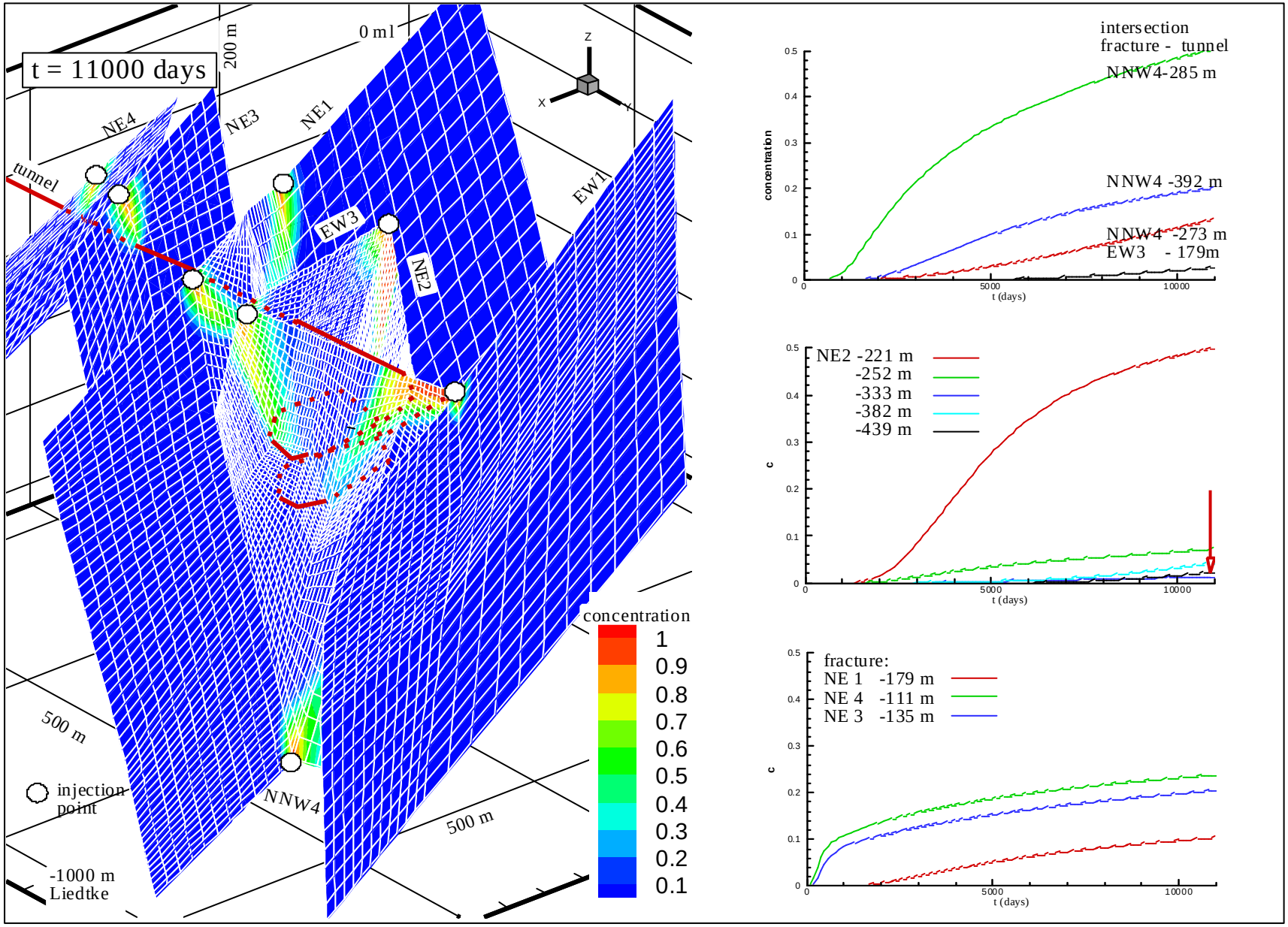
t = 11000 days
200 m
0 ml
NE4
NE3
NE1
EW1
EW3
NE2
tunnel
z
x
y
concentration
1
0.9
0.8
0.7
0.6
0.5
0.4
0.3
0.2
0.1
500 m
500 m
injection point
NNW4
-1000 m
Liedtke
intersection
fracture - tunnel
NNW4-285 m
NNW4 -392 m
NNW4 -273 m
EW3 - 179m
concentration
t (days)
NE2 -221 m
-252 m
-333 m
-382 m
-439 m
c
t (days)
fracture:
NE 1 -179 m
NE 4 -111 m
NE 3 -135 m
c
t (days)

Appendix 3.5

fracture (days)	z	first arrival time (days)	t_5	t_{10}	t_{50}	distance	velocity v_0	v_5	v_{10}	v_{50}
(m)	(m)					(m)	(m/day)	(m/day)	(m/day)	(m/day)
NNW4	-273	1000	6500	9400	-	340	2.9	0.2	0.1	
NNW4	-285	500	1500	1900	-	307	1.6	0.3	0.3	
NNW4	-392	1300	3600	5200	-	480	2.7	0.4	0.3	
NNW4	-417	3200	-	-	-	450	7.1			
EW3	-179	1800	-	-	-	322	5.6			
NE2	-221	1000	2700	3300	11000	340	2.9	0.4	0.3	0.1
NE2	-252	1100	7300	-	-	555	2.0	0.2		
NE2	-333	2100	-	-	-	422	5.0			
NE2	-382	1500	-	-	-	685	2.2			
NE2	-439	3700	-	-	-	579	6.4			
NE1	-179	1000	5000	10500	-	391	2.6	0.2	0.1	

max = 10,000 days

Flow velocity
in the fractures

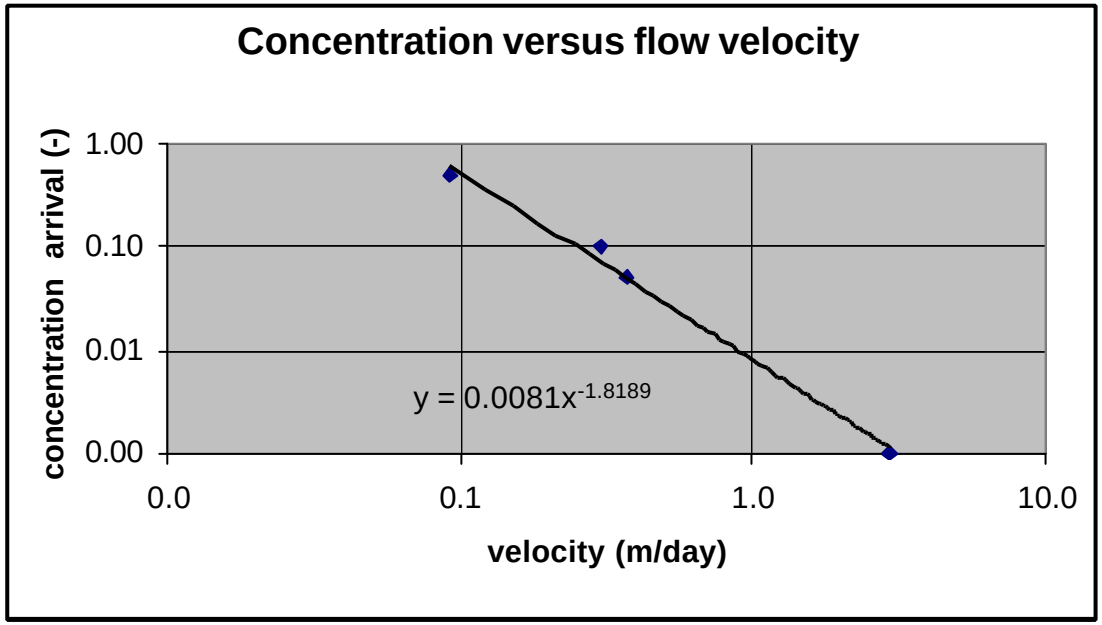

Appendix 3.6

Appendix 4

Modelling Questionnaire for Task 5

MODELLING QUESTIONNAIRE FOR TASK 5, BMWi

worked October 1999

This is a Modelling Questionnaire prepared by SKB based on discussions within the Task Force group. It should be answered when reporting Task 5 in order to simplify the evaluation process of the modelling exercise. Preferably, include this response in an appendix to your forthcoming report.

1. SCOPE AND ISSUES

a) What was the purpose for your participation in Task 5?

- *Validate the numerical tool that was used for flow and transport simulations; further development of this tool with respect to chemical and density effects*
- *Similar to the objectives set up for Task 5: use and integration of hydrochemical data; application of a chemical model simultaneous to hydrological computations with the aim of finally coupling different models; achieve consistency of the models*
- *Furthermore, the purpose was to demonstrate the possibility of calculating transport processes with a large scale 3-dimensional hydraulic mode, and to identify flow paths and flow velocities considering chemical components and possible reactions. In this way - knowing the permeability distribution - the expansion of radioactive substances to the biosphere after the backfilling of a future repository is possible. The Äspö HRL serves as a modelling example for the procedure.*

b) What issues did you wish to address through participation in Task 5?

- *Assess the extent of influence of chemical reactions on the groundwater chemistry at Äspö (granitic environment)*

2. CONCEPTUAL MODEL AND DATA BASE

a) Please describe your models using tables 1-3 in the appendix.

- *See tables 1 to 3*

b) To what extent have you used the data sets delivered? Please fill in Table 4 in the appendix.

- *See table 4*

c) Specify more exactly what data in the data sets you actually used? Please fill in "Comments" in Table 4

- *See table 4*

d) What additional data did you use if any and what assumptions were made to fill in data not provided in the Data Distributions but required by your model? ? Please add in the last part of Table 4.

- *See table 4*

e) Which processes are the most significant for the situation at the Äspö site during the simulation period?

- *The changes in the flow pattern due to the excavation of the tunnel are the most important processes for the simulation period and have to be considered. The resulting drawdown controls the mixing processes as well as the flow velocities and flow direction. From the chemical point of view, the abundance of oxygen contained in the inflowing surface water also has a great influence on the dominant chemical reactions and existing species.*

2. MODEL GEOMETRY/STRUCTURAL MODEL

a) How did you geometrically represent the ÄSPÖ site and its features/zones?

- *The Äspö site is represented by a number of deterministic fracture zones that were treated as two-dimensional planes cropping out at the surface; the rock matrix (rock mass domains) between the hydraulic features was ignored*

b) Which features were considered the most significant for the understanding of flow and transport in the ÄSPÖ site, and why?

- *The selected discrete fracture zones (specified in Table 1) were considered to be the most important ones. On the one hand, they show the highest transmissivities or inflow rates to the tunnel respectively that justify their importance in the dynamic system. On the other hand, they are representative of the regional fracture system, they are located in the central area of the HRL, and extend to several hundred metres. For this reason, fractures are also included that are not intersected by the tunnel.*

c) Motivate selected numerical discretization in relation to used values of correlation length and/or dispersion length.

- *The stability and available time for the calculations were decisive for the numerical discretization. The used values for dispersion were defined considering the element dimensions.*

4a. MATERIAL PROPERTIES – HYDROGEOLOGY

a) How did you represent the material properties in the hydraulic units used to represent the ÄSPÖ SITE?

- *The distribution of the material properties depends on the fracture zones involved. For the most part, the parameters were assigned to the features as a constant value (T, porosity); a few material properties differ from fracture to fracture (width) and have the potential to control characteristic fracture behaviour, e.g. the flow rates to the tunnel.*

b) What is the basis for your assumptions regarding material properties?

- *Material properties are strongly dependent on local conditions that can be observed by a wide scattering of the property parameters in the literature; the varying parameters were taken into consideration to estimate an order of magnitude of the parameter involved which can then be included in the model.*
- *Rock matrix can be ignored.*

c) Which assumptions were the most significant, and why?

- *Almost all fractures are represented by the same material properties; all fractures are comparable; variations of parameter values in one fracture are limited to local areas; the variation of parameter values can for the most part be compensated by an averaged value.*
- *Ignoring the rock mass domains may have an influence on the storage capacity; the drawdown simulated in the fractures is too fast in some cases and has to be controlled with recharge rates.*

4b. CHEMICAL REACTIONS – HYDROCHEMISTRY

a) What chemical reactions did you include?

- *A part of the reactions suggested in the paper of M. Laaksoharju: " Groundwater reactions to consider within the Task 5 modelling" delivered with data 14*
- *Chemical calculations are carried out independently of the regional flow and transport model; specific control points were chosen to carry out chemical investigations*
- *Sulphate and carbonate chemistry (diss./prec. of calcite, gypsum, dolomite, degassing of CO2(g))*

b) What is the basis for your assumptions regarding the chosen chemical reactions?

- *Every chemical component was assigned one characteristic chemical reaction that explains gain or loss of this species. A comparison of calculated element concentrations following the conservative mixing model approach compared to measured element concentrations in the water samples was used to identify deviations which may be explained by chemical reactions.*
- *Available and usable data base from measurements and sampling; Al-measurements were not available thus e.g. silicate reactions could not be included*

c) Which reactions were the most significant, and why?

- *The assessment of which reactions are the most significant depends on the identification of deviations in measured concentrations and the modelled mixing distribution. The most significant deviations occur for Ca^{2+}, Mg^{2+}, HCO_3^-, and SO_4^{2-}. The reactions looked at more closely include these components.*

5a. BOUNDARY CONDITIONS FOR HYDROGEOLOGICAL MODEL (Flow and Transport)

a) What boundary conditions were used in the modelling of the ÄSPÖ site tests?

- *No-flow at bottom*
- *Recharge rate for Äspö Island (upper boundary)*
- *Prescribed groundwater heads of zero at vertical boundaries and for the Baltic Sea (upper boundary)*
- *Prescribed inflow rates to the tunnel (internal boundaries)*

- *For transport calculations: interpolation of grid data from M3 calculations with boundary and initial conditions; hydrochemical conditions were assigned to the discrete fractures*
- *Vertical, upper and bottom boundaries: fixed water composition corresponding to the initial conditions*

b) What was the basis for your assumptions regarding boundary conditions?

- *BC must represent the regional hydraulic and chemical conditions*
- *Construct a model that represents large scale processes and focuses on the spiral tunnel as the central part of the model*
- *Usefulness of interpolated grid data for the mixing proportions*
- *Model not sensitive to boundary conditions, model border not reached; but very sensitive to initial distribution*

c) Which assumptions were the most significant, and why?

- *Measured pressure values in boreholes can be used to estimate the lateral extension of the drawdown funnel and the maximum depth of the groundwater table*
- *Vertical and bottom boundaries are for the most part not reached by changes of the flow system and do not influence the central part of the model; fixed pressure and concentrations can be chosen for an influx with a constant composition*

5b. BOUNDARY/INITIAL CONDITIONS FOR HYDROCHEMICAL MODEL

a) What boundary conditions were used in the modelling of the ÄSPÖ site tests?

- *Distribution of reference waters according to M3 grid data*
- *Element concentrations calculated from mixing proportions of reference waters resulting from the transport model*
- *Measured element concentrations at boreholes*

b) What was the basis for your assumptions regarding boundary conditions?

- *Deviations of modelled and measured concentrations of conservative elements are negligible*
- *Conservative elements must be explained by pure mixing, e.g. dilution*

c) Which assumptions were the most significant, and why?

- *Classification and element composition of reference waters according to M3 data is suitable for decribing chemical characteristics at the Äspö site*
- *Deviations of non-conservatives compared to mixing compositions are due to reactions*

6. MODEL CALIBRATION

a) To what extent did you calibrate your model on the provided hydraulic information? (Steady state and transient hydraulic head etc.)

- *Influx to the tunnel measured at the weirs used for assigning flow rates to specific fractures*
- *Inflow of meteoric water into the fractures at top boundaries derived from recharge rate on Äspö given in the literature*
- *Several runs to achieve correspondence with measured time series of heads and flux*

b) To what extent did you calibrate your model on the provided "transport data"? (Breakthrough curves etc.)

- *Change of concentration of the water content*

c) To what extent did you calibrate your model on the provided hydrochemical data? (Mixing ratios; density/salinity etc.)

- *Best fit of mixing proportions / element concentrations at control points and correspondence with time-dependent changes*
- *Change of concentration with time due to mixing processes identified by investigation of conservative species Cl and 18O*

d) What parameters did you vary?

- *Fracture width, permeability, recharge rate, specific storage coefficient; the number of fractures included in the model has been increased permanently*

e) Which parameters were the most significant, and why?

- *Fracture width at tunnel intersection points were varied to control the influx and the recharge rate had great influences on the drawdown extension*

f) Compare the calibrated model parameters with the initial data base - comments?

- *In the whole, the transmissivity has been changed by two orders of magnitude; locally the changes covered three orders of magnitude (+/-); other parameters were varied only in a small range and are mostly similar to the initial parameters*

7. SENSITIVITY ANALYSIS

Identify the sensitivity in your model output to:
a) the discretization used

- *sensitive to irregular shaped (long, narrow) elements and elements with three edges (oscillation); uniform quadrilateral elements preferred*

b) the transmissivity/hydraulic conductivity (distribution) used
c) transport parameters used

- *After calculation of the flow velocity, the transport calculation was carried out based on the flow field. This process was executed until the deviations of the measured heads, the amount of water and the concentration had been reduced to an acceptable amount. All three parameters were examined during the calculation process. Therefore, the flow field was controlled several times before the transport was calculated and was compared with the hydraulic parameters*
- *After each iteration process 3-4 fracture zones were added to the fracture network. At first, the most dominant fracture with respect to the hydraulic conditions was examined. At present, 10 fractures have been examined which are connected with each other. The 14-fracture model is ongoing. The concentration of the four waters was controlled by the amounts and flow velocity. Each water has a single meaning during the iteration process.*

d) chemical mixing parameters used

- *Sensitive with regard to initial - interpolated - distribution of mixing fractions*
- *Disagreement of mixing fractions and conservative element concentrations*

e) chemical reaction parameters used

8. LESSONS LEARNED

a) Given your experience in implementing and modelling the ÄSPÖ site, what changes do you recommend with regards to:

- **Experimental site characterisation?**

- *No changes*

- **Presentation of characterisation data?**

- *No changes*

- Performance measures and presentation formats?

- *No changes*

b) What additional site-specific data would be required to make a more reliable prediction of the tracer experiments?

- *Analysis of additional conservative tracers in the water samples (Bromine, reliable Tritium data)*
- *Comparable time series of hydrological and hydrochemical measurements at boreholes; complete or additional analysis (Br^-, Tritium, Al, C and S isotope data), e.g. to consider additional conservative tracers or to assess incongruent hydrolysis processes*

c) What conclusions can be made regarding your conceptual model utilised for the exercise?

- *Conceptual model is suitable for identifying and modelling significant flow and mixing processes connected to the Äspö HRL at the site scale*

- *Main processes included in considering deterministic fractures and ignoring matrix effects*
- *Reproduction of conservative mixing in terms of four reference waters is satisfactory, but must be improved by considering conservative elements like chloride*
- *Groundwater classification into different types very helpful for identification of mixing processes*

d) What additional generic research results are required to improve the ability to carry out predictive modelling of transport on the site scale?

- *Higher resolution and consideration of local differences concerning material properties and model parameters to implement less important features that are controlled by small scale effects*
- *In general bring together the effects identified at different scales to better represent natural conditions and optimise the model output*
- *Recharge rate and amount of infiltration at depth*

9. RESOLUTION OF ISSUES AND UNCERTAINTIES

a) What inferences did you make regarding the descriptive structural-hydraulic model on the site scale for the ÄSPÖ site?

- *Available data base provides an understanding of the hydrological and hydrochemical conditions and allows the development of a suitable conceptual model that accounts for the most significant processes occurring during tunnel construction*
- *Groundwater system can be reproduced including the main structural elements of the site and ignoring the rock mass domain*

b) What inference did you make regarding the active hydrochemical processes, hydrochemical data provided and the hydrochemical changes calculated?

- *The induced mixing processes can largely explain the changing chemical compositions*
- *Conservative mixing approach helps to identify deviations of reactive species*
- *Further deviations can be understood by assuming chemical reactions which are mostly due to changes in the chemical boundary conditions (pH, Eh, which in turn control reactions like calcite dissolution/precipitation, pyrite dissolution, and ion exchange*

c) What issues did your model application resolve?

- *Disturbance of groundwater system as a result of tunnel construction; drawdown funnel; identification of transport processes; illustration of water distribution in the fractures; identification or exclusion of possible reactions; trend of chemical evolution*

d) What additional issues were raised by the model application?

- *Difficulties in explaining chemical development for every component at control points; deviation from general trend may be due to local conditions (e.g. grouting, pumping, in situ tests)*

- *Influence of density effects*
- *It has not been possible to calculate the groundwater lowering three dimensionally considering the two phase flow in the area of Äspö island*
- *The influence of the annual precipitation on the recharging of meteoric water is dependent on the groundwater depression cone of the single fracture system associated with tunnel excavation, theses influences have not been examined sufficiently*

10. INTEGRATION OF THE HYDOGEOLOGICAL AND HYDROCHEMICAL MODELLING

a) How did you integrate the hydrogeological and hydrochemical work?

- *Flow and transport calculations were carried out for a fracture network on a site scale considering chemical conditions by setting up a conservative mixing model using the M3 reference waters*
- *A tool was developed to perform batch reactions with PHREEQC that carries out speciation calculations for the whole fracture network resulting from the mixing model;*
- *chemical calculations carried out with PHREEQC refer to selected control points as well as to the whole fracture domain; the aim wa to identify chemical reactions that account for changes in the chemical water composition at the whole site; integration was achieved by comparing the results of the mixing model with measured element concentrations – deviations indicate possible reactions*

b) How can the integration of the hydrogeological and hydrochemical work be improved?

- *Develop a method for directly coupling conservative transport with a reactive transport model; changing concentrations of non-conservative elements due to reactions must have an influence on ongoing transport calculations and on the characteristics of the chemical environment*

c) Hydrogeologist: How has the hydrochemistry contributed to your understanding of the hydrogeology around the Äspö site?

- *Mixing fractions resulting from M3 approach is a helpful tool to increase the understanding of dominant processes; conservative mixing model contributes to improvement of hydrological model, but does not explain further deviations of non-conservative species*

d) Hydrochemist: How has the hydrogeology contributed to your understanding of the hydrochemistry around the Äspö site?

- *Only if the hydrogeology has been understood completely can assumptions be made on chemical effects; it is necessary to follow a kind of chronological order with iterative interactions*

Table 1 Description of model for water flow calculations

TOPIC	Example	*Our Model*
Type of model	Stochastic continuum model	*Discrete fracture network*
Process description	Darcy´s flow including density driven flow. (Transport equation for salinity is used for calculation of the density)	*Transient saturated Darcy's flow disregarding density effects*
Geometric framework and parameters	Model size: 1.8x1.8x1 km^3 . Deterministic features: All deterministic features provided in the data set. Rock outside the deterministic features modelled as stochastic continuum.	*2 x 1.8 x 1 km^3* *A selection of 10 deterministic features provided in the data set (NE-1, NE-2, NE-3, NE-4, NNW-2, NNW-4, NNW-7, EW-1 78°, EW-1 88°, EW-3)* *Rock domain ignored between deterministic fractures*
Material properties and hydrological properties	Deterministic features: Transmissivity (T), Storativity(S) Rock outside deterministic features: Hydraulic conductivity(K), Specific storage (Ss)	*Deterministic features: Permeability (K), Storativity (S), Fracture aperture (b)* *Rock domain ignored between deterministic fractures*
Spatial assignment method	Deterministic features: Constant within each feature (T,S). No changes due to calibration. Rock outside deterministic features: (K,Ss) log normal distribution with correlation length xx. Mean, standard deviation and correlation based on calibration of the model	*Deterministic features: Constant within each feature (K, S) Fracture aperture different within each fracture, e.g. at tunnel locations* *Rock domain ignored between deterministic fractures*

Boundary conditions	Surface: Constant flux. Sea: Constant head Vertical-North: Fixed pressure based on vertical salinity distribution. Vertical-East: Fixed pressure based on vertical salinity distribution. Vertical-South: Fixed pressure based on vertical salinity distribution. Vertical-West: Fixed pressure based on vertical salinity distribution. Bottom: No flux. Linear change by time based regional simulations for undisturbed conditions and with Äspö tunnel present.	*Surface: Constant flux* *Sea: Constant head* *Vertical-North: Fixed pressure* *Vertical-East: Fixed pressure* *Vertical-South: Fixed pressure* *Vertical-West: Fixed pressure* *Bottom: No flux* *Inner: Flow rates or constant heads respectively* *The water flux in the model is a function of the size of the cone of depression, which depends on the location of the tunnel*
Numerical tool	PHOENICS	*DURST / Rockflow*
Numerical method	Finite volume method	*Finite element method*
Output parameters	Head, flow and salinity field.	*Heads* *Flow field* *Flow velocity and corresponding amount of water*

Table 2 Description of model for tracer transport calculations

TOPIC	EXAMPLE	*Our model*
Type of model	Stochastic continuum model	*Discrete fracture network*
Process description	Advection and diffusion, spreading due to spatially variable velocity and molecular diffusion.	*Advection* *Dispersion* *Diffusion*
Geometric framework and parameters	Model size: 1.8x1.8x1 km^3 . Deterministic features: All deterministic features provided in the data set. Rock outside the deterministic features modelled as stochastic continuum.	*2 x 1.8 x 1 km^3* *A selection of 10 deterministic features provided in the data set (NE-1, NE-2, NE-3, NE-4, NNW-2, NNW-4, NNW-7, EW-1 78°, EW-1 88°, EW-3)* *Rock domain ignored between deterministic fractures*
Material properties	Flow porosity (ne)	*Porosity* *Longitudinal and transverse dispersion* *Diffusion* *Tortuosity*
Spatial assignment method	ne based on hydraulic conductivity value (TR 97-06) for each cell in model, including deterministic features and rock outside these features.	*Deterministic values for all features*
Boundary conditions	Mixing ratios for end members as provided as initial conditions in data sets.	*Mixing ratios for reference waters derived and interpolated for discrete fractures as provided as initial conditions in data sets.*
Numerical tool	PHOENICS	*DURST / Rockflow*
Numerical method	Particle tracking method or tracking components by solving the advection/diffusion equation for each component	*Finite element method*
Output parameters	Breakthrough curves	*Concentrations of reference waters*

Table 3 Description of model for chemical reactions calculations

TOPIC	EXAMPLE	*Our model*
Type of model	xxx	*Equilibrium and Batch Calculations*
Process description	Mixing. Reactions: Xx, Yy,Zz,Dd…..	*Mixing processes of different water distributions at the control points* *Equilibrium calculations*
Geometric framework and parameters	Modelling reactions within one fracture zone, NE-1.	*Modelling chemical equilibrium at specific control points and in fractures* *Identifying chemical environmental parameters by equilibrium calculations for each time step at each node (batch reactions)*
Reaction parameters	Xx: a=ff, b=gg,… Yy: c=. Zz: d=...	*PH, Eh, T*
Spatial distribution of reactions assumed	Xx: seafloor sediments Yz: Bedrock below seafloor, superficial Dd: Bedrock ground surface, superficial Yz: Bedrock below seafloor, at depth Zz: Bedrock ground surface, at depth Yy, Zz: near tunnel	
Boundary/initial conditions for the reactions	Xx: aaa… Yy: bbb…	
Numerical tool	Phreeque	*Phreeqc*
Numerical method	xx	
Output parameters	xx	*Element concentrations in molarities* *pH* *pe* *species distribution* *saturation indices*

Table 4a Summary of data usage

Data del. No	Data	Importance of data (see notes)	*Comment*
1	Hydrochemical data 1		
1a	Surface boreholes undisturbed conditions, Äspö-Laxemar	P	*Samples: Mixing fractions, element concentrations and environmental parameters*
1b	Surface boreholes disturbed conditions (by tunnel excavation), Äspö	P	*Samples: Mixing fractions, element concentrations and environmental parameters*
1c	Surface boreholes undisturbed conditions, Ävrö	-	
1d	Surface boreholes sampled during drilling, Äspö	P	*Samples: Mixing fractions, element concentrations and environmental parameters*
1e	Data related to the Redox experiment	-	
1f	Tunnel and tunnel boreholes disturbed conditions	P	*Samples: Mixing fractions, element concentrations and environmental parameters*
2	Hydrogeological data 1		
2a1	Annual mean air temperature	X	
2a2	Annual mean precipitation	p	
2a3	Annual mean evapotranspiration	X	
2b1	Tunnel front position by time	P	*Date of penetration point of the fractures*
2b2	Shaft position by time	p	*Date of penetration point of the fractures*
2c1	Geometry of main tunnel	P	*x-, y-, z-values in Äspö coordinate system*
2c2	Geometry of shafts	p	*x-, y-, z-values in Äspö co-ordinate system*
2d	Hydrochemistry at weirs (chloride, pH, electrical conductivity, period: July 1993 - Aug 1993)	p	*Electrical conductivity compared to depth or tunnel length respectively*
2e	Geometry of the deterministic large hydraulic features (Most of them are fracture zones)	P	*Dip and Azimuth (Rhén et al. 1997) Extensions*

Table 4b Summary of data usage

Data del. No	Data	Importance of data (see notes)	*Comment*
3	Hydrogeological data 2		
3a	Monthly mean flow rates measured at weirs. Tunnel section 0-2900m, period May 1991 – January 1994	P	*Location of weirs and flow rate to assign inflow rates to specific fractures*
3b	Piezometric levels for period June 1st 1991 – May 21st 1993. Values with 30 day intervals (Task 3 data set)	P	*Time dependent lowering of water table representing the drawdown*
3c	Salinity levels in borehole sections for period Sept 1993. (Task 3 data set)	-	
3d	Undisturbed piezometric levels	p	
3e	Co-ordinates for borehole sections	P	*x-, y-, z-values in Äspö co-ordinate system;* *assign borehole sections to penetrated fractures*
3f	Piezometric levels for period July 1st 1990 – January 24th 1994. Daily values.	P	*Time dependent lowering of water table representing the drawdown*
4	Hydrochemical data 2	-	*Use of data 7 instead of 4*
4a	Chemical components, mixing proportions and deviations for all borehole sections used in the M3 calculations	-	*Use of data 7a instead of 4a*
4b	Boreholes with time series, > 3 samples (part of 4a)	-	*Use of data 7b instead of 4b*
4c	Borehole sections interpreted to intersect deterministic large hydraulic features (Most of them are fracture zones) (part of 4a)	-	*Use of data 7c instead of 4c*
4d	Chemical components, mixing proportions and deviations. Grid data based on interpolation. Undisturbed conditions	-	*Use of data 7d instead of 4d*
4e	Chemical components, mixing proportions and deviations. Grid data based on interpolation. Disturbed conditions (from tunnel excavation)	-	*Use of data 7e instead of 4e*

4f	Boundary and initial conditions. Chemical components, mixing proportions and deviations (1989). Grid data for vertical boundaries based on interpolation. Undisturbed conditions	-	*Use of data 7f instead of 4f*
4g	Boundary conditions after tunnel construction (1996) Chemical components, mixing proportions and deviations. Grid data for vertical boundaries based on interpolation. Disturbed conditions (from tunnel excavation)	-	*Use of data 7g instead of 4g*

Table 4c Summary of data usage

Data del. No	Data	Importance of data (see notes)	Comment
5	Geographic data 1		
5a	Äspö coastline	M	*Easting and Northing in Äspö coordinate system for separation of upper boundary conditions*
5b	Topography of Äspö and the surrounding area	m	*Investigation of topography concerning possible sources of infiltrating surface water (fresh water)*
6	Hydro tests and tracer tests		
6a	Large scale interference tests (19 tests)	-	
6b	Long time pump and tracer test, LPT2	-	
7	Hydrochemical data 3, update of data delivery 4 based on new end members. Recommended to be used instead of 4.	P	*Used instead of data 4*
7a	Chemical components, mixing proportions and deviations for all borehole sections used in the M3 calculations	P	*Chemical components and mixing proportions at selected control points;* *Deviations in element concentrations resulting from mixing model used for assessing hydraulic model and for identifying chemical reactions*
7b	Boreholes with time series, > 3 samples (part of 7a)	P	*Partly used at control points: chemical components, mixing fractions*
7c	Borehole sections interpreted to intersect deterministic large hydraulic features (Most of them are fracture zones) (part of 7a)	P	*In specific hydraulic features partly used at control points:* *chemical components, mixing fractions*
7d	Chemical components, mixing proportions and deviations. Grid data based on interpolation. Undisturbed conditions	P	*Use of grid data for interpolation of initial distribution of mixing proportions in fracture zones*
7e	Chemical components, mixing proportions and deviations. Grid data based on interpolation. Disturbed conditions (from tunnel excavation)	p	*Comparison with modelled distribution in fracture zones*

7f	Boundary and initial conditions. Chemical components, mixing proportions and deviations (1989). Grid data for vertical boundaries based on interpolation. Undisturbed conditions	P	*Use of grid data for interpolation of boundary and initial distribution of mixing proportions in fracture zones*
7g	Boundary conditions after tunnel construction (1996) Chemical components, mixing proportions and deviations. Grid data for vertical boundaries based on interpolation. Disturbed conditions (from tunnel excavation)	p	*Comparison with modelled distribution in fracture zones*

Table 4d Summary of data usage

Data del. No	Data	Importance of data (see notes)	Comment
8	Performance measures and reporting 1		
8a	Performance measures	M	
8b	Suggested control points. 6 points in tunnel section 0-2900m and 3 points in tunnel section 2900-3600m.	M	
8c	Suggested flowchart for illustration of modelling	M	
9	Hydrogeological data 3		
9a	Monthly mean flow rates measured at weirs. Tunnel section 0-2900m, period: May 1991- Dec 1996.	P	*Location of weirs and flow rate to assign inflow rates to certain fractures*
10	Geographic data 2		
10a	Topography of Äspö and the surrounding area (larger area than 5b)	M	*Easting and Northing in Äspö co-ordinate system for separation of upper boundary conditions*
10b	Co-ordinates for wetlands	-	
10c	Co-ordinates for lakes	-	
10d	Co-ordinates for catchments	-	
10e	Co-ordinates for streams	-	
10f	Co-ordinate transformation Äspö system- RAK	X	
11	Boundary and initial conditions		
11a	Pressure before tunnel construction, from the regional SKB model (TR 97-09)	m	
11b	Salinity before tunnel construction, from the regional SKB model (TR 97-09)	m	
11c	Pressure after tunnel construction, from the regional SKB model (TR 97-09)	m	
11d	Salinity after tunnel construction, from the regional SKB model (TR 97-09)	m	

Table 4e Summary of data usage

Data del. No	Data	Importance of data (see notes)	*Comment*
12	Performance measures and reporting 2		
12a	Suggested control points. 6 points in tunnel section 0-2900m and 3 points in tunnel section 2900-3600m (same as 8b) and 2 outside the tunnel.	M	*Suggested control points were used as far as they could be assigned to discrete fractures used in the model*
13	Transport parameters compiled		
13a	LPT2 tracer tests	X	
13b	Tracer test during passage of fracture zone NE-1	X	
13c	Redox tracer tests	X	
13d	TRUE-1 tracer tests	X	
14	Hydrochemical data 4		
14a	Groundwater reactions to consider within TASK5 modelling (Description of how M3 calculates the contribution of reactions and the identification of dominant reactions based on the M3 calculations.	X	
15	Co-ordinates for the test sections defining the control points	P	
16	Co-ordinates for boreholes drilled from the tunnel	P	

Table 4f Summary of data usage

Data del. No	Data	Importance of data (see notes)	*Comment*
17	Hydrogeological data - prediction period		
17a	Hydrochemistry at weirs (chloride, pH, electrical conductivity, period: July 1993 - Dec 1995)	P	
17b	Piezometric levels for period July 1st 1990 – Dec 1996. Daily values.	P	
18	Hydrochemical data - prediction period.		
18a	Chemical components, mixing proportions and deviations for all borehole sections used in the M3 calculations. Data for tunnel section 2900-3600m.	P	
18b	Boreholes with time series, > 3 samples (part of 18a)	P	
18c	Borehole sections interpreted to intersect deterministic large hydraulic features (Most of them are fracture zones) (part of 18a)	P	
	Other data (part of data in Task 1, 3 and 4)	X	
	Fracture orientation, fracture spacing and trace length – tunnel data	P	
	Fracture orientation, fracture spacing– mapping of cores	-	
	Fracture orientation, fracture spacing and trace length – mapping of outcrops	-	

P = data of great importance for quantitative estimation of model parameters
p = data of less importance for quantitative estimation of model parameters
M = data of great importance used qualitatively for setting up model
m = data of less importance used qualitatively for setting up model
X = data useful as general background information
- = data not use